NUCLEON TRANSFER IN HEAVY ION REACTIONS

Luigi Lo Monaco

Balliol College

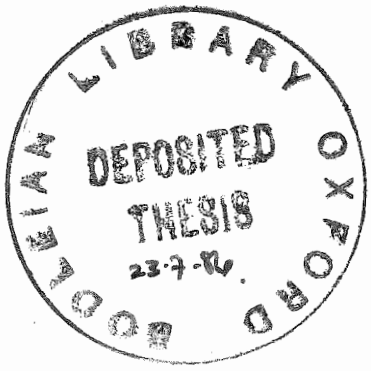

A thesis submitted for the degree of Doctor of Philosophy in the

University of Oxford

Michaelmas Term 1985

'How do people find the time for quotations

in their theses?'

L. Lo Monaco

Nucleon Transfer in Heavy Ion Reactions

Luigi Lo Monaco, Balliol College

Abstract of thesis submitted for the degree of Doctor of Philosophy
in the University of Oxford,
Michaelmas Term 1985.

An analytical formula is derived for the amplitude for transfer of a nucleon in quasi-elastic reactions between heavy ions. The derivation takes advantage of the semiclassical conditions found in peripheral collisions between heavy ions. The relative motion of the two nuclei is treated classically and the transfer amplitude is calculated by a perturbation method. Under the approximation of small overlap between the nuclear potentials, the semiclassical amplitude is reduced to a surface integral. This can be calculated analytically by using Hankel function forms for the bound-state wavefunctions and by approximating the actual orbit by a constant velocity orbit tangential to it at the distance of closest approach. These approximations seem reasonable in strong absorption conditions. Corrections to the formula of the amplitude are evaluated. The analytical form of the amplitude exhibits an exponential behaviour as a function of the distance of closest approach. The decay constant of the exponential is given explicitly and it is found to be an important parameter of the reaction. Kinematical conditions for maximum transfer are derived which relate the incident energy to the reaction Q-value. The physical interpretation of the amplitude is discussed. In the case of proton transfer, the effect of Coulomb potential results in a shift of the binding energy of the proton. With this prescription we still obtain the same form of the transfer amplitude for both neutrons and protons. The formula for the semiclassical tranfer amplitude is used to calculate angular distributions within a simplified formalism derived from the distorted wave Born approximation (DWBA). The reactions considered are $^{208}Pb(^{16}O,^{15}O)^{209}Pb$, $^{26}Mg(^{11}B,^{10}B)^{27}Mg$ and $^{34}S(^{32}S,^{33}S)^{33}S$ for neutron transfer and $^{208}Pb(^{16}O,^{15}N)^{209}Bi$ for proton transfer. It is found that the shapes of the present angular distributions agree with full DWBA calculations but the magnitude of the former depends on whether the distance of closest approach is that of the initial channel, the final channel or some average of the two. Conditions for the selective population of definite states are discussed in relation to the reaction Q-value, energy and initial and final states involved. It is found that an inversion of the selectivity with respect to the spins of the initial and final state occurs when the energy of relative motion at distance of closest approach equals the reaction Q-value. An approximate formula for the angle-integrated cross section has also been derived.

ACKNOWLEDGEMENTS

This thesis was done in the Department of Theoretical Physics. I have great pleasure in thanking Pofessor R. J. Elliott and the staff for welcoming me to the Department.

I would particularly like to express my gratitude to

Dr. D. M. Brink, my supervisor, for his help and for the patience shown during my research and the writing of this thesis;

Dr. R. A. Baldock for help in the calculation of bound-state wavefunctions and job-hunting consultancy, Dr. A. Bonaccorso for discussions and encouragement, Dr. S. M. Marsh for help in the computation of elastic-scattering phase shifts;

the many students in the Nuclear Structure group I have met in the last few years, who have made work in the Department such a social event; I should mention in particular Constança Providencia, Orfeu Bertolami, Hasnita Hashim and Peter Hopkins for their invaluable help in the very, very late stages of this thesis;

D. G. Lewis and P. N. Shotton for their (unknowing) help with the formatting of this thesis;

Fondazione A. Della Riccia, Florence, Italy, for partial financial support during the first two years of my course.

The use of the computing and typesetting facilities of the Nuclear Physics Laboratory is gratefully acknowledged.

Finally, I would like to thank my parents for their constant support throughout these years.

CONTENTS

p.t.o.

CONTENTS

Chapter I. Introduction

I.1

Nuclear reactions can nowadays be produced by accelerating nuclei over a wide range of energies. They provide a great volume of data which need to be interpreted through a reaction theory in order gain information on the structure of nuclei. In this work we consider one of the simplest nuclear reactions, the rearrangement collision

$$a_1 + c_2 \longrightarrow c_1 + a_2$$

or

$$(c_1 + x) + c_2 \longrightarrow c_1 + (c_2 + x)$$

which can be described as the transfer of one or more nucleons x from the projectile to the target or viceversa, leaving the final nuclei in bound states. Transfer reactions are highly selective in the nuclear levels they populate. This indicates that they are very sensitive to the relationship between the initial and final nuclear states involved and hence can be very useful as probes of nuclear structure. While inelastic scattering responds strongly to collective correlations in nuclear wavefunctions, one-nucleon transfers probe the single particle character of the states, two-nucleon transfers reveal nucleon-nucleon correlations such as pairing, two-neutron, two-proton transfers may reveal alpha clustering, and so on.

Transfer reactions take place when the tails of the single-particle wave functions in one nucleus start to overlap with the attractive nuclear field of the other. In fact typical distances for these processes are larger than those relevant for nuclear inelastic scatter-

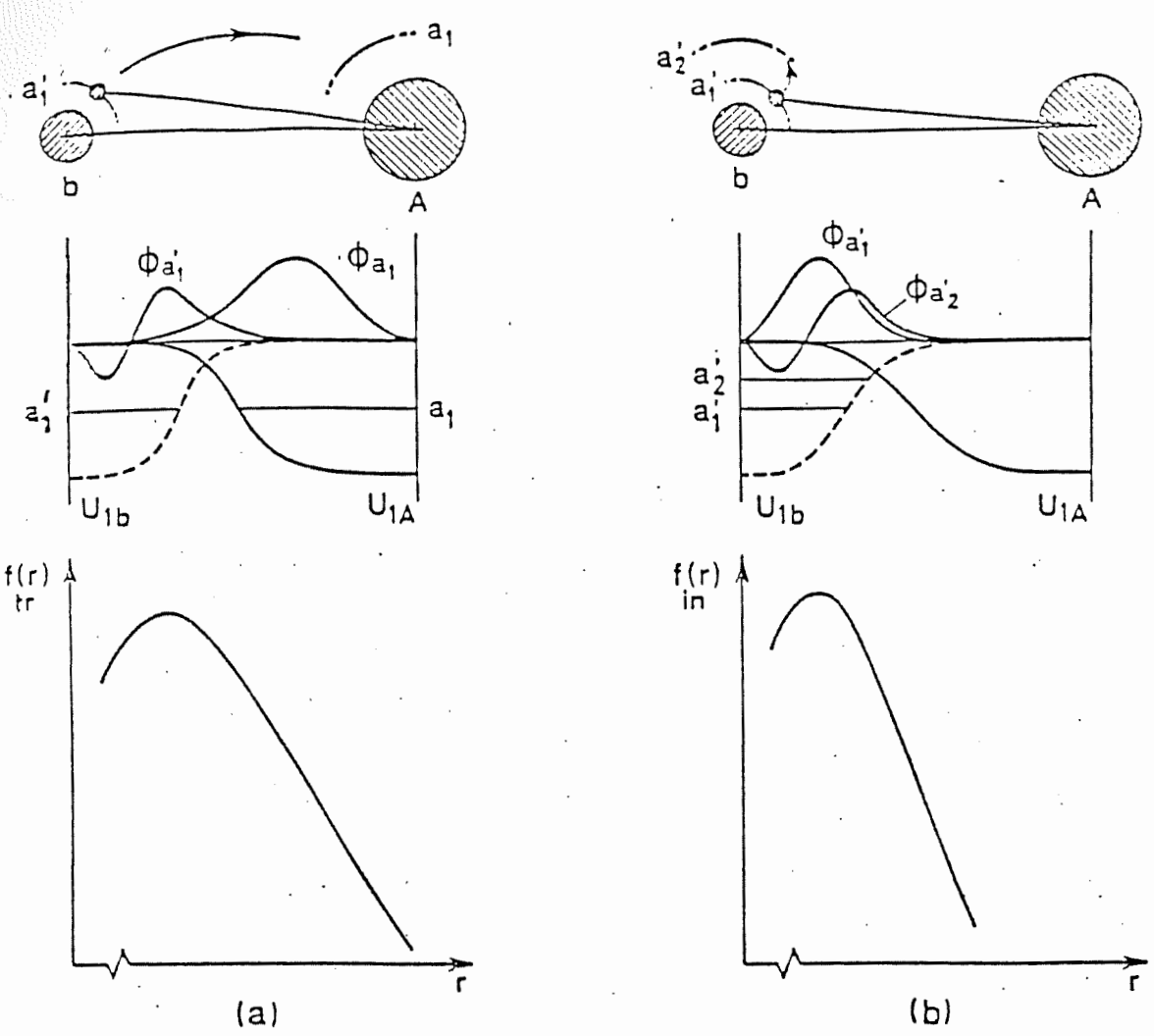

Fig. I.1

Schematic representation of the radial dependence of the one-particle transfer and inelastic formfactors. In (a) a nucleon moving in the orbital with quantum numbers a_1' in the projectile a is transferred under the action of the shell model potential U_{1A} to the target nucleus A into an orbital a_1. The dependence of the formfactor on the distance between the two nuclei is determined by the overlap of the product of the single-particle wavefunctions ϕ_{a_1} and $\phi_{a_1'}$ with the potential U_{1A}. A schematic representation of this dependence is given at the bottom of (a).

In (b) a nucleon in the projectile a is excited under the influence of the target field U_{1A}, from the single-particle orbital with quantum numbers a_1' to the orbital with quantum numbers a_2'. The dependence of the formfactor on the distance between the cores is here determined by the overlap of the product of the functions $\phi_{a_1'}$ and $\phi_{a_2'}$ with the potential U_{1A}. A representation of this dependence is shown at the bottom of (b). (From Broglia and Winther 1985)

ing. This is because the associated form factors $f_{tr}(r)$ are proportional to the overlap of the nucleon single-particle wavefunctions in the initial and final nucleus with the nuclear potential (Fig. I.1a). Then $f_{tr}(r)$ has a longer range than the inelastic scattering form factor $f_{in}(r)$, which is proportional to the overlap between the initial and final nucleon wavefunctions of the same nucleus with the potential (Fig. I.1b).

In closer collisions, although the properties of individual states lose their importance, transfer reactions play an important rôle in the damping of the relative motion leading to deep inelastic collisions and fusion reactions as they dominate the frictional forces acting between the nuclear surfaces. They also usually control the depopulation of elastic channels and thus are a major component of the absorptive potential for grazing reactions.

When more than one nucleon is transferred multistep processes, especially through inelastic channels, are important and in some cases dominant (Fig. I.2).

Here we consider only one-step direct processes, which account for most of the one-nucleon transfer reactions between heavy ions. The difference with respect to experiments with light ions, like the (d,p) reaction, arises from the large mass, charge, linear and angular momenta involved and the wide variety of systems that can be brought together in heavy ion reaction. We shall return to the implications of using heavy ions after briefly reviewing, in §I.2, the experimental situation for transfer reactions. In §I.3 we discuss some theories developed for these reactions and in §I.4 we give an overview of the present work. Most of the material in this chapter is taken from excellent reviews and books on the subject (Ascuitto and Seglie 1984, Broglia and Winther 1985, Glendenning 1983, Goldfarb and Von Oertzen 1979, Hasan 1976, Hodgson 1971 and 1978, Satchler 1983).

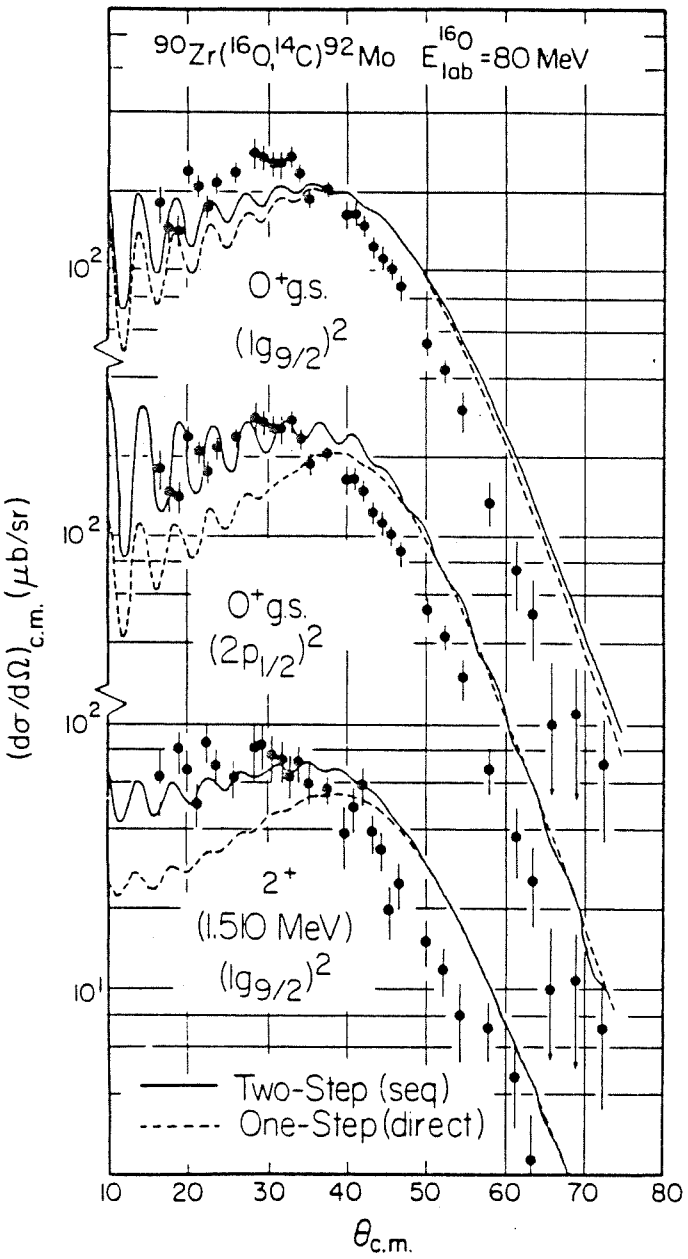

$E_{c.m.} = 68$ MeV

$V_{cB} = 46$ MeV

$n = 22.6$

Figure 1.2. Comparison of calculations for sequential and direct transfer for the pure configurations $(g_{9/2})^2$ and $(2p_{1/2})^2$. The measured angular distributions are also shown. The influence from configurational effects is evident at forward angles. Source: P. P. Tung, K. A. Erb, M. W. Sachs, G. B. Sherwood, R. J. Ascuitto, and D. A. Bromley, *Phys. Rev. C* **18**:1663 (1978).

I.2 Some phenomenology of transfer reactions.

In this section we show some experimental results from the literature on transfer reactions, although it is difficult to select examples that can be regarded as "typical", especially for heavy ions. The angular distributions are different for transfers below and above the Coulomb barrier, so we consider the two cases separately.

The cross sections for sub-Coulomb transfers are considerably smaller than those for higher energies and angular distributions are quite featureless and almost independent of the ℓ transfer (see §V11.1 for its definition). They increase monotonically to maxima at 180° (Fig. I.3).

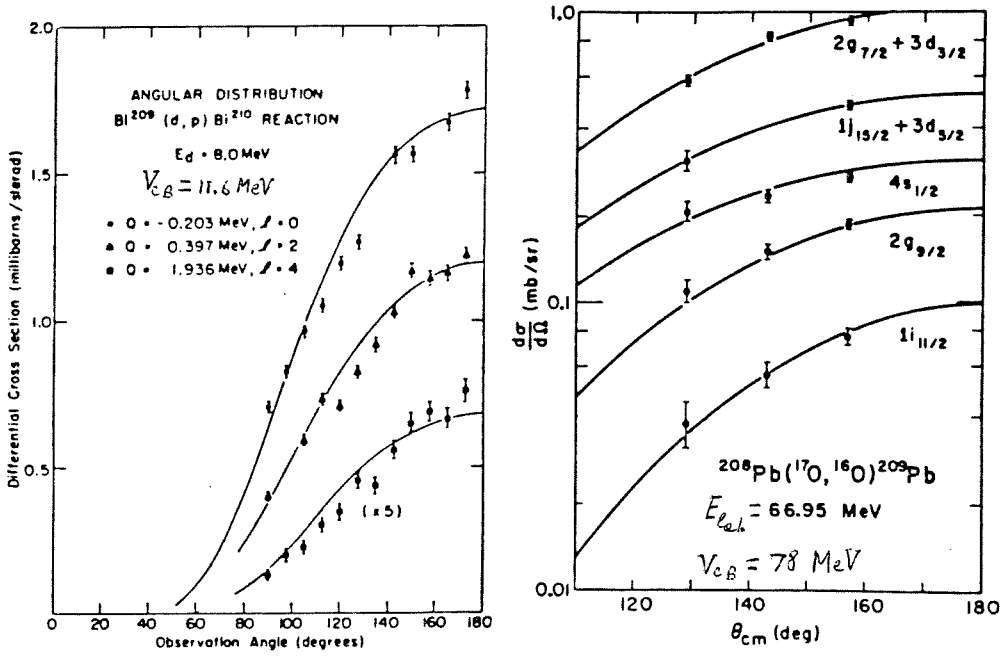

FIG. I.3. Angular distributions for nucleon transfer at sub-Coulomb energies for several different l transfers. The curves are the results of DW calculations. (a) The (d, p) reaction at 8 MeV. (From Erskine, Buechner and Enge 1962.) (b) The (^{17}O, ^{16}O) reaction at 67 MeV. (From Franey et al. 1979.)

As the energy rises up to and above the Coulomb barrier diffractionlike peaks begin to appear at the forward angles and they grow until they dominate the angular distribution (Figs. I.4 and I.5)

An interesting qualitative account can be given which explains some important features of transfer reactions. To fix ideas we first consider a reaction much studied in the past, the neutron stripping from deuterons. Fig. I.6 shows a typical spectrum of protons from a (d, p) reaction. This consists in general of a number of discrete peaks at the higher energies, which become closer together and merge into a continuous distribution at lower energies. The angular distributions of these protons show that, when averaged over a suitable energy interval, the continuous distribution is symmetrical about 90°, and usually almost isotropic. These protons are therefore due to the compound nucleus process. The more energetic protons resolved into discrete peaks, however, are often peaked in the forward direction at high incident energies (Fig. I.7a) and in the backward direction at low incident energies (Fig. I.7b). In addition, the magnitude of the cross-section is often much greater than that given by statistical theory. This indicates that the protons leaving the system in discrete, low-lying states are the result of direct reactions.

For light ions, at energies up to few tens of MeV above the Coulomb barrier, the number of partial waves participating is not large and the angular distributions show a correspondingly moderate amount of structure (Fig. I.8). The position of the first and main peak indicates the ℓ transfer as it is usually predicted unambiguously by, say, distorted wave Born approximation (DWBA). Matching of the momenta and angular momenta of the entrance and exit channels has also an important effect on angular distributions. An

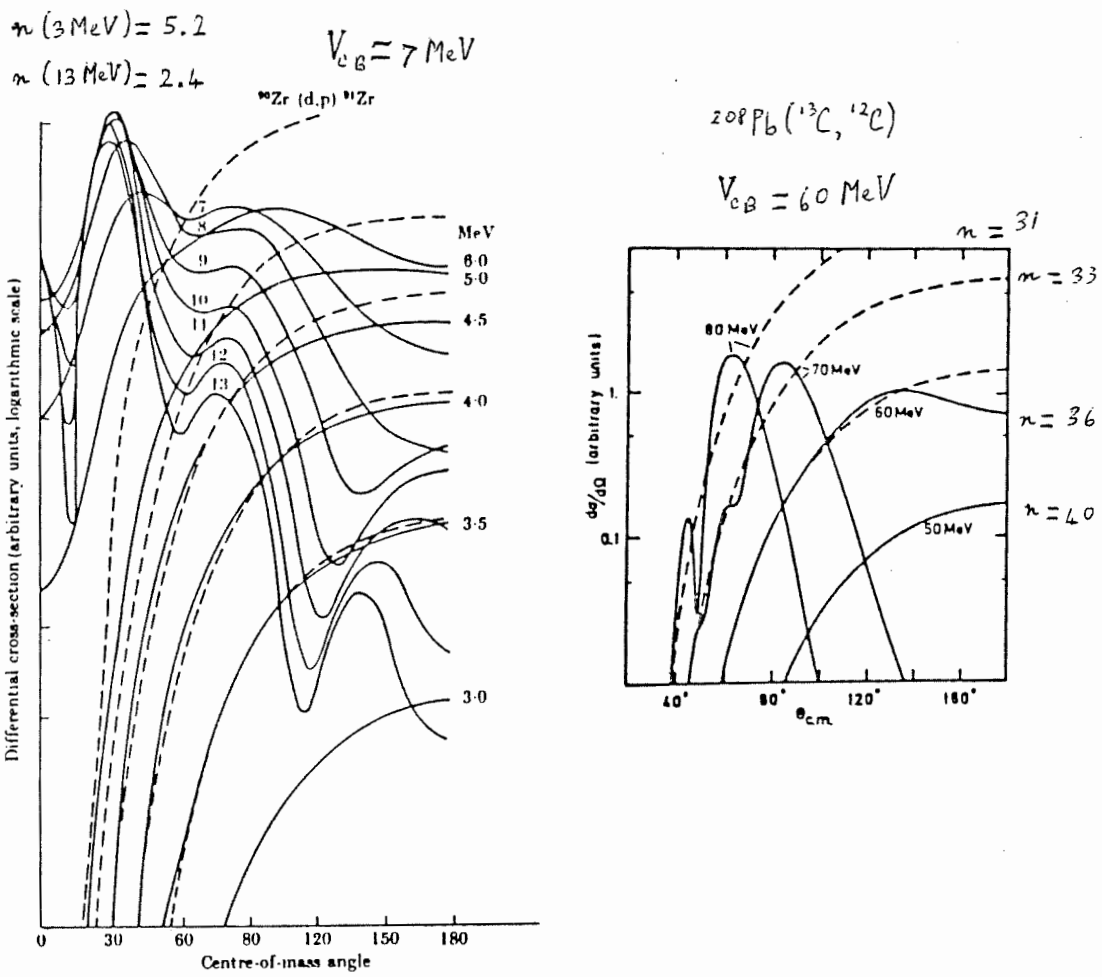

FIG. 1.4. Showing the evolution of diffraction structure from Coulomb-dominated transfer angular distributions. Both transitions are for $l = 0$. Dashed curves are for Coulomb waves alone and correspond to neglect of nuclear absorption and refraction. On the left, ^{90}Zr(d, p) reaction. (From Goldfarb 1966.) On the right, ^{208}Pb(^{13}C, ^{12}C) reaction. (From Traber et al. 1977.)

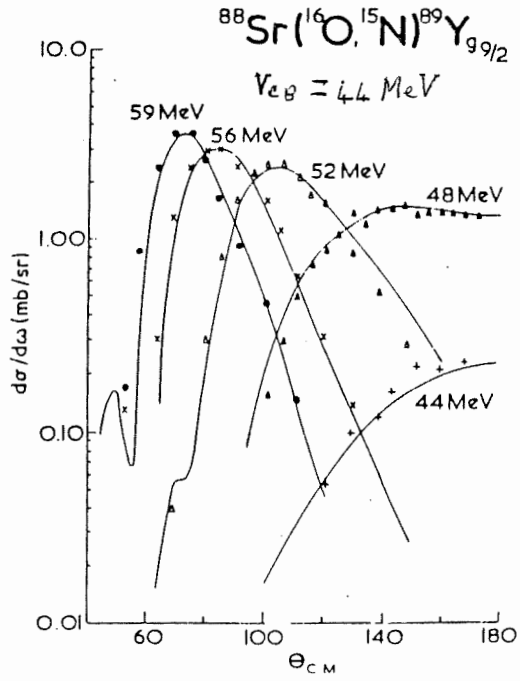

Fig. 1.5. Angular distributions for the ground state ^{88}Sr(^{16}O, ^{15}N)^{89}Y reaction for beam energies varying from 44 MeV to 59 MeV (Anantaraman 1973). The curves are associated with DWBA calculations; but with variable normalization factors (Bouldin and Goldfarb 1973).

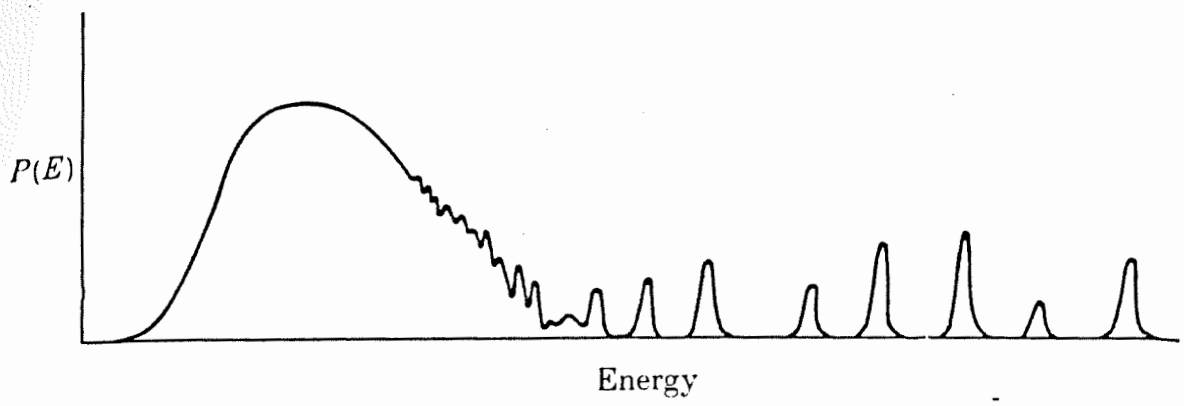

FIG. I .6. Energy distribution of protons from a (d, p) reaction.

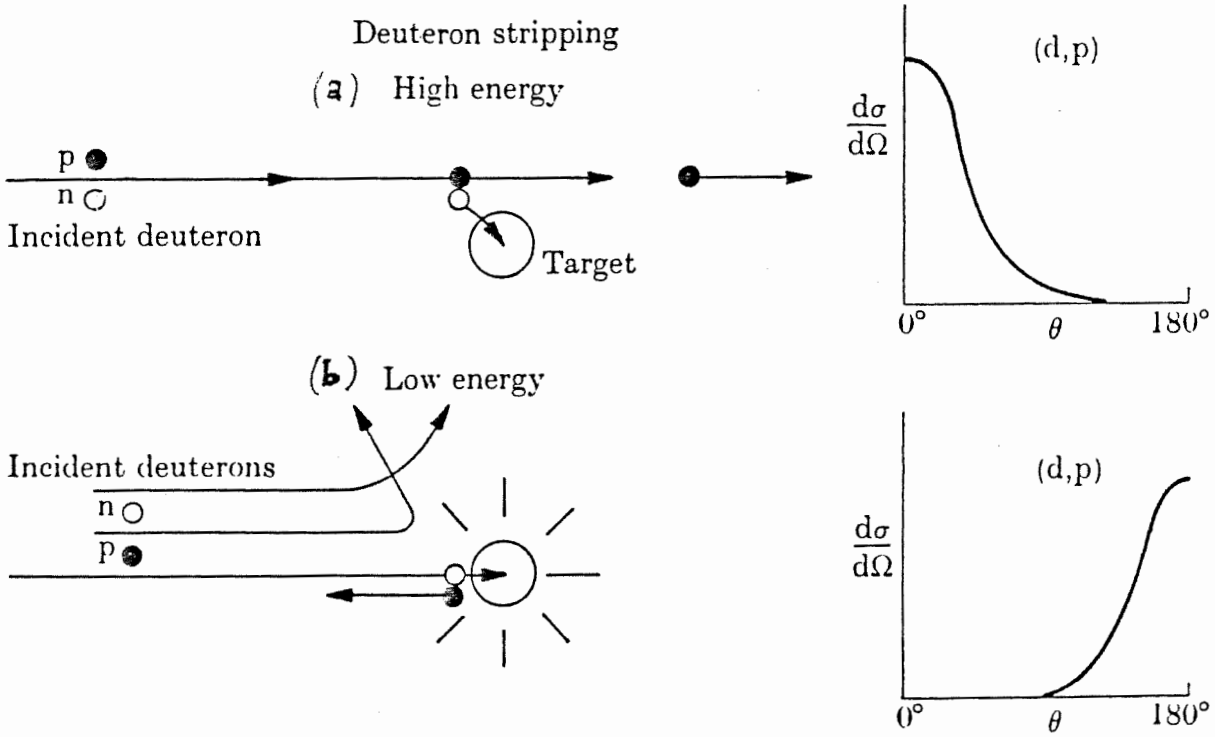

FIG. I.7 Deuteron stripping at high and low energy.

The figures in this page are from Hodgson 1971, p. 434-5.

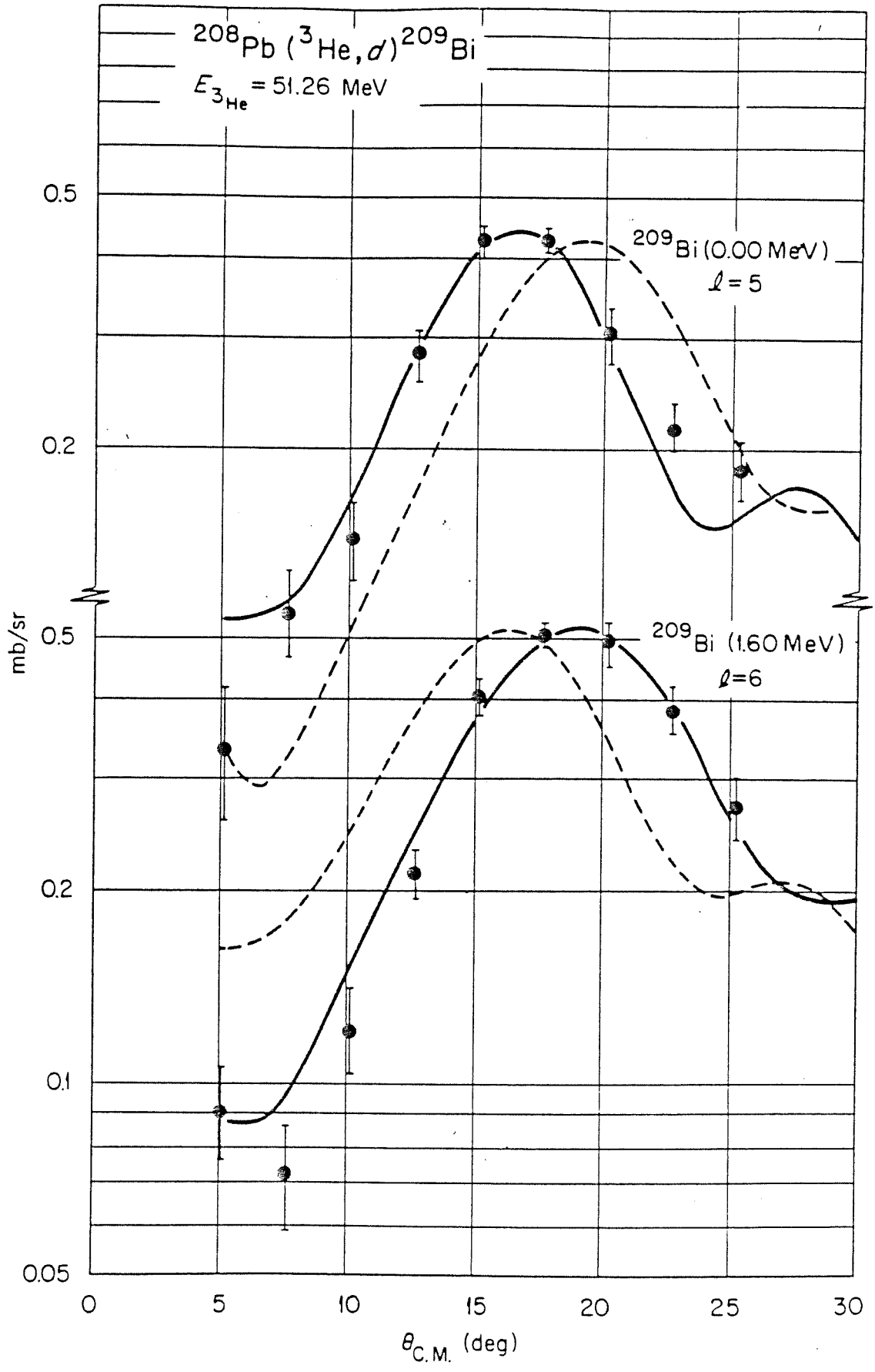

FIG. I.8. Illustrating the identification of the l transfer from the main forward peak of the angular distributions of a light-ion stripping reaction. The curves are from DW calculations. The solid curves fit the data and correspond to the l-values shown. The dashed curves correspond to the other l value in each case. (From Wildenthal et al. 1967.)

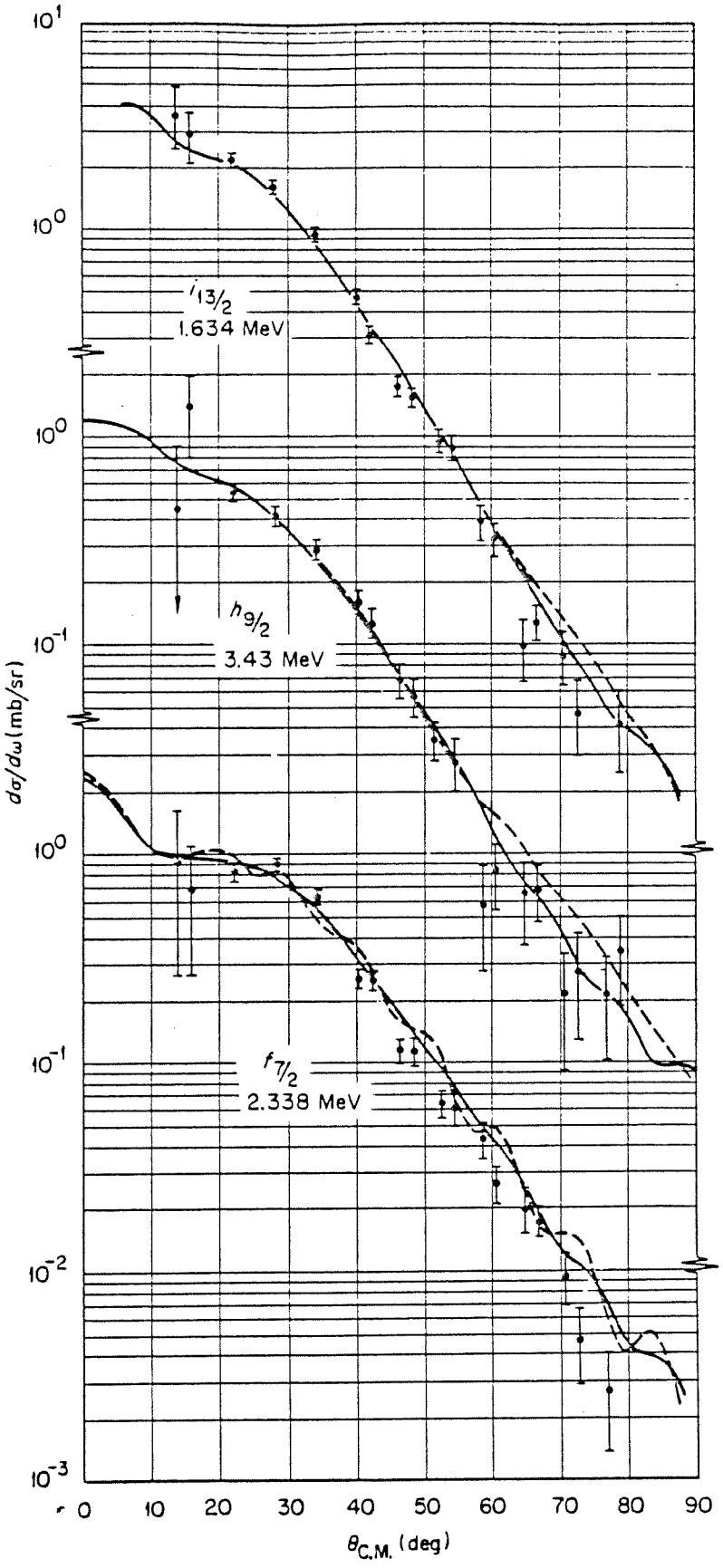

FIG. 1.9. Rather featureless angular distributions for ^{208}Pb(^{3}He, α) at 47.5 MeV for the transitions indicated. This reaction is poorly matched; the favoured l transfer is $l \approx 6$. The cross section (per unit spectroscopic factor) calculated for $l = 1$ transfer is only about $\frac{1}{10}$ that for $l = 6$. The curves result from DW calculations with two different optical potentials. (From Satchler et al. 1969.)

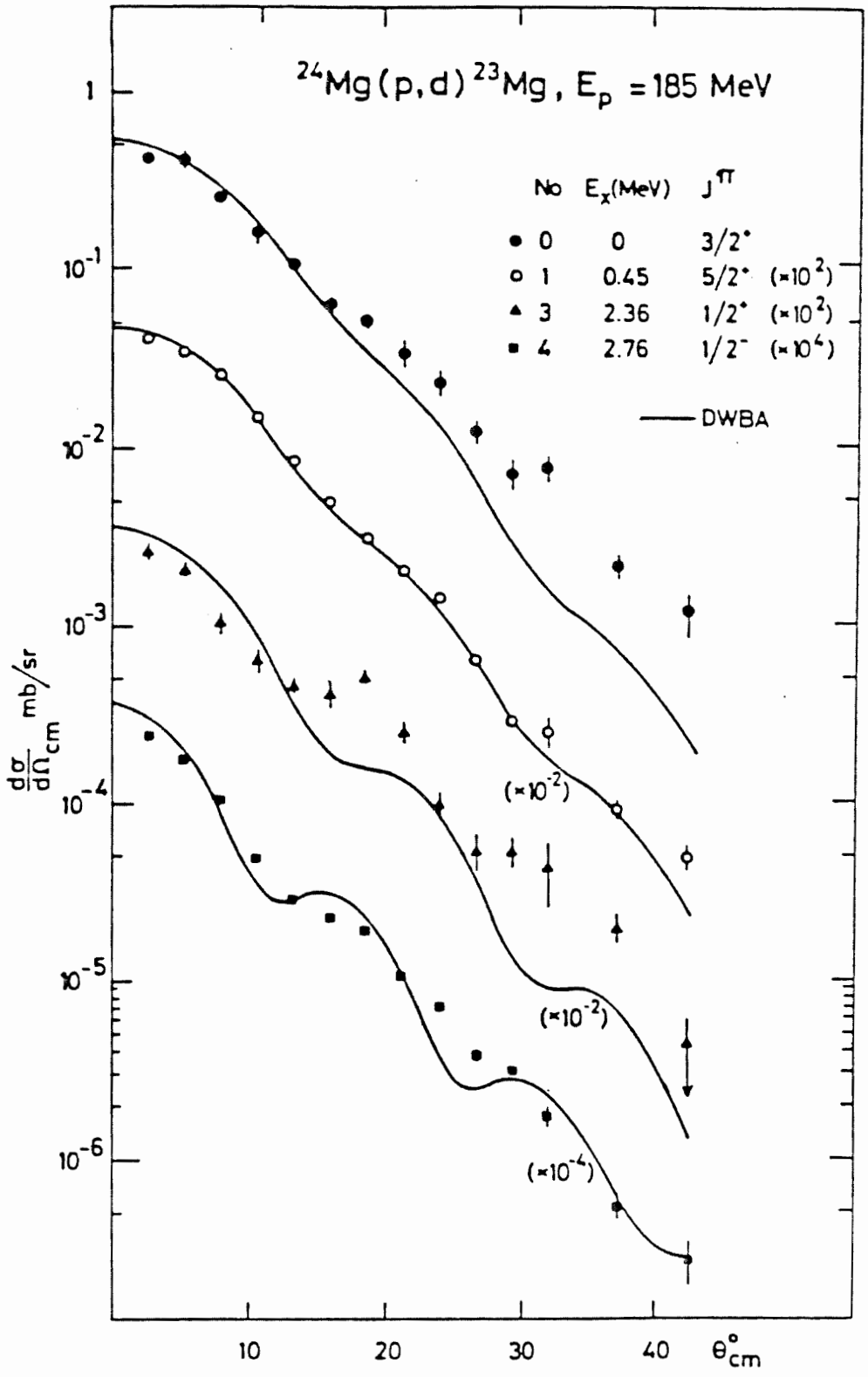

Fig. I.10. Examples of angular distributions for medium-energy (p,d) reactions. The curves are distorted wave calculations. (From Källne and Fagerstström 1975).

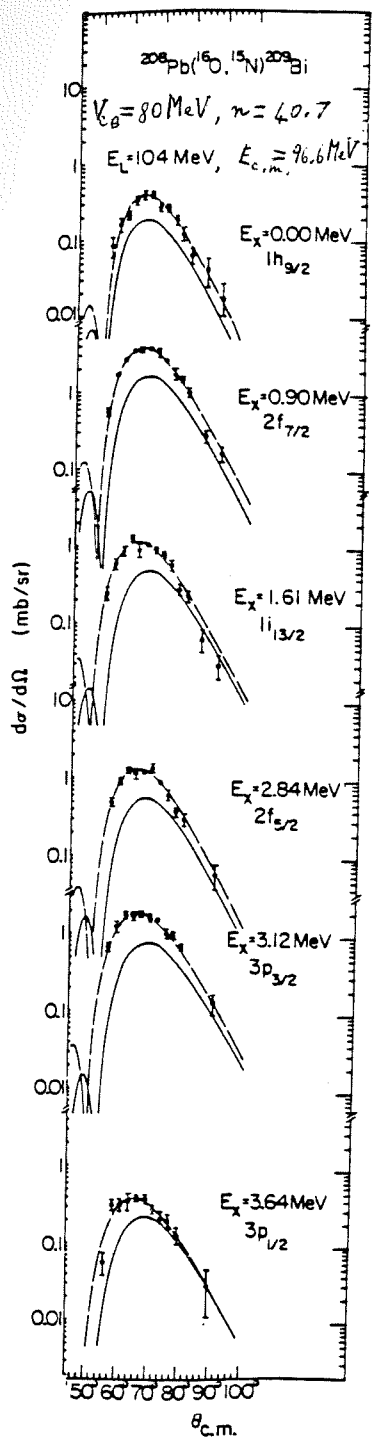

Fig. I.11. Differential cross sections for the $^{208}Pb(^{16}O,^{15}N)^{209}Bi$ reactions. The solid curves are the results of DWBA calculations. The dashed curves are those calculations shifted in angle and renormalized to best fit the data. (From Pieper et al. 1978)

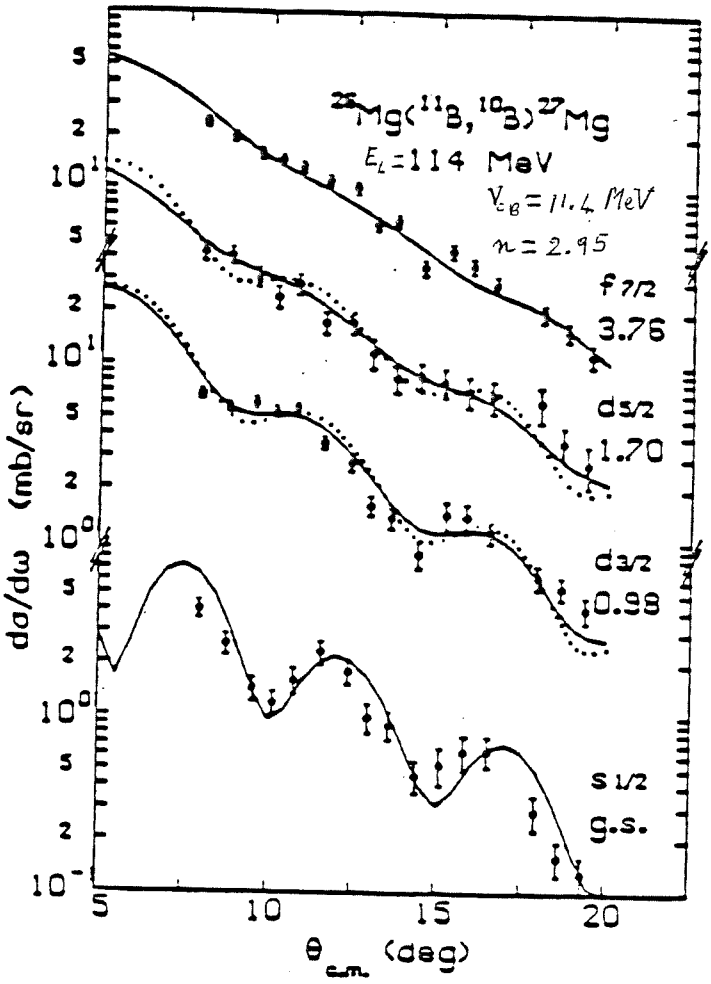

Fig. I.12. Differential cross sections for the $^{26}Mg(^{11}B,^{10}B)^{27}Mg$ reactions. The solid curves are DWBA calculations The dotted curves correspond to the $L_{max} = 3$ component of the cross section. (From Paschopoulos et al. 1975)

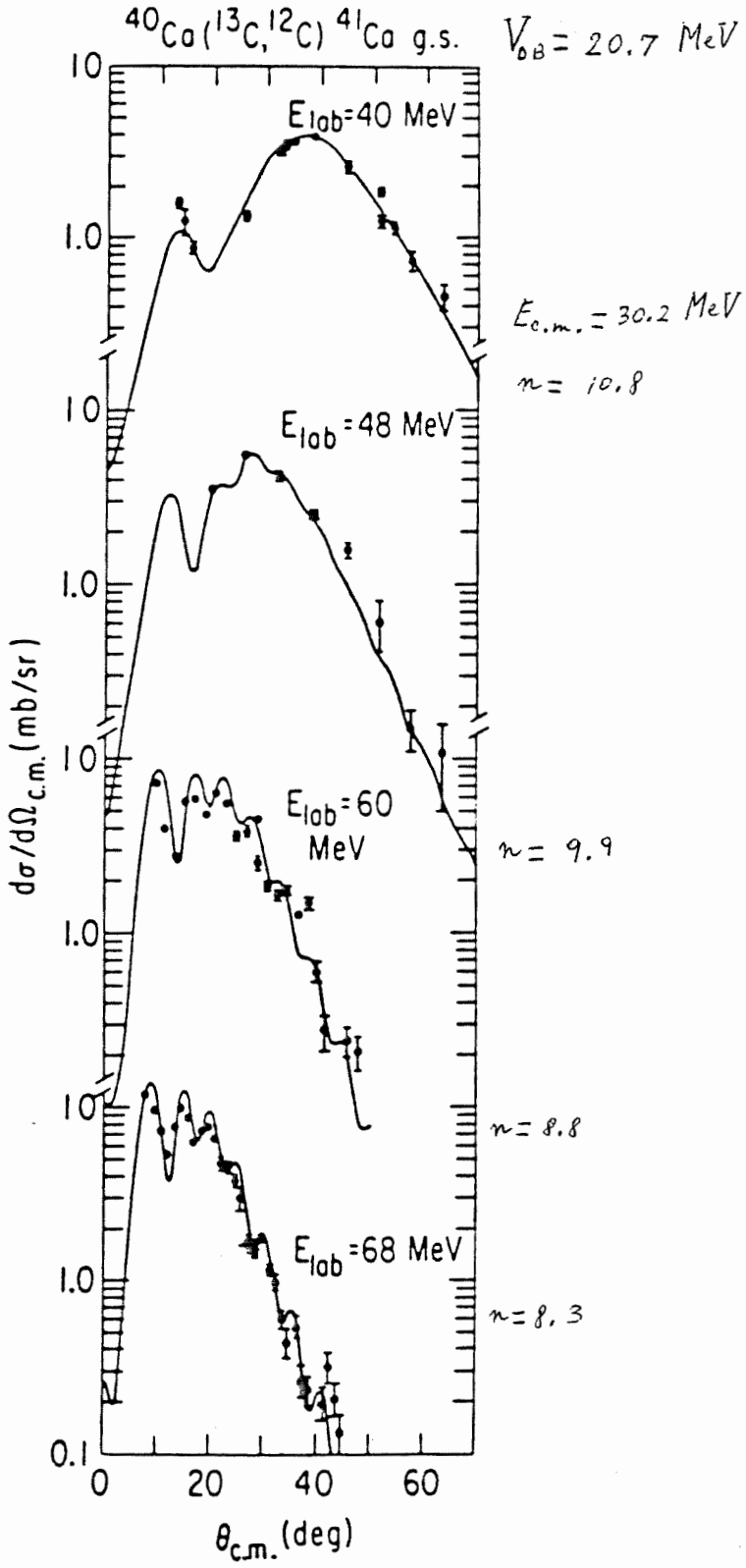

FIG. I.13. Example of the evolution from a bell-shaped distribution to the appearance of diffraction structure as the energy is raised. (From Kahana and Baltz 1977.)

example is the reaction $(^3He, \alpha)$ shown in Fig. I.9. Since the Q value is large, the incoming and outcoming wave are poorly matched and the angular distribution is quite structureless. At higher energies the forward peaking of the angular distribution becomes even more marked, as Fig. I.10 shows for the (p, d) reaction.

The effects of strong absorption are usually more pronounced in transfer reactions with heavy ions. This, together with their shorter wavelengths and larger angular momenta, results in a sharper localization of the reaction on the nuclear surface. There are essentially two types of angular distributions for heavy ion transfer reactions above the Coulomb barrier: the simple "bell-shaped" angular distributions centered near the scattering angle for grazing collisions (Fig. I.11) and more diffractionlike structures (Fig. I.12). Some systems may evolve from the first to the second type as the energy is increased (Fig. I.13) while others maintain the bell-shaped angular distributions (Fig. I.14).

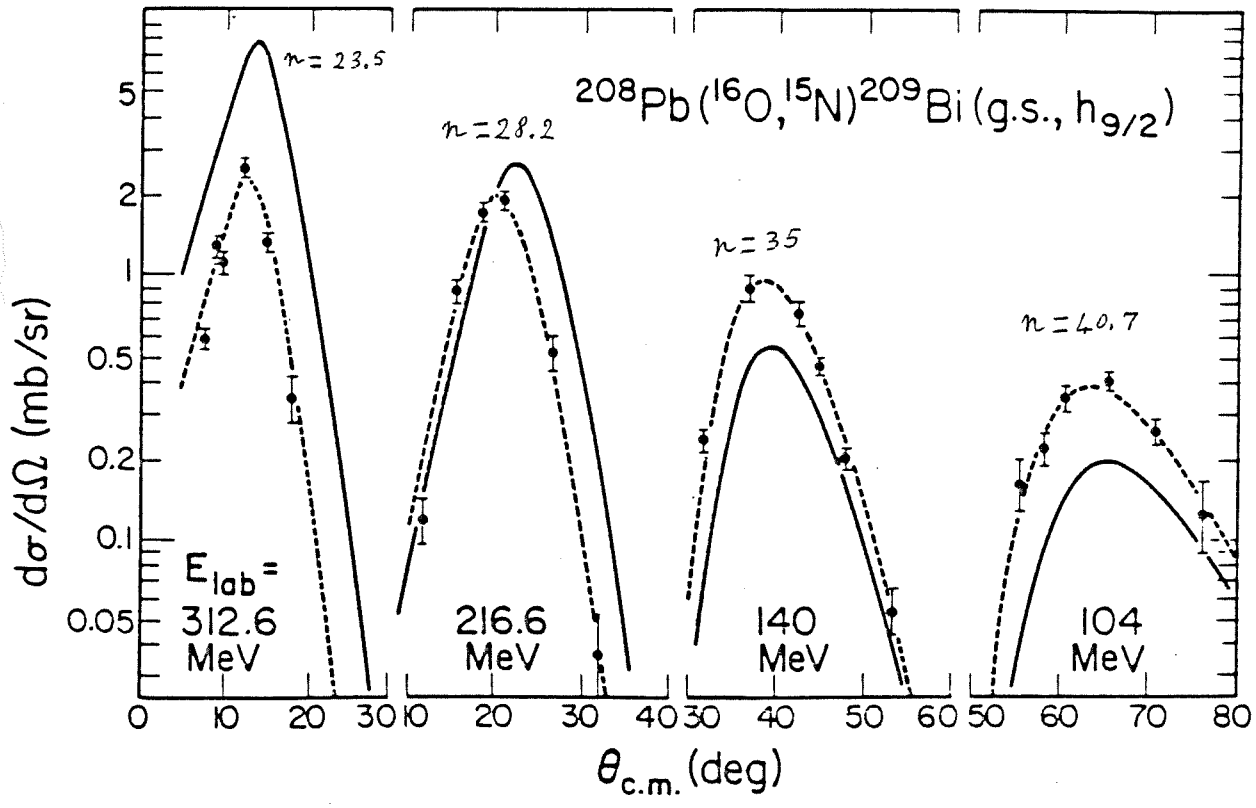

Fig. I.14. Measured and calculated cross sections for one-proton transfer to ^{208}Pb at four bombarding energies. The solid curves are DWBA predictions, using a spectroscopic factor $S = 0.95$. The dashed lines are these curves arbitrarily shifted in magnitude and angle to obtain the best fit to the data. As the energy increases the angular distributions become narrower and are peaked at a lower angle but maintain their "bell" shape. (From Olmer et. al. 1978)

This behaviour has been interpreted in a way similar to that used for elastic scattering where one envisages Fresnel scattering when the Sommerfeld parameter $n \gg 1$ and Fraunhofer scattering when $n \lesssim 1$. Relevant values of the Sommerfeld parameter n and the Coulomb barrier V_{CB} are included in the previous examples of experimental data. For transfer one considers waves scattered from the near-side and far-side and their interference. At the lower energies the transfer occurs only from waves scattering from the near-side of the target, because of the diverging effect of the Coulomb potential. But, as the energy increases, the Coulomb deflection is reduced and contributions from the far-side begin to interfere with the near-side amplitudes. Hence the interference pattern is characterized by an angular period $\Delta\theta \sim \pi/kR$, where k is the incident wave-number and R is the nuclear radius. However, for a more detailed interpretation of experimental data one needs to consider a theory of transfer reactions. A brief review follows.

I.3 Theories of transfer reactions.

Several methods have been used to study transfer reactions since they were discovered. The neutron stripping in reactions induced by deuterons -(d,p) for short- helped recognizing that a different mechanism than compound nucleus formation is responsible for an important class of nuclear reactions, which are then called direct. Although the latter account for a small part of the total cross section they are invaluable for the study of low lying levels in nuclei. Oppenheimer and Phillips (1935) first proposed the mechanism of direct capture of the neutron to explain the data obtained by Lawrence et al. (1935) in reactions induced by low energy (0-3.6 MeV) deuterons. Later on Serber (1947) suggested

a very simple model to explain the forward peaking of (d, n) reactions at high energies observed by Helmotz et al. (1947). The theory of (d, p) reactions proposed by Butler (1950, 1951) showed the relevance of linear and angular momentum transfers in these relatively simple reactions. However, this theory was soon recognized as inadequate in that it made use of plane waves to describe the relative motion. One cannot neglect the refractive effects that absorption inside the nuclear surface has on the plane waves. Therefore a distorted wave theory is a better approximation and, for one-step reactions, is the best we can do to date.

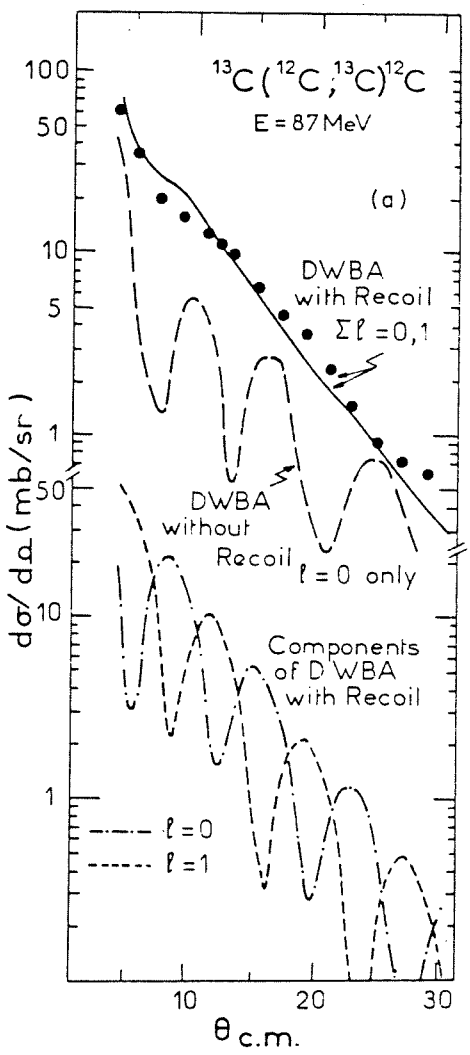

Fig. I.15. Example of recoil effects in heavy-ion transfer reactions. The no-recoil approximation leaves out the nonnormal-parity $\ell = 1$ amplitude and results in an oscillatory angular distribution. Addition of the $\ell = 1$ terms in an exact calculation results in a structureless distribution in agreement with the data. Even for $\ell = 0$ the no-recoil distribution differs from the exact one. The backward-angle elastic scattering predicted by the optical model in this region is completely negligible. (From de Vries 1973)

In the application of DWBA to transfer reactions approximations have been made in order to simplify and calculate the six-dimensional integral of the transition matrix. Zero-range and no-recoil approximations were used with some success to calculate cross sections for transfer induced by light ions. It was initially thought that a no-recoil approximation would be justified for heavy ion reactions because the mass of the transferred particle is small compared to that of the nuclei. However, recoil effects cannot be neglected in general without losing a good deal of the physics in heavy ion transfer reactions, as it was shown by Dodd and Greider (1969). Fig. I.15 shows that the no-recoil approximation can predict a completely wrong angular distribution.

In the early analyses of transfer reactions semiclassical theories were used as an aid to understand the physics of the process and as an alternative to impossible computations. Nowadays exact finite range DWBA computations of one-nucleon transfer reactions (which include recoil) are routine practice since programs have been written to do so. As a result we are more demanding and require that semiclassical theories give a quantitative description of the reactions, while keeping the simplicity that characterizes them. In this respect for heavy ion reactions we are particularly fortunate in that a classical description of the relative motion is accurate enough while in many cases "a purely quantum-mechanical description may be too complicated to be either possible or interesting" (Nörenberg and Weidenmüller 1980, p. 1).

In most semiclassical theories one considers the nuclei moving along classical trajectories specified by an impact parameter or relative angular momentum. The transfer process is then treated quantum-mechanically and one calculates a transfer amplitude, A_{tr}, along

a given trajectory. From this the cross section can be calculated, for instance as a product of probabilities:

$$\sigma = |S|^2 |A_{tr}|^2 \sigma_{elastic}, \qquad (I.1)$$

where the reflection coefficient $|S|^2$ gives the probability that the system escapes absorption into other inelastic channels. The classical formula $(I.1)$ is the simplest way to obtain a cross section, but it has many drawbacks, as we shall discuss in chapter III. For the moment we look at several possible ways to calculate the transfer amplitude. Broglia and Winther (1972 a and b) expand the total wave function into a linear combination of the channel wavefunctions. The coefficients of this expansion, $c_{\alpha\beta}$, give the amplitude for transfer from the initial channel α to the final channel β as a function of time t, with the initial condition $c_{\alpha\beta}(-\infty) = \delta_{\alpha\beta}$. They obtain a set of coupled first order differential equations for these coefficients, which can be solved approximatively to arrive at a formula for the transfer amplitude $c_{\alpha\beta}(+\infty)$.

Some semiclassical theories consider a partial-wave expansion for the reaction amplitude $f(\theta)$ of the form

$$f(\theta) = \sum_L g_L \; h_L(\theta), \qquad (I.2)$$

where g_L is a partial wave amplitude and $h_L(\theta)$ is a known function of the scattering angle θ, e.g. a spherical harmonic or a rotation matrix. The amplitude g is then parametrized in a suitable form, which is peaked in L-space (e.g. Strutinsky 1964, 1973). This reflects the assumption that small L waves are absorbed while for much larger L's there is no transfer. Attempts have been made to understand this simple semiclassical parametrization of the scattering amplitude with several methods. Broglia et al. (1974) identify g_L with

the solutions of their semiclassical coupled equations times $e^{i\delta_L}$, where δ_L are the elastic scattering phase shifts:

$$g_L \sim c_{\alpha\beta} e^{2i\delta_L}. \qquad (I.3)$$

Koeling and Malfliet (1975) use a path integral formalism to derive a transition amplitude. Other approaches start with the expression for the transition matrix in DWBA and, under high-energy, short-wavelength conditions, utilize the WKB approximation to obtain simplified expressions for the distorted waves and derive a formula of the type $(I.2)$ (Landowne et al. 1976, Hasan and Brink 1978). In the latter work the amplitude g_L is factorized in a form similar to *eq.* $(I.3)$:

$$g_L \sim A_{tr}(2,1)\ e^{2i\delta_L}, \qquad (I.4)$$

where $A_{tr}(2,1)$ is identified as the semiclassical transfer amplitude of Brink (1972). Then $A_{tr}(2,1)$ is integrated numerically and it is shown to decay exponentially with the angular momentum of relative motion or with the distance of closest approach. The form $I.4$ is discussed in chapter III, after integrating analytically the semiclassical transfer amplitude in chapter II.

The problem of particle transfer between two bound states in potential wells moving along classical trajectories has been solved numerically (Esbensen et al. 1983). In fact even the more realistic problem of the time dependent Hartree-Fock approximation (TDHF), where the particles to be transferred move in the self-consistent field of all other particles, can be solved numerically. A different point of view has been taken by Révai (1985), who proposes a simultaneous treatment of all reaction channels, elastic, rearrangement (transfer) and break-up. With this method, by using separable potentials and straight-

line trajectories, probabilities for various reaction channels have been computed (Milek et al. 1985). Although these calculations are in principle better approximations or even exact results, the amount of computation involved seems considerable and no comparison with directly observable quantites has been made so far. Therefore a simple semiclassical description is still of relevance to understand what are the most important physical parameters of the process.

In this work we consider transfer reactions between heavy ions. The difference with respect to experiments with light ions like the (d,p) reaction comes from their large charge, mass, angular momenta involved and the wide variety of systems that can be brought together in a heavy ion reaction. These have implications in the following ways:

(i) The large charges emphasize the rôle of the Coulomb interaction. Even at energies far exceeding the Coulomb barrier, cross sections can be attributed to certain angular regions with the dominant action of the Coulomb field. (ii) The large masses allow first for the possibility of localization of the reactions in a peripheral way. This is simply because of the comparatively small de Broglie wave lengths that come into play. (iii) Concomitant with the large masses are the large linear and angular momenta of the relative motion. With the availability of large amounts of angular momenta to transfer to the internal motion, transitions to states with high spins are a possibility. There is also an important difference in the possible values of the transferred angular momentum ℓ for the transition from the initial single particle state $\ell_1\ j_1$ to the final state $\ell_2\ j_2$. For reactions induced by light ions the initial state is $s1/2$, so there are only two possible values $\ell = j_2 \pm 1/2$, while for heavy ions the allowed values are in general given by the selection rules $|j_1 - j_2| \leq \ell \leq j_1 + j_2$

and $|\ell_1 - \ell_2| \leq \ell \leq \ell_1 + \ell_2$ (iv) The composite nature of the projectile and the multiplicity of possible reactions lead to loss of flux in break-up channels. High levels of absorption become apparent. The exclusion principle also plays a rôle with the low compressibility of the nucleus. The result is an inaccessibility of the nuclear interior and with this we gain in the interpretation of phenomena. (v) The diversity of heavy ions as projectiles provides the advantage of choice of beams in order to study particular states of nuclei as the same final state can be populated in a number of reactions.

I.4 Overview.

In chapter II, under the approximation of small overlap between the two nuclei, we calculate the semiclassical transfer amplitude $A(2,1)$ which enters in *eq.* $(I.2)$ analytically. The formula obtained is then used to study the kinematical conditions that favour nucleon transfer. This is partially done in chapter II where we consider a physical interpretation of the amplitude and more in detail in chapter VII.

In chapter III the semiclassical amplitude is related to cross sections. A product-of-probabilities classical formula is first considered and the conditions to apply it to heavy ion transfer reactions are discussed. Then we recall a partial-wave formula for the transition amplitude derived from the DWBA by Hasan and Brink (1978). One advantage of a simple analytical formula for the semiclassical transfer amplitude is that one can use the same formula to calculate the cross section in two ways: i) from the classical expression $I.1$, whenever it is applicable to angular distributions, or ii) from the partial-wave formula $(I.2)$ when diffraction effects are important. We show, however, that the two formulæ give

the same angle-integrated transfer cross section. Therefore the simpler classical formula *eq.* ($I.1$) can be used to study the spin selectivity of transfer reactions and their energy dependence, as it is done in chapter VII.

In chapter IV we apply the theory to one-neutron transfer reactions induced by heavy ions. Several calculations for this case are presented and compared with experimental data.

In chapter V the calculation of the semiclassical amplitude is extended to proton transfer and results for this case are presented in chapter VI.

In chapter VII we introduce some possible angular momentum couplings to study the selectivity of the reaction with respect to the spins of the initial and final levels. We also look at the energy dependence of the cross section and extrapolate it to a higher energy regime where it decreases exponentially (Transfert à Grande Vitesse).

Conclusions are drawn in chapter VIII.

The main advantage of using the semiclassical approach presented in this work for the analysis of transfer reactions is its simplicity. At the same time we obtain an agreement with experimental data comparable to that of complete DWBA calculations, as it is shown in chapters IV and VI. It is worth mentioning that our expressions include recoil through an exponential factor deriving from the Galilean transformation of one of the bound-state wave functions. Therefore we can use our analytical formula for the semiclassical transfer amplitude to study the conditions favouring a particular transfer at low, medium and high energy. The physical interpretation of the process that results is more transparent than a full DWBA computation. The use of a formula of the type $I.2$ to study transfer reactions

allows a certain flexibility in the choice of the optical potential determining the phase shifts in *eq.* *I*.3. These can be obtained either by numerical solution of the Schrödinger equation with a complex potential $U = U_C + U_N$ or by first order WKB approximation. Considering the whole nuclear potential U_N as a perturbation one obtains for the nuclear part of the phase shifts (e.g. Brink 1978, p. 13)

$$\delta_L^N \approx -\frac{1}{2\hbar}\int_{-\infty}^{\infty} U_N[r_C(\Lambda,t)]\ dt, \qquad (I.5)$$

where the integral is taken along the Coulomb orbit corresponding to classical angular momentum $\Lambda = (L+1/2)\hbar$. Alternatively, one can parametrize the nuclear part of the radial S-matrix $S_N(L) \equiv \exp(2i\delta_L^N)$ and study, for example, the energy dependence of the cross section without the intermediate step of an optical potential, as it is done in chapter VII. Moreover, it has been pointed out (Broglia et al. 1981) that the transfer process gives the main contribution to the long-range part, $W_{transfer}$, of the absorptive potential. This can be related to the transfer probability per unit time, ω, by

$$W_{transfer} = \frac{1}{2}\hbar\omega, \qquad (I.6)$$

The present theory has been developed for the simple case of one-nucleon transfer from/to single particle levels. However, it could reasonably be extended to transfer of clusters of nucleons, e.g. alpha particles. It applies to incident energies above the Coulomb barrier because we approximate the actual trajectory by a straight line tangential to it at the distance of closest approach. Clearly this would be a bad approximation for angular distributions that are not forward peaked, as in sub-coulomb transfer. On the other hand there are certain advantages when the bombarding energy is so low that the system of the

two initial nuclei $a_1 + c_2$ cannot surmount their mutual Coulomb barrier, and the Q value is such that the same is true for $c_1 + a_2$ in the exit channel. Since the nuclei are kept far apart by their Coulomb repulsion the probability of compound nucleus formation is negligible. Then any observed transfer reaction is a direct one. At the same time, distortion of the elastic Coulomb waves by the nuclear potentials is either negligible or small enough that its effects can be easily assessed. As a result the analysis of the reaction is free of the uncertainties associated with optical potentials. Another simplicity arising from the lack of close approach is that one needs the overlap of only the asymptotic parts of the initial and final wavefunctions of the transferred particle and the form of these asymptotic parts is known precisely for a single nucleon. However, for heavy ion reactions we are usually in a strong absorption condition, so that we need not consider the interior of the nuclear region and only the 'tails' of the nucleon wavefunctions are relevant to the transfer process.

Chapter II. The Transfer Amplitude

II.1 Definition of the Amplitude.

Here we derive an analytical formula for the amplitude in a transfer reaction of the type

$$a_1 + c_2 \longrightarrow c_1 + a_2$$

or

$$(c_1 + x) + c_2 \longrightarrow c_1 + (c_2 + x)$$

For most of this chapter we follow the derivation of Lo Monaco and Brink (1985). First we consider the simpler case of neutron transfer ($x = n$) between bound states. Let Ψ_1 be the initial state of the neutron bound in a single particle potential $V_1(\mathbf{r}, t)$ which represents the shell model potential of the nucleus a_1. The neutron is transferred into a single particle state Ψ_2 in the potential $V_2(\mathbf{r}, t)$ which represents the final nucleus a_2. The potential V_1 moves past V_2 during the transfer and the relative motion is described by an orbit $\mathbf{s}(t)$, where s is the distance between the centres of V_1 and V_2. $s \to \infty$ when $t \to \pm\infty$.

The initial and final states $\Psi_\alpha(\mathbf{r}, t)$ satisfy the time-dependent Schrödinger equation for the neutron bound in the potential $V_\alpha(\mathbf{r}, t)$, where $\alpha = 1, 2$,

$$i\hbar \frac{\partial \Psi_\alpha}{\partial t} = (T + V_\alpha)\Psi_\alpha \qquad (II.1)$$

Here $T = -(\hbar^2/2m)\nabla^2$ is the kinetic energy operator and m is the mass of the transferred particle. During the transfer process the wave function of the neutron, Ψ, is affected by

both potentials V_1 and V_2 and therefore satisfies the equation

$$i\hbar\frac{\partial\Psi}{\partial t} = (T + V_1 + V_2)\Psi \qquad (II.2)$$

with the initial condition that $\Psi \rightarrow \Psi_1$ when $t \rightarrow -\infty$. The transfer amplitude, $A(2,1)$, can be defined as the overlap between the wave function Ψ and the final state Ψ_2 when $t \rightarrow \infty$:

$$A(2,1) = < \Psi_2|\Psi >_{t=\infty} \qquad (II.3)$$

A perturbation formula can be derived for the transfer amplitude A(2,1) in the following way (e.g. Brink 1977). Using *eqs.* $(II.1)$ and $(II.2)$ it is easy to check that

$$i\hbar\frac{\partial}{\partial t} < \Psi_2|\Psi > = < \Psi_2|V_1\Psi >$$

Integrating between $t = -\infty$ and $t = \infty$ we obtain

$$A(2,1) = \frac{1}{i\hbar}\int_{-\infty}^{+\infty} < \Psi_2|V_1|\Psi > dt \qquad (II.4)$$

In deriving eq. (II.4) we used the initial condition that there is no overlap between the initial and final neutron bound states long before the collision takes place, i.e.

$$< \Psi_2|\Psi >_{t=-\infty} = < \Psi_2|\Psi_1 >_{t=-\infty} = 0.$$

Eq. $(II.4)$ is an exact formula. The four-dimensional integral vanishes for values of $(\mathbf{r}, t)$ such that $V_1 = 0$. In the region where $V_1 \neq 0$ we approximate Ψ by Ψ_1 and we have

$$A(2,1) \simeq \frac{1}{i\hbar}\int_{-\infty}^{+\infty} < \Psi_2|V_1|\Psi_1 > dt \qquad (II.5a)$$

$$= \frac{1}{i\hbar}\int_{-\infty}^{+\infty} < \Psi_2|V_2|\Psi_1 > dt \qquad (II.5b)$$

The equality between $(II.5a)$ and $(II.5b)$ shows that in first order one can use either the initial or the final nuclear potential (post-prior equivalence).

A method which uses expressions similar to *eqs.* $(II.5)$ was developed by Oppenheimer (1928) to compute the transition probability for the ionization of hydrogen atoms in a constant electric field.

Eqs. $(II.5)$ are a reasonable approximation for our problem because in a peripheral collision leading to transfer the potentials do not overlap appreciably. If they do there is absorption into other channels (e.g. deep inelastic or fusion reactions) than the simple transfer considered here. In the case of a peripheral collision *eqs.* $(II.5)$ can be transformed into a simpler form involving a surface integral. Let Σ be a surface which lies between the two potentials V_1 and V_2 (fig. II.1) and which divides the space into two regions R_1 and R_2.

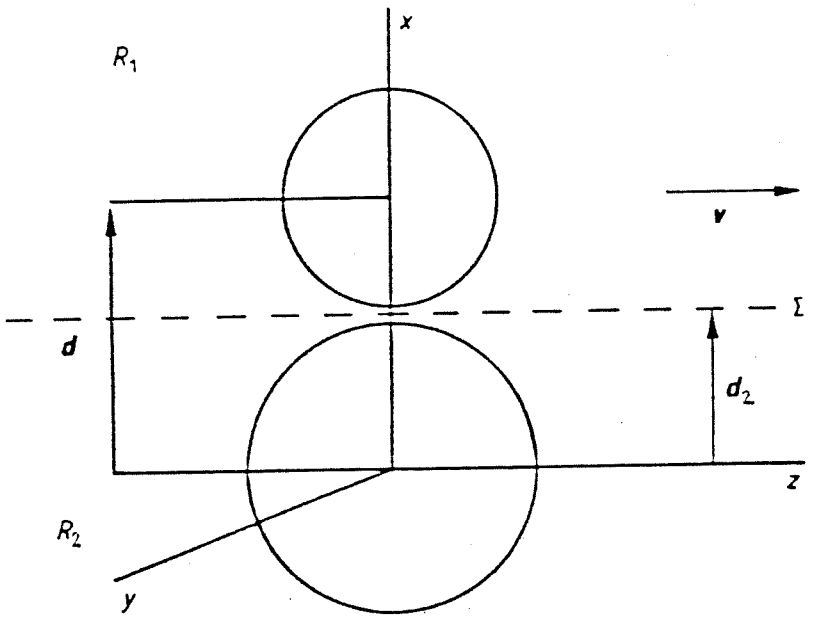

Figure II.1 Coordinate system for the transfer amplitude.

Then the matrix element in *eq.* $(II.5a)$ can be written as

$$< \Psi_2|V_1|\Psi_1 >= \int_{R_1} \Psi_2^*(\mathbf{r},t)V_1(\mathbf{r},t)\Psi_1(\mathbf{r},t)d^3\mathbf{r} + \int_{R_2} \Psi_2^*(\mathbf{r},t)V_1(\mathbf{r},t)\Psi_1(\mathbf{r},t)d^3\mathbf{r} \quad (II.6)$$

The first term in eq. (II.6) can be simplified by using eq. (II.1) to write

$$\int_{R_1} \Psi_2^* V_1 \Psi_1 d^3\mathbf{r} = \int_{R_1} \Psi_2^* \left(i\hbar\frac{\partial}{\partial t} + \frac{\hbar^2}{2m}\nabla^2 \right) \Psi_1 d^3\mathbf{r}$$

Since we are dealing with bound states the integration region can be thought of as finite. Then it is possible to apply Green's theorem which reduces the above integral to

$$\int_{R_1} \Psi_2^* V_1 \Psi_1 d^3\mathbf{r} = \frac{\hbar^2}{2m}\int_\Sigma d\mathbf{S}\cdot(\Psi_2^*\nabla\Psi_1 - \Psi_1\nabla\Psi_2^*)$$

$$+\int_{R_1}\left(i\hbar\frac{\partial\Psi_2}{\partial t} + \frac{\hbar^2}{2m}\nabla^2\Psi_2\right)^*\Psi_1 d^3\mathbf{r} + i\hbar\frac{\partial}{\partial t}\int_{R_1}\Psi_2^*\Psi_1 d^3\mathbf{r} \qquad (II.7)$$

where dS is a surface element normal to Σ directed out of R_1. If eq. (II.7) is integrated over time between $t = -\infty$ and $t = \infty$ the third term on the *r.h.s.* vanishes because the potentials V_1 and V_2 are very far away from each other as $t \to \pm\infty$ and Ψ_1 and Ψ_2 have no overlap. By using eq. (II.1) for Ψ_2 the second term in eq. (II.7) can be expressed as an integral containing V_2. Hence eq. (II.5 a) becomes

$$A(2,1) = \frac{\hbar}{2mi}\int_{-\infty}^{+\infty} dt \int_\Sigma d\mathbf{S}\cdot(\Psi_2^*\nabla\Psi_1 - \Psi_1\nabla\Psi_2^*)$$

$$+\frac{1}{i\hbar}\int_{-\infty}^{+\infty} dt\left(\int_{R_1}\Psi_2^*V_2\Psi_1 d^3\mathbf{r} + \int_{R_2}\Psi_2^*V_1\Psi_1 d^3\mathbf{r}\right) \qquad (II.8).$$

Eq.(II.8) is exactly equivalent to eqs.(II.5). It is a perturbative expression for the transfer amplitude (II.3) or (II.4) symmetrical in the initial and final states and potentials. This reflects the equality between $(II.5a)$ and $(II.5b)$. If in a peripheral collision there is

no overlap between the potentials V_1 and V_2 it is possible to choose Σ so that $V_2(\mathbf{r},t) = 0$ for all points $\mathbf{r}$ in R_1 on one side of the surface, while $V_1(\mathbf{r},t) = 0$ for all points $\mathbf{r}$ in R_2 on the other side. Then the last two terms in *eq.* $(II.8)$ vanish and

$$A(2,1) = \frac{\hbar}{2mi} \int_{-\infty}^{+\infty} dt \int_{\Sigma} d\mathbf{S} \cdot (\Psi_2^* \nabla \Psi_1 - \Psi_1 \nabla \Psi_2^*) \qquad (II.9)$$

In eq. (II.9), which resembles a quantal probability current, the bound state wavefunctions Ψ_1 and Ψ_2 are only required on the surface Σ. If Σ is outside the range of V_1 and V_2 the wavefunctions can be replaced by their asymptotic forms, proportional to Hankel functions. Eq. (II.9) is equivalent to eqs. (II.5) if V_1 and V_2 do not overlap during the collision. For large distances, the bound-state potentials decrease as $exp(-r/a)$, where a is the diffuseness parameter, while the wavefunctions decrease as $exp(-\gamma r)$, where γ is related to the binding energy of the transferred neutron by eq. (II.21). For typical values of diffuseness and neutron binding energies, the slope $1/a$ is greater than γ by a factor of about two or three (see table IV.2). Therefore the "tail" of the potential decays faster than that of the bound-state wavefunction. In § II.2 we evaluate the amplitude by assuming that the condition of no overlap is satisfied. We discuss corrections to eq. (II.9) in § II.4. A formula similar to eq. (II.9) has been used by Nogami (1973) to discuss α decay.

II.2 Evaluation of the amplitude.

In this section we evaluate the transfer amplitude, eq. (II.9), when the orbit of relative motion is a Coulomb orbit. If the scattering angle is small then the orbit can be replaced by a constant velocity orbit $\mathbf{s}(t)$ tangential to it at the point of closest approach (fig. II.1). This is a reasonable approximation because the acceleration in the Coulomb orbit is small.

It would not be a good approximation for large angle scattering. The transfer amplitude depends only on the relative velocity, so we can assume that V_2 is at rest and V_1 has velocity $\mathbf{v}$, where $\mathbf{v}$ is the tangential relative velocity at the distance of closest approach d. The coordinate system is shown in fig. II.1. It is convenient to take the z axis parallel to the direction of relative motion and the x axis in the plane of the orbit. We write the equation of the orbit relative to the centre of V_2 as

$$\mathbf{s}(t) = \mathbf{d} + \mathbf{v}t \tag{II.10}$$

where $\mathbf{v}$ is in the z direction and $\mathbf{d}$ in the x direction.

If $\Phi_1(\mathbf{r})$ and $\Phi_2(\mathbf{r})$ are bound-state wave functions in the static potentials V_1 and V_2 with energies ε_1 and ε_2

$$[T + V_\alpha(\mathbf{r}_\alpha)]\Phi_\alpha(\mathbf{r}_\alpha) = \varepsilon_\alpha \Phi_\alpha(\mathbf{r}_\alpha), \qquad \alpha = 1, 2, \tag{II.11}$$

then the time dependence is given by

$$\Psi_1(\mathbf{r}, t) = \Phi_1\left[\mathbf{r} - \mathbf{s}(t)\right] \exp\left\{(i/\hbar)\left[m\mathbf{v}\cdot\mathbf{r} - \left(\varepsilon_1 + \frac{1}{2}mv^2\right)t\right]\right\} \tag{II.12}$$

$$\Psi_2(\mathbf{r}, t) = \Phi_2(\mathbf{r}) \exp(-i\varepsilon_2 t/\hbar) \tag{II.13}$$

The wavefunction Ψ_1 is obtained from Φ_1 by a Galilean transformation. If the surface Σ in the transfer amplitude $(II.9)$ is taken to be the plane $x = d_2$ (see fig. II.1) then the surface integral in *eq.* $(II.9)$ is over the variables y and z:

$$A(2,1) = \frac{-\hbar}{2mi}\int_{-\infty}^{+\infty} dt \int_{-\infty}^{+\infty} dy \int_{-\infty}^{+\infty} dz [\Phi_2^*(d_2, y, z)\frac{\partial}{\partial d_2}\Phi_1(d_2 - d, y, z - vt)$$

$$-\Phi_1(d_2 - d, y, z - vt)\frac{\partial}{\partial d_2}\Phi_2^*(d_2, y, z)] \exp\left\{\frac{i}{\hbar}\left[mvz + \left(\varepsilon_2 - \varepsilon_1 - \frac{1}{2}mv^2\right)t\right]\right\}. \tag{II.14}$$

There is a minus sign in front of *eq.* $(II.14)$ because the direction of $d\mathbf{S}$ in *eq.* $(II.9)$ is opposite to that of the x-component of the gradient operator. By making the change of variables

$$(z,t) \longrightarrow (z, z_1 = z - vt)$$

the argument of the exponential in eq. (II.14) becomes

$$\frac{i}{\hbar v}\left[\left(\frac{1}{2}mv^2 + \varepsilon_2 - \varepsilon_1\right) z + \left(\frac{1}{2}mv^2 + \varepsilon_1 - \varepsilon_2\right) z_1\right]$$

and

$$\int_{-\infty}^{+\infty} dz \int_{-\infty}^{+\infty} dt \longrightarrow -\frac{1}{v}\int_{-\infty}^{+\infty} dz \int_{-\infty}^{+\infty} dz_1.$$

Now the integrals over z and z_1 in *eq.* $(II.14)$ can be separated into a product:

$$A(2,1) = -\frac{i\hbar}{2mv}\int_{-\infty}^{+\infty} [\tilde{\Phi}_2^*(d_2, y, k_{2z})\frac{\partial}{\partial d_2}\tilde{\Phi}_1(d_2 - d, y, k_{1z})$$

$$-\tilde{\Phi}_1(d_2 - d, y, k_{1z})\frac{\partial}{\partial d_2}\tilde{\Phi}_2^*(d_2, y, k_{2z})]dy \qquad (II.15)$$

where

$$\tilde{\Phi}(x,y,k) \stackrel{\text{def}}{=} \int_{-\infty}^{+\infty} e^{-ikz}\Phi(x,y,z)dz, \qquad (II.16)$$

$$k_{1z} = -\left(Q + \frac{1}{2}mv^2\right)/(\hbar v), \qquad k_{2z} = -\left(Q - \frac{1}{2}mv^2\right)/(\hbar v), \qquad (II.17)$$

and

$$Q = \varepsilon_1 - \varepsilon_2 \qquad (II.18)$$

is the reaction Q-value. We assume that Σ is outside the range of the potentials V_1 and V_2 during the whole collision. Then $\Phi_1(\mathrm{r})$ and $\Phi_2(\mathrm{r})$ can be replaced by their asymptotic

expressions which are related to Hankel functions (see Appendix II.A for their precise definition)

$$\Phi_\alpha(\mathbf{r}) = C_{\ell_\alpha}\gamma_\alpha\chi_{\ell_\alpha}(\gamma_\alpha r)Y_{\ell_\alpha\lambda_\alpha}(\theta,\varphi), \qquad \alpha = 1,2,$$
$$\chi_l(\gamma r) = -i^l h_l^{(1)}(i\gamma r). \tag{II.19}$$

With this choice

$$\chi_l(\gamma r)\sim e^{-\gamma r}/(\gamma r)$$
$$\Phi_\alpha(\mathbf{r})\sim C_{\ell_\alpha}\exp(-\gamma_\alpha r)r^{-1}Y_{\ell_\alpha\lambda_\alpha}(\theta,\varphi) \tag{II.20}$$

when r is large. In *eqs.* (*II*.19) and (*II*.20) ℓ_1 and ℓ_2 are the orbital angular momentum quantum numbers of the initial and final bound states Ψ_1 and Ψ_2, λ_1 and λ_2 are their projections along the z axis in fig. II.1, C_{ℓ_1} and C_{ℓ_2} are normalization constants given by the ratio between the solution of the radial Schrödinger equation for the neutron bound in the potential V_1 or V_2 and the function $\gamma_{1,2}\chi_{\ell_{1,2}}(\gamma_{1,2}r_{1,2})$; γ_1 and γ_2 are related to the bound state energies ε_1 and ε_2 by

$$\varepsilon_\alpha = -\hbar^2\gamma_\alpha^2/(2m) \tag{II.21}$$

The Fourier transform (*II*.16) is calculated in Appendix II.A by using *eqs.* (*II*.19) and (*II*.20). As in *eq.* (*II*.15) we have the derivatives of the $\tilde{\Phi}$'s with respect to d_2 it is convenient to rewrite the result of the Fourier transform, *eq.* (*II.A*.26), in a form which shows the dependence on the x-coordinate explicitly. By using the integral representation of the modified Bessel function (Abramowitz and Stegun, 1970, p. 376)

$$K_n(z) = \frac{1}{2}\int_{-\infty}^{\infty}\exp(-z\cosh t + nt)dt \tag{II.22}$$

we have

$$K_\lambda(\eta\rho)e^{i\lambda\varphi} = \frac{1}{2}\int_{-\infty}^{\infty}\exp[-\eta\rho\cosh t + \lambda(t+i\varphi)]dt \tag{II.23}$$

By changing the integration variable from t to $u = t + i\varphi$ the argument of the exponential becomes

$$-\eta\rho\cos\varphi\cosh u + i\eta\rho\sin\varphi\sinh u + \lambda u = -\eta x\cosh u + i\eta y\sinh u + \lambda u,$$

while the branches (1) and (2) of the u-integration-path (see fig. II.3) cancel and we get

$$K_\lambda(\eta\rho)e^{i\lambda\varphi} = \frac{1}{2}\int_{-\infty}^{\infty}\exp(-\eta x\cosh u + i\eta y\sinh u + \lambda u)du. \qquad (II.24)$$

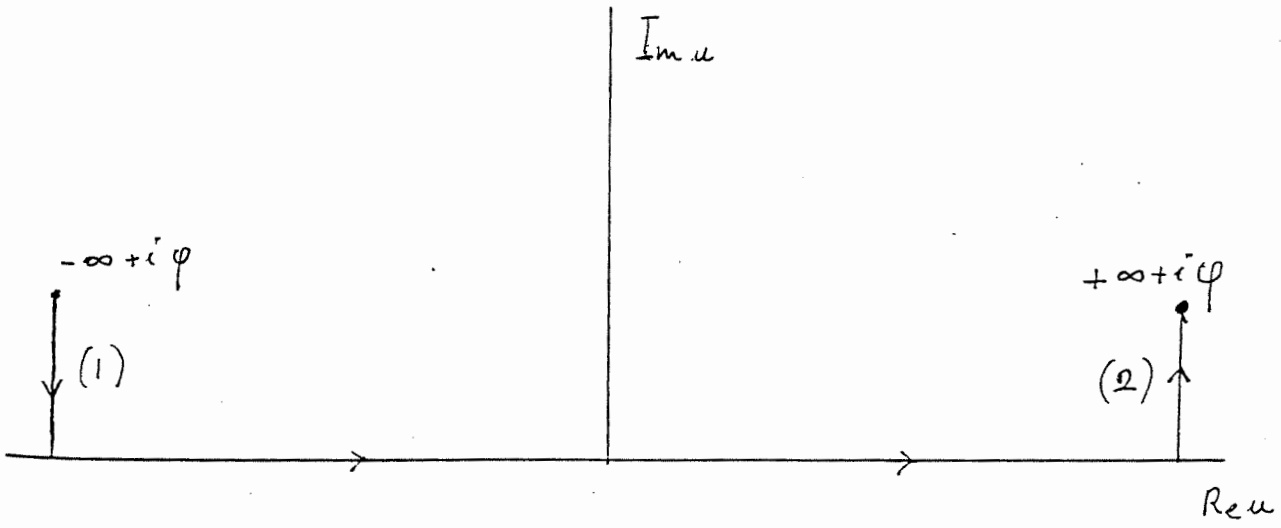

Fig. II.3. Integration path for eq. (II.24).

Then *eq.* (*II.A.*26) gives for the derivatives of the Fourier transforms in *eq.* (*II.*15):

$$\frac{\partial}{\partial d_2}\tilde{\Phi}_{\ell_1\lambda_1}(d_2-d,y,k_{1z}) = C_{\ell_1}Y_{\ell_1\lambda_1}(\beta_1,0)$$

$$\cdot\int_{-\infty}^{\infty}(-\eta\cosh u_1)\exp[\eta(d-d_2)\cosh u_1 + i\eta y\sinh u_1 + \lambda_1 u_1]du_1$$

$$= C_{\ell_1}Y_{\ell_1\lambda_1}(\beta_1,0)(-1)^{\lambda_1}\int_{-\infty}^{\infty}\eta\cosh u'\exp(-\eta d_1\cosh u' - i\eta y\sinh u' + \lambda_1 u')du', \quad (II.25a)$$

where $u' = u_1 + i\pi$ and $d_1 = d - d_2$;

$$\frac{\partial}{\partial d_2}\tilde{\Phi}^*_{\ell_2\lambda_2}(d_2,y,k_{2z}) = C_{\ell_2}Y^*_{\ell_2\lambda_2}(\beta_2,0)$$

$$\cdot\int_{-\infty}^{\infty}(-\eta\cosh u_2)\exp(-\eta d_2\cosh u_2 - i\eta y\sinh u_2 + \lambda_2 u_2)du_2. \quad (II.25b)$$

The complex angles β_1 and β_2 have the same meaning as θ_0 in Appendix A. According to *eq.* (*II.A.*22) they are then defined by

$$\cos\beta_\alpha = -i\,\frac{k_{\alpha z}}{\gamma_\alpha}, \qquad \sin\beta_\alpha = \frac{\eta}{\gamma_\alpha}, \qquad \alpha = 1,2. \quad (II.26)$$

They give the 'direction' of the complex vector $\mathbf{k}_\alpha$ of neutron momenta before and after transfer. This vector has components $\mathbf{k}_\alpha \equiv (i\eta, 0, k_{\alpha z})$, where $k_{\alpha z}$ are defined by *eqs.* (*II.*17), and $\sqrt{k_{\alpha x}^2 + k_{\alpha y}^2 + k_{\alpha z}^2} = i\gamma_\alpha$. It is complex because the neutron is in a bound state (with negative energy). By substituting *eqs.* (*II.*25) into the transfer amplitude (II.15) we find

$$A(2,1) = -\frac{i\hbar}{2mv}C_{\ell_1}C_{\ell_2}(-1)^{\lambda_1}Y_{\ell_1\lambda_1}(\beta_1,0)Y^*_{\ell_2\lambda_2}(\beta_2,0)$$

$$\cdot\int_{-\infty}^{\infty}du'\int_{-\infty}^{\infty}du_2\;\eta(\cosh u' + \cosh u_2)\exp[-\eta(d_1\cosh u' + d_2\cosh u_2) + \lambda_1 u' + \lambda_2 u_2]$$

$$\cdot\int_{-\infty}^{\infty}e^{-i\eta(\sinh u' + \sinh u_2)y}\,dy \quad (II.27)$$

Then *eq.* (*II.A.*26) gives for the derivatives of the Fourier transforms in *eq.* (*II.*15):

$$\frac{\partial}{\partial d_2}\tilde{\Phi}_{\ell_1\lambda_1}(d_2-d,y,k_{1z}) = C_{\ell_1}Y_{\ell_1\lambda_1}(\beta_1,0)$$

$$\cdot\int_{-\infty}^{\infty}(-\eta\cosh u_1)\exp[\eta(d-d_2)\cosh u_1 + i\eta y\sinh u_1 + \lambda_1 u_1]du_1$$

$$= C_{\ell_1}Y_{\ell_1\lambda_1}(\beta_1,0)(-1)^{\lambda_1}\int_{-\infty}^{\infty}\eta\cosh u'\exp(-\eta d_1\cosh u' - i\eta y\sinh u' + \lambda_1 u')du', \quad (II.25a)$$

where $u' = u_1 + i\pi$ and $d_1 = d - d_2$;

$$\frac{\partial}{\partial d_2}\tilde{\Phi}^*_{\ell_2\lambda_2}(d_2,y,k_{2z}) = C_{\ell_2}Y^*_{\ell_2\lambda_2}(\beta_2,0)$$

$$\cdot\int_{-\infty}^{\infty}(-\eta\cosh u_2)\exp(-\eta d_2\cosh u_2 - i\eta y\sinh u_2 + \lambda_2 u_2)du_2. \quad (II.25b)$$

The complex angles β_1 and β_2 have the same meaning as θ_0 in Appendix A. According to *eq.* (*II.A.*22) they are then defined by

$$\cos\beta_\alpha = -i\,\frac{k_{\alpha z}}{\gamma_\alpha}, \qquad \sin\beta_\alpha = \frac{\eta}{\gamma_\alpha}, \qquad \alpha = 1,2. \quad (II.26)$$

They give the 'direction' of the complex vector $\mathbf{k}_\alpha$ of neutron momenta before and after transfer. This vector has components $\mathbf{k}_\alpha \equiv (i\eta, 0, k_{\alpha z})$, where $k_{\alpha z}$ are defined by *eqs.* (*II.*17), and $\sqrt{k_{\alpha x}^2 + k_{\alpha y}^2 + k_{\alpha z}^2} = i\gamma_\alpha$. It is complex because the neutron is in a bound state (with negative energy). By substituting *eqs.* (*II.*25) into the transfer amplitude (II.15) we find

$$A(2,1) = -\frac{i\hbar}{2mv}C_{\ell_1}C_{\ell_2}(-1)^{\lambda_1}Y_{\ell_1\lambda_1}(\beta_1,0)Y^*_{\ell_2\lambda_2}(\beta_2,0)$$

$$\cdot\int_{-\infty}^{\infty}du'\int_{-\infty}^{\infty}du_2\;\eta(\cosh u' + \cosh u_2)\exp[-\eta(d_1\cosh u' + d_2\cosh u_2) + \lambda_1 u' + \lambda_2 u_2]$$

$$\cdot\int_{-\infty}^{\infty}e^{-i\eta(\sinh u' + \sinh u_2)y}\,dy \quad (II.27)$$

The integral over y gives a δ-function:

$$2\pi\delta(\eta(\sinh u' + \sinh u_2)) = \frac{2\pi}{\eta \cosh u'}\delta(u' + u_2)$$

and the integrals over u' and u_2 in *eq.* $(II.27)$ reduce to

$$4\pi \int_{-\infty}^{\infty} \exp[-\eta d \cosh u + (\lambda_1 - \lambda_2)u]\, du = 8\pi K_{\lambda_1 - \lambda_2}(\eta d),$$

where we used the integral representation $(II.22)$ again and put $d = d_1 + d_2$. Substitution into *eq.* $(II.27)$ gives the final expression for the transfer amplitude

$$A(2,1) = -4\pi i \frac{\hbar}{mv} C_{\ell_1} C_{\ell_2} (-1)^{\lambda_1} Y_{\ell_1 \lambda_1}(\beta_1, 0) Y^*_{\ell_2 \lambda_2}(\beta_2, 0) K_{\lambda_1 - \lambda_2}(\eta d). \qquad (II.28)$$

When the product $\eta d \gg 1$ the modified Bessel function K can be substituted by the asymptotic expression (II.A.13). By introducing the unit vectors

$$\hat{k}_\alpha = \frac{\mathbf{k}_\alpha}{|\mathbf{k}_\alpha|} = \frac{1}{\sqrt{\eta^2 + k_{\alpha z}^2}}(i\eta, 0, k_{\alpha z}),$$

eq. (II.28) can be written as

$$A(2,1) \approx -4\pi i \frac{\hbar}{mv} C_{\ell_1} C_{\ell_2} (-1)^{\lambda_1} Y_{\ell_1 \lambda_1}(\hat{k}_1) Y^*_{\ell_2 \lambda_2}(\hat{k}_2) \sqrt{\frac{\pi}{2\eta d}}\, e^{-\eta d}. \qquad (II.29)$$

Eq. (II.29) exhibits two important features of the semiclassical transfer amplitude.

i) It decays exponentially with the distance of closest approach d, the decay constant being given by the quantity η. For a given d (for instance the 'grazing' distance) the amplitude has a maximum when η has a minimum. From eqs. (II.A.9), (II.17) and (II.21) we have

$$\eta^2 = k_{1z}^2 + \gamma_{1z}^2 = k_{2z}^2 + \gamma_{2z}^2 = -\frac{2m}{\hbar^2}\bar{\varepsilon}, \qquad (II.30)$$

where

$$\bar{\varepsilon} = \frac{1}{2}(\varepsilon_1 + \varepsilon_2) - \frac{1}{4}\left(\frac{Q^2}{\frac{1}{2}mv^2} + \frac{1}{2}mv^2\right) \qquad (II.31)$$

is a kind of average bound-state energy. Then maximum transfer is obtained when the tangential velocity v satisfies the condition:

$$\frac{1}{2}mv^2 = |Q| \qquad (II.32)$$

that is the kinetic energy of the transferred particle compensates for the reaction Q-value. This is essentially the same formula given by Siemens et al. (1971).

ii) The semiclassical transfer amplitude transforms under rotations as the product

$$Y_{\ell_1\lambda_1}(\hat{k}_1)Y^*_{\ell_2\lambda_2}(\hat{k}_2).$$

Thus one can use the addition theorem for spherical harmonics (of complex angles) to calculate an explicit expression for the transfer probability by summing over the final magnetic substates and averaging over the initial ones

$$P_{tr}(\ell_2, \ell_1) = \frac{1}{2\ell_1 + 1}\sum_{\lambda_1\lambda_2} |A(\ell_2\lambda_2, \ell_1\lambda_1)|^2. \qquad (II.33)$$

Eq. (II.33) gives the probability for transfer between single-particle states specified by their orbital angular momentum ℓ_α and energy ε_α ($\alpha = 1, 2$). However, one is usually interested in the single particle angular momentum $\mathbf{j} = \boldsymbol{\ell} + \mathbf{s}$, where $\mathbf{s}$ is the spin of the transferred particle. Therefore the transfer amplitude $A(\ell_2\lambda_2, \ell_1\lambda_1)$ needs to be re-coupled to j. This is discussed in chapter VII.

It is worth noting that the amplitude ($II.28$) contains recoil effects. This can be seen by comparing it with the factorized DWBA amplitude of Dodd and Greider (1969) [cf. Anyas-Weiss et al. 1974], where a recoil term of the form $\exp(im\mathbf{v}\cdot\mathbf{r})$ appears in the form factor. The channel coordinates $\mathbf{r}_i$ and $\mathbf{r}_f$ are related to the separation $\mathbf{s}$ between the two cores and the coordinate $\mathbf{r}_2$ of the transferred particle x with respect to the core c_2 by (see fig. II.4)

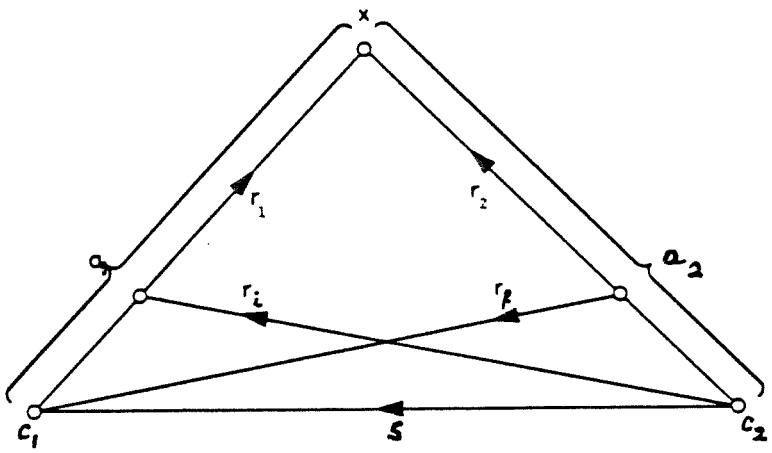

Fig. II.4. Coordinates to illustrate recoil in the reaction $a_1(=c_1+x)+c_2\rightarrow c_1+a_2(=c_2+x)$.

$$\mathbf{r}_i=\frac{c_1}{c_1+x}\mathbf{s}+\frac{x}{c_1+x}\mathbf{r}_2,$$

$$\mathbf{r}_f=\mathbf{s}-\frac{x}{c_2+x}\mathbf{r}_2.$$

The term in $\mathbf{r}_2$ is due to the centre of mass of the composite system being shifted (by "recoil") from the centre of mass of the core.

In our semiclassical approach the exponential $\exp(im\mathbf{v}\cdot\mathbf{r})$ arises from the Galilean transformation ($II.12$). In this form it may contain the masses of the cores c_1 and c_2 if $\mathbf{v}$ is an average velocity. Even in the case when $\mathbf{v}$ is simply the relative velocity at closest

approach (in the initial or final channel) we still have "recoil" effects due to the finite transferred mass m.

One implication of recoil is its effect on angular momentum and parity transfer. In the no-recoil approximation to DWBA the form factor can be expanded in multipoles proportional to $Y_{\ell m}(\hat{r})$, where ℓ is the transferred angular momentum (defined in §VII.1). Then the allowed ℓ-transfers are limited by the "normal parity" rule

$$\pi = (-)^{\ell_1+\ell_2} = (-)^{\ell}.$$

This is no longer true if the recoil phase $\exp(im\mathbf{v}\cdot\mathbf{r})$ is included. In fact the expansion of this phase into partial waves introduces terms with additional angular momentum, so that ℓ is no longer restricted to normal parity values but obeys the more general selection rules of §VII.1.

The same conclusions on angular momentum transfer can be reached from our final expression $(II.29)$. If $\hat{k}_1 = \hat{k}_2$ the multipole expansion of $A(\ell_2\lambda_2, \ell_1\lambda_1)$ will contain only ℓ-terms with normal parity $(-)^{\ell} = (-)^{\ell_1+\ell_2}$. From *eqs.* $(II.26)$ and $(II.17)$ we can see that this happens only if the mass of the transferred particle $m = 0$ and $\varepsilon_1 = \varepsilon_2$. In general $\hat{k}_1 \neq \hat{k}_2$ and this introduces non-normal parity transfers.

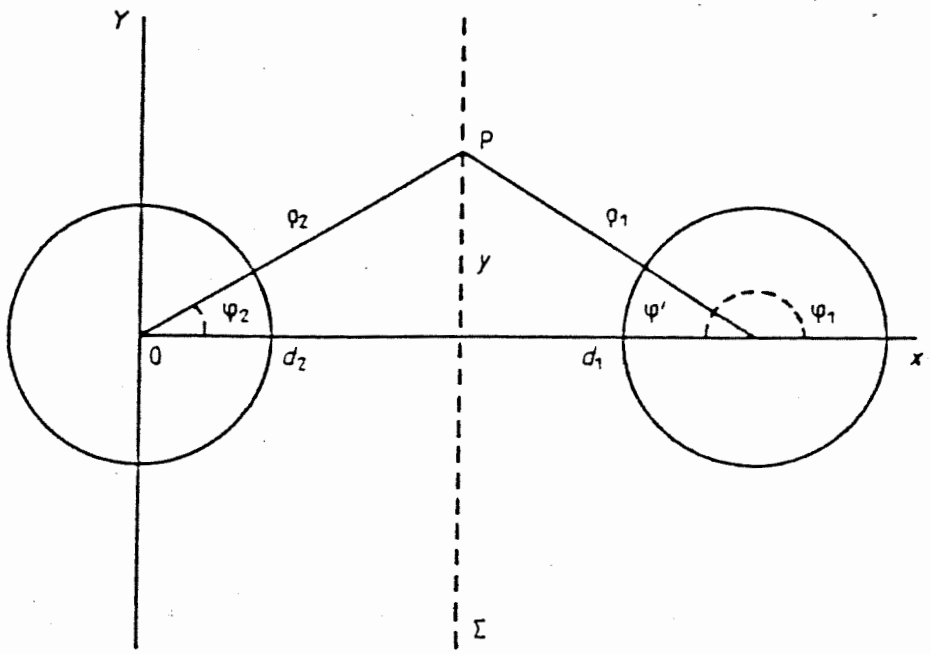

Figure II.2.

Projection of coordinate system for the transfer amplitude onto the $x-y$ plane.

II.3 Physical Interpretation of the Amplitude.

The transfer amplitude formula ($II.28$) gives the population of the various magnetic substates and depends only on the existence of the surface Σ between the two nuclei introduced in §II.1 and on their separation d. The arguments presented in this section are based on a particular location of Σ given by d_2 and $d_1 = d - d_2$ (fig.II.1), and they lead to an approximate factorization of the transfer amplitude and to a matching condition. The physical interpretation obtained in this way is not completely satisfactory because the location of Σ is not defined exactly. This may not be too serious because the qualitative features of the matching condition are not very sensitive to the precise division of d into

d_1 and d_2. The ratio d_1/d_2 must be near the ratio of the nuclear radii and a typical choice would be $d_1/d_2 = A_1^{1/3}/A_2^{1/3}$, where A_1 and A_2 are the mass numbers of the two nuclei. First we write the transfer amplitude $(II.28)$ in a different form:

$$A(\ell_2\lambda_2, \ell_1\lambda_1) = -i\pi(\hbar/mv)F(\lambda_1, \lambda_2, \eta d)\tilde{\Phi}^*_{\ell_2\lambda_2}(d_2, 0, k_{2z})(-1)^{\lambda_1}\tilde{\Phi}_{\ell_1\lambda_1}(d_1, 0, k_{1z}). \tag{II.34}$$

Here $\tilde{\Phi}$ is the result of the Fourier transform in eq. (II.A.26):

$$\tilde{\Phi}_{l\lambda}(x, y, k_z) = 2C_l Y_{l\lambda}(\beta, \varphi)K_\lambda[\eta(x^2 + y^2)^{1/2}], \tag{II.35}$$

where β, φ and η are given by *eqs.* $(II.26)$, $(II.A.3)$ and $(II.A.9)$ in terms of the arguments of $\tilde{\Phi}$ and the binding energy parameter γ of eq. (II.21). If the neutron wavefunction is $\Phi(x, y, z)$ in the initial or final state then $|\tilde{\Phi}(x, y, k_z)|^2$ is the probability density for finding the neutron with position (x, y) in the plane perpendicular to that of the relative motion of the two nuclei and momentum $\hbar k_z$ parallel to the relative velocity v (fig. II.1). Thus $\tilde{\Phi}^*_{\ell_2\lambda_2}(d_2, 0, k_{2z})$ is the amplitude for the neutron in the final state Ψ_2 to be on the surface Σ with $y = 0$ and z component of the momentum $\hbar k_{2z}$ relative to the final nucleus. The quantity $(-1)^{\lambda_1}\tilde{\Phi}_{\ell_1\lambda_1}(d_1, 0, k_{1z})$ is a similar amplitude for the initial state. The factor $(-1)^{\lambda_1}$ occurs because $\varphi_1 = \pi$ at the point of transfer in the initial state (see fig. II.2). The quantity F in eq. (II.34) is defined as

$$F(\lambda_1, \lambda_2, \eta d) = \frac{K_{\lambda_1 - \lambda_2}(\eta d)}{K_{\lambda_1}(\eta d_1)K_{\lambda_2}(\eta d_2)}. \tag{II.36}$$

Later in this section we show that F expresses a λ-matching condition.

One feature of formulæ $(II.28)$ or $(II.34)$ for the transfer amplitude is that the z components of the neutron momentum, $\hbar k_{1z}$ relative to the initial nucleus and $\hbar k_{2z}$ relative

to the final nucleus, are fixed by the kinematical matching conditions (II.17). This result comes out automatically in the quantal calculation of § II.2, but it is expected from the following classical argument. Suppose that at the point of transfer on Σ (see fig. II.1) the neutron has z-components of the velocity v_{1z} relative to the initial nucleus and v_{2z} relative to the final nucleus. If the transition from one nucleus to the other is smooth then v_{1z} should add to the relative velocity v of the two nuclei at the point of closest approach to give the final velocity :

$$v_{1z} + v = v_{2z}. \qquad (II.37)$$

If the velocity component of the neutron in the (x, y) plane is $v_\perp$ at the point of transfer on Σ and if the potentials $V_1 = V_2 = 0$ on Σ then the initial and final energies of the neutron are related to the velocities by

$$\varepsilon_1 = \frac{1}{2}m(v_{1z}^2 + v_\perp^2) \qquad \varepsilon_2 = \frac{1}{2}m(v_{2z}^2 + v_\perp^2) \qquad (II.38)$$

Subtracting gives

$$Q \equiv \varepsilon_1 - \varepsilon_2 = \frac{1}{2}m(v_{1z}^2 - v_{2z}^2). \qquad (II.39)$$

Now we solve eqs. (II.37) and (II.39) to obtain

$$v_{1z} = -(Q + \frac{1}{2}mv^2)/(mv), \qquad v_{2z} = -(Q - \frac{1}{2}mv^2)/(mv) \qquad (II.40)$$

These relations are equivalent to eq. (II.17) because $k_{1z} = \frac{mv_{1z}}{\hbar}$ and $k_{2z} = \frac{mv_{2z}}{\hbar}$. The perpendicular component of momentum is

$$p_\perp = mv_\perp = i\hbar\eta \qquad (II.41)$$

and is purely imaginary. This is because ε_1 and ε_2 are negative for bound states and eq. (II.38) can be satisfied only if $v_\perp$ is imaginary.

Now we discuss the quantity F, which is defined in *eq.* $(II.36)$ and appears in the expression $(II.34)$ for the transfer ampltude. When w is large and positive and n is not too large the Bessel function $K_n(w)$ can be approximated by

$$K_n(w) \approx (\pi/2w)^{1/2} \exp\left(-w + \frac{1}{2}n^2/w\right). \qquad (II.42)$$

This form can be obtained from the integral representation (II.22) by approximating

$$\cosh t \simeq 1 + \frac{1}{2}t^2$$

Using *eq.* $(II.42)$ we obtain

$$F(\lambda_1, \lambda_2, \eta d) \approx \left(\frac{2\eta d_1 d_2}{\pi d}\right)^{1/2} \exp\left[\frac{(\lambda_1 - \lambda_2)^2}{2\eta d} - \frac{\lambda_1^2}{2\eta d_1} - \frac{\lambda_2^2}{2\eta d_2}\right]. \qquad (II.43)$$

The leading terms in the exponent cancel because $d = d_1 + d_2$. If $\hbar k_{1y}$ and $\hbar k_{2y}$ are the y-components of the neutron momentum on Σ just before and just after transfer then

$$\lambda_1 \approx -k_{1y} d_1, \qquad \lambda_2 \approx k_{2y} d_2$$

Substituting these expressions into the exponent of *eq.* $(II.43)$ gives

$$\begin{aligned} F(\lambda_1, \lambda_2, \eta d) &\sim \left(\frac{2\eta d_1 d_2}{\pi d}\right)^{1/2} \exp\left[\frac{-d_1 d_2}{2\eta d}(k_{1y} - k_{2y})^2\right] \\ &\sim \left(\frac{2\eta d_1 d_2}{\pi d}\right)^{1/2} \exp\left[\frac{-d_1 d_2}{2\eta d}\left(\frac{\lambda_1}{d_1} + \frac{\lambda_2}{d_2}\right)^2\right]. \end{aligned} \qquad (II.44)$$

Eq. $(II.44)$ is a λ-matching condition. It implies that F is large only if $k_{1y} \approx k_{2y}$ or $\lambda_1/d_1 \approx -\lambda_2/d_2$.

Eq. $(II.28)$ gives a closed-form expression for the transfer amplitude in the case of neutron transfer when the coordinate system is chosen as in fig. II.1, with the z axis parallel

to the direction of relative motion. It is well known (Brink 1972, 1977, Hasan and Brink 1978, Bond 1980) that when the relative velocity is large, the states populated in neutron transfer are polarized perpendicular to the reaction plane. This has been discussed by using a coordinate system with z axis perpendicular to the reaction plane. However, in this system it is not possible to obtain a closed-form expression like *eq.* $(II.28)$.

II.4 Corrections to the Amplitude.

When there is some overlap between the potentials V_1 and V_2 during the collision there are corrections to the transfer amplitude of § II.1 and II.2. These are of two kinds: first, the integrals containing V_1 and V_2 in *eq.* $(II.8)$ are not zero; second, the Hankel function form $(II.19)$ for the bound-state wavefunctions Φ_α is not exact. The radial wavefunctions are modified because V_1 and V_2 are not zero on the surface Σ. Here we estimate these corrections and show that they are of opposite sign.

To estimate the second correction, we write the exact wavefunctions Ψ_1 and Ψ_2 of the initial and final states as

$$\Psi_\alpha = [1 - b_\alpha(r_\alpha)]\Psi^0_\alpha, \qquad \alpha = 1, 2, \tag{II.45}$$

where Ψ^0_α are the Hankel functions forms in *eq.* $(II.19)$. The quantities $b_\alpha(r_\alpha)$ are positive functions because the effect of V_α is to reduce the radial wavefunctions below their free-particle values. By using *eq.* $(II.8)$ the transfer amplitude can be written as

$$A(2,1) = A^0(2,1) + \Delta A,$$

where A^0 is the amplitude given by *eq.* $(II.28)$. To lowest order in V_1 and V_2 we write the correction as

$$\Delta A = \Delta A_1 + \Delta A_2,$$

with

$$\Delta A_1 = \frac{1}{i\hbar}\int_{-\infty}^{+\infty} dt \left[\int_{R_1} \Psi_2^{0^*} V_2 \Psi_1^0 (1 - b_1 - b_2) d^3\mathbf{r} + \int_{R_2} \Psi_2^{0^*} V_1 \Psi_1^0 (1 - b_1 - b_2) d^3\mathbf{r}\right], \tag{II.46}$$

$$\Delta A_2 = -\frac{\hbar}{2mi}\int_{-\infty}^{+\infty} dt \int_\Sigma d\mathbf{S} \cdot (\Psi_2^{0^*} \nabla \Psi_1^0 - \Psi_1^0 \nabla \Psi_2^{0^*})\ (b_1 + b_2). \tag{II.47}$$

In obtaining these formulæ, we replaced Ψ_1 and Ψ_2 in *eq.* $(II.8)$ by the expressions $(II.45)$ and neglected terms containing the products $b_1 b_2$ and the derivatives of b_1 and b_2. In the expression for ΔA_2, Ψ_2^0 decays exponentially in the positive x-direction (see fig. II.1) while Ψ_1^0 decays exponentially in the opposite direction. To estimate ΔA_2, we replace the component of the gradient operator acting on Ψ_1^0 in the direction $d\mathbf{S}$ by $-\eta$ and the component of the same operator acting on Ψ_2^0 by η. We do this because according to *eq.* $(II.41)$ $i\hbar\eta$ is the component of the momentum of the transferred neutron in a plane perpendicular to the reaction plane and the biggest contribution to the integral $(II.47)$ comes from the region of the Σ plane near the point of closest approach, $y = 0$ in fig. II.2. With these replacements ΔA_2 simplifies to

$$\Delta A_2 = \frac{\hbar\eta}{im}\int_{-\infty}^{+\infty} dt \int_\Sigma \Psi_2^{0^*} \Psi_1^0 (b_1 + b_2)\ dS. \tag{II.48}$$

The factor that multiplies $\frac{1}{i\hbar}\Psi_2^{0^*}\Psi_1^0$ in *eq.* $(II.46)$, $V_\alpha(1 - b_1 - b_2)$, is negative because such are the binding potentials V_α $(\alpha = 1, 2)$, while the corresponding factor in *eq.* $(II.48)$, $\frac{\hbar^2\eta}{m}(b_1 + b_2)$, is positive. Thus it is clear that ΔA_1 and ΔA_2 have opposite signs. A simple

estimate of b_1 and b_2 gives

$$b_\alpha(r_\alpha) \simeq -\frac{m}{\hbar^2\gamma_\alpha}\int_{r_\alpha}^{\infty} V_\alpha(r)\ dr. \qquad (II.49a)$$

If we substitute this into *eq.* $(II.48)$ we see that ΔA_1 and ΔA_2 have comparable magnitudes, so that the correction ΔA is smaller than the individual parts ΔA_1 and ΔA_2. A condition for ΔA_2 and hence ΔA to be small is that both b_1 and b_2 are small compared to unity. By using the exponential approximation for the potential $V_\alpha(r) = V_\alpha(r_\alpha)e^{-\frac{r-R}{a}}$ we have

$$b_\alpha(r_\alpha) \simeq -\frac{ma}{\hbar^2\gamma_\alpha}V_\alpha(r_\alpha) = \frac{V_\alpha(r_\alpha)}{\varepsilon_\alpha}\ \frac{a\gamma_\alpha}{2} \ll 1. \qquad (II.49b)$$

II.5 An alternative way of calculating the amplitude.

Here we give a different derivation of *eq.* $(II.28)$, which makes use of a two-dimensional Fourier transform, *eq.*$(II.50)$ below. This formulation, used by Bonaccorso, Piccolo and Brink (1985), allows a better understanding of the physical meaning of the semiclassical transfer amplitude and is more easily extended to proton-transfer. We introduce

$$\tilde{\tilde{\Phi}}(x,k_y,k_z) \stackrel{\text{def}}{=} \int_{-\infty}^{+\infty} e^{-ik_y y}\ \tilde{\Phi}(x,y,k_z)dy$$

$$= \int_{-\infty}^{+\infty} dy \int_{-\infty}^{+\infty} dz\ e^{-i(k_y y + k_z z)}\ \Phi(x,y,z), \qquad (II.50)$$

where $\tilde{\Phi}(x,y,k_z)$ is defined by *eq.* $(II.16)$. Then

$$\tilde{\Phi}(x,y,k_z) = \frac{1}{2\pi}\int_{-\infty}^{+\infty} \tilde{\tilde{\Phi}}(x,k_y,k_z)\ e^{ik_y y}\ dk_y. \qquad (II.51)$$

If *eq.* $(II.51)$ is substituted into *eq.* $(II.15)$ the integral over y gives a δ-function

$$2\pi\delta(k_{2y} - k_{1y})$$

which shows that the momentum component of the neutron perpendicular to the reaction plane is not changed by the transition from the initial to the final nucleus. This is the same condition given by the approximate form $(II.44)$. Then *eq.* $(II.15)$ reduces to

$$A(2,1) = -\frac{i\hbar}{4\pi mv}\int_{-\infty}^{+\infty}[\tilde{\tilde{\Phi}}_2^*(d_2,k_y,k_{2z})\frac{\partial}{\partial d_2}\tilde{\tilde{\Phi}}_1(d_2-d,k_y,k_{1z})$$
$$-\tilde{\tilde{\Phi}}_1(d_2-d,k_y,k_{1z})\frac{\partial}{\partial d_2}\tilde{\tilde{\Phi}}_2^*(d_2,k_y,k_{2z})]dk_y \qquad (II.52)$$

From *eqs.* $(II.50)$ and $(II.11)$ we obtain

$$\frac{\partial^2}{\partial x^2}\tilde{\tilde{\Phi}}(x,k_y,k_z) = \int_{-\infty}^{+\infty}dy\int_{-\infty}^{+\infty}dz\; e^{-i(k_y y+k_z z)}\left(\nabla^2-\frac{\partial^2}{\partial y^2}-\frac{\partial^2}{\partial z^2}\right)\Phi(x,y,z)$$
$$=\frac{2m}{\hbar^2}\int_{-\infty}^{+\infty}\int_{-\infty}^{+\infty}e^{-i(k_y y+k_z z)}V(x,y,z)\Phi(x,y,z)dydz+(\gamma^2+k_y^2+k_z^2)\tilde{\tilde{\Phi}}(x,k_y,k_z), \quad (II.53)$$

where we dropped the subscript $\alpha = 1,2$ for simplicity. In *eq.* $(II.52)$ the two-dimensional Fourier transforms $\tilde{\tilde{\Phi}}_{1,2}$ are required for a coordinate $x = d_2$ or $x = d_2 - d$ on the surface Σ where the potentials vanish. For these values of x *eq.* $(II.53)$ gives

$$\left(\frac{\partial^2}{\partial x^2}-\xi^2\right)\tilde{\tilde{\Phi}}(x,k_y,k_z) = 0, \qquad (II.54)$$

where

$$\xi = \sqrt{\gamma^2+k_y^2+k_z^2} = \sqrt{\eta^2+k_y^2}. \qquad (II.55)$$

Eq. $(II.54)$ can be solved to give

$$\tilde{\tilde{\Phi}}(x,k_y,k_z) = B(k_y,k_z)e^{-\xi|x|} \qquad (II.56)$$

So the x-dependence of $\tilde{\tilde{\Phi}}$ is a simple exponential, while the quantity B has to be determined. By substituting *eq.* $(II.56)$ into $(II.52)$ we find

$$A(2,1) = -\frac{i\hbar}{2\pi mv}\int_{-\infty}^{+\infty}\xi\;\tilde{\tilde{\Phi}}_2^*(d_2,k_y,k_{2z})\tilde{\tilde{\Phi}}_1(d_2-d,k_y,k_{1z})dk_y$$

$$= -\frac{i\hbar}{2\pi mv}\int_{-\infty}^{+\infty} \xi\ e^{-\xi d}\ B_2^*(k_y,k_{2z})B_1(k_y,k_{1z})\ dk_y. \qquad (II.57)$$

Even before calculating explicitly the quantities B and before the final integration on k_y *eq.* $(II.57)$ shows that the semiclassical transfer amplitude decreases exponentially with the distance of closest approach d. The coefficient $B(k_y,k_z)$ is calculated in Appendix II.B. By substituting the result, *eq.* $(II.B.15)$, into the transfer amplitude $(II.57)$ we find

$$A(\ell_2\lambda_2,\ell_1\lambda_1) = -2\pi i\frac{\hbar}{mv}C_{\ell_1}C_{\ell_2}(-1)^{\lambda_1}\int_{-\infty}^{+\infty}\frac{e^{-\xi d}}{\xi}Y^*_{\ell_2\lambda_2}(\hat{k}_2)Y_{\ell_1\lambda_1}(\hat{k}_1)\ dk_y \qquad (II.58a)$$

$$= -2\pi i\frac{\hbar}{mv}C_{\ell_1}C_{\ell_2}(-1)^{\lambda_1}Y_{\ell_1\lambda_1}(\beta_1,0)Y^*_{\ell_2\lambda_2}(\beta_2,0)\int_{-\infty}^{+\infty}e^{i(\lambda_2-\lambda_1)\varphi_{02}}\ \frac{e^{-\xi d}}{\xi}\ dk_y, \qquad (II.58b)$$

where

$$\hat{k}_\alpha = \frac{1}{\sqrt{\xi^2+k_y^2+k_{\alpha z}^2}}(i\xi,k_y,k_{\alpha z}), \qquad (\alpha=1,2). \qquad (II.59)$$

The vectors $\hat{k}_\alpha$ in § II.2 are a particular case for $k_y = 0$. This is because in that coordinate representation the reaction plane $(x-z)$ is a symmetry plane. In *eqs.* $(II.58a)$ to $(II.58b)$ we used *eqs.* $(II.B.9)$ and $(II.B.10)$ which show that $\theta_0 \equiv \beta$ does not depend on k_y and $\cos\varphi_{01} = -\frac{\xi}{\eta} = -\cos\varphi_{02}$ while $\sin\varphi_{01} = \sin\varphi_{02}$ and then $\varphi_{01} = \pi - \varphi_{02}$. By expressing ξ and φ_{02} from *eqs.* $(II.56)$ and $(II.B.10)$ in terms of η and k_y the integral in *eq.* $(II.58b)$ can be written as

$$\int_{-\infty}^{+\infty}\frac{\exp[-\eta d\sqrt{1+(k_y/\eta)^2}]}{\eta\sqrt{1+(k_y/\eta)^2}}\left[\sqrt{1+(k_y/\eta)^2}+\frac{k_y}{\eta}\right]^{\lambda_2-\lambda_1}\ dk_y$$

$$= \int_{-\infty}^{+\infty} e^{-\eta d\cosh u+(\lambda_2-\lambda_1)u}\ du = 2K_{\lambda_2-\lambda_1}(\eta d), \qquad (II.60)$$

where we changed the integration variable from k_y to u, defined by $k_y = \eta\sinh u$, and used the integral representation $(II.22)$. Then *eq.* $(II.58)$ gives

$$A(2,1) = -4\pi i\ \frac{\hbar}{mv}\ C_{\ell_1}C_{\ell_2}\ (-1)^{\lambda_1}\ Y_{\ell_1\lambda_1}(\beta_1,0)\ Y^*_{\ell_2\lambda_2}(\beta_2,0)\ K_{\lambda_2-\lambda_1}(\eta d), \qquad (II.61)$$

which is the same as *eq.* $(II.28)$ because $K_\nu(z) = K_{-\nu}(z)$.

Now we consider the physical interpretation of the double Fourier transform

$$\tilde{\tilde{\Phi}}_{\ell\lambda}(x, k_y, k_z) = 2\pi i \; C_\ell \; Y_{\ell\lambda}(\hat{k}) \; \frac{e^{-\xi|x|}}{\xi}, \qquad (II.62)$$

The quantity $|\tilde{\tilde{\Phi}}(x, k_y, k_z)|^2$ gives the probability density that the particle be found at a distance x between the two nuclei with z-component of its momentum (along the axis of relative motion of the two nuclei - cf. Fig. II.1) given by the kinematical conditions $(II.17)$. *Eq.* $(II.57)$ gives the transfer amplitude essentially as the overlap of two factors: the amplitude $\tilde{\tilde{\Phi}}_1(d_2 - d, k_y, k_{1z})$ that the particle be on the surface Σ before transfer with momentum

$$k_{1z} = -\left(Q + \frac{1}{2}mv^2\right)/(\hbar v)$$

times the amplitude $\tilde{\tilde{\Phi}}_2^*(d_2, k_y, k_{2z})$, where the momentum has changed to

$$k_{2z} = -\left(Q - \frac{1}{2}mv^2\right)/(\hbar v).$$

That is when the neutron jumps from one nucleus to the other it compensates for the relative motion by "running" in opposite directions before and after the jump (cf. Von Oertzen 1985).

Moreover, the form $(II.58a)$ of the semiclassical amplitude can be used in alternative to the approximation $(II.29)$ to calculate the transfer probability, *eq.* $(II.33)$, between single particle states of specified orbital angular momenta ℓ_1 and ℓ_2. By making use of the addition theorem for spherical harmonics (of complex angles) we find

$$P_{tr}(\ell_2, \ell_1) = \left(\frac{\hbar C_{\ell_1} C_{\ell_2}}{2mv}\right)^2 (2\ell_2 + 1) \int_{-\infty}^{+\infty} \int_{-\infty}^{+\infty} \frac{e^{-(\xi+\xi')d}}{\xi\xi'} \; P_{\ell_1}(\hat{k}_1^* \cdot \hat{k}_1') P_{\ell_2}(\hat{k}_2^* \cdot \hat{k}_2') dk_y dk_y', \qquad (II.63)$$

where P_ℓ is a Legendre polynomial. One can evaluate numerically the double integral in *eq.* $(II.63)$ but it is interesting to make a further approximation and single out the dependence of the transfer probability on the product ηd. In *eq.* $(II.63)$ the main contribution comes from $k_y \approx 0 \approx k'_y$. Then, from *eq.* $(II.55)$,

$$\xi \simeq \eta + \frac{k_y^2}{2\eta}$$

and we also assume

$$\xi\xi' \simeq \eta^2 + \frac{k_y^2}{2} + \frac{k_y'^2}{2} + \left(\frac{k_y k'_y}{2\eta}\right)^2 \simeq \eta^2.$$

With these approximations Stancu and Brink (1985) obtain

$$P_{tr}(\ell_2, \ell_1) = \frac{\pi}{2}\left(\frac{\hbar C_{\ell_1} C_{\ell_2}}{mv}\right)^2 (2\ell_2 + 1)\frac{e^{-2\eta d}}{\eta d}\, M_{\ell_1 \ell_2}, \qquad (II.64)$$

where the quantity $M_{\ell_1 \ell_2}$ contains only a one-dimensional integral to evaluate numerically. From numerical comparison with *eq.* $(II.63)$ they find this result accurate within 1%. *Eq.* $(II.64)$ shows explicitly the exponential decrease of P_{tr}. This expression has been used by the same authors to calculate the imaginary part, W_{trans}, of the optical potential due to transfer between heavy ions. The latter is related to the transfer probability from all levels in nucleus 1 to all levels in nucleus 2 by

$$\frac{2}{\hbar}\int_{-\infty}^{+\infty} W_{trans}[\mathbf{R}(t)]dt = P_{21} + P_{12}, \qquad (II.65)$$

where $\mathbf{R}(t)$ is the classical trajectory. The expression $(II.64)$ suggests for the potential at the strong absorption radius d

$$W_{trans}(d) = W_0 e^{-2\eta d}. \qquad (II.66)$$

As we saw in *eqs.* $(II.30)$ and $(II.31)$, the quantity η depends on the energies of the single particle levels taking part in the transition. Therefore the absorptive potential is obtained by summing *eq.* $(II.66)$ over all possible transfers from nucleus 1 to 2 and viceversa. In this way one studies the effect of the shell structure on the depopulation of the elastic channel. Stancu and Brink (1985) find that sometimes very few (or one) transitions contribute to W_{trans} while in general at higher incident energy more transitions are important. This can be explained in terms of the damping parameter η. *Eq.* $(II.64)$ shows that the maximum transfer probabilty occurs when η is minimum, which happens when the incident energy per nucleon $E_d \equiv 1/2\ mv^2$ at the distance of closest approach d satisfies the condition $(II.32)$. If one assumes d as the radius of the Coulomb barrier V_{CB}, the energy E_d is given by (cf. chapter VII)

$$E_d = \frac{A_1 + A_2}{A_1 A_2}\ (E_{c.m.} - V_{CB}) = E_n - \frac{A_1 + A_2}{A_1 A_2} V_{CB}, \qquad (II.67)$$

where $E_n = E_{lab}/A_1$ is the incident energy per nucleon and A_2 is the target mass number.

For $E_d = |Q|$ the quantity η takes the value

$$\eta_{min} = \begin{cases} \frac{1}{\hbar}\sqrt{-2m\varepsilon_1} = \gamma_1, & \text{if } Q < 0; \\ \frac{1}{\hbar}\sqrt{-2m\varepsilon_2} = \gamma_2, & \text{if } Q > 0. \end{cases} \qquad (II.68)$$

When $E_d < |Q|$ the quantity η decreases with increasing incident energy. Then one expects the contribution of the transition $\varepsilon_1 \rightarrow \varepsilon_2$ $(Q = \varepsilon_1 - \varepsilon_2)$ to the absorptive potential $(II.66)$ to become stronger. When $E_d > |Q|$ the quantity η increases with the incident energy and the transfer probability $(II.64)$ decreases.

For a given value of the initial binding energy ε_1 and relative energy E_d, we have maximum transfer when

$$\varepsilon_2 = \varepsilon_1 + E_d \qquad (II.69)$$

and η attains the value $\gamma_1 = \sqrt{-2m\varepsilon_1}/\hbar$. The relation $(II.69)$ means that as the incident energy is increased a transition from a bound state ($\varepsilon_1 < 0$) favours an increasingly 'loose' final state, to the point that when $E_d \gtrsim |\varepsilon_1|$ the energy ε_2 can be positive. This implies that for high incident energies transfer to continuum levels becomes important and should be included in the calculation of the absorptive potential.

For the particular case $\varepsilon_1 = \varepsilon_2 = \varepsilon(< 0)$, e.g. the ground state transition

$$^{12}C(^{13}C, ^{12}C)^{13}C$$

studied by Von Oertzen (1985), we have from *eq.* $(II.30)$

$$\eta(E_d, Q = 0) = \frac{1}{\hbar}\sqrt{m\left(\frac{E_d}{2} - 2\varepsilon\right)}, \qquad (II.70)$$

which is a monotonically increasing function of the incident energy. Then one expects the transfer probability to decrease steadily with increasing energy. The energy dependence of transfer cross sections is discussed in more detail in chapter VII.

Appendix II.A Calculation of a Fourier transform.

Here we calculate the Fourier transform $\tilde{\Phi}$ which appears in *eq.* $(II.15)$ and is defined by *eq.* $(II.16)$:

$$\tilde{\Phi}_{l\lambda}(x,y,k) \stackrel{\text{def}}{=} \int_{-\infty}^{+\infty} e^{-ikz}\Phi_{l\lambda}(x,y,z)dz, \qquad (II.A.1)$$

where we now introduced the orbital angular momentum quantum numbers l, λ of the bound state wavefunction Φ.

The form of $\Phi_{l\lambda}$ gives some immediate constraints for the Fourier transform $\tilde{\Phi}_{l\lambda}$. If the binding potentials V_1 and V_2 have radial symmetry or vanish -as we shall assume later on- the wave function $\Phi_{l\lambda}$ in polar coordinates can be separated into the product of a radial part, f, and a spherical harmonic Y:

$$\Phi_{l\lambda}(r,\theta,\varphi) = f_l(r)Y_{l\lambda}(\theta,\varphi) = f_l(r)Y_{l\lambda}(\theta,0)e^{i\lambda\varphi} = \Phi_{l\lambda}(r,\theta,0)e^{i\lambda\varphi}. \qquad (II.A.2)$$

The spherical polar coordinates (r,θ,φ) are related to the rectangular coordinates (x,y,z) by

$$x = \rho\cos\varphi, \quad y = \rho\sin\varphi, \quad z = r\cos\theta, \qquad (II.A.3)$$

where

$$\rho = \sqrt{x^2+y^2} = r\sin\theta \qquad (II.A.4)$$

defines the relation to the cylindrical polar coordinates (ρ,φ,z). Since φ does not depend on z, substituting *eq.* $(II.A.2)$ into *eq.* $(II.A.1)$ gives for the Fourier transform in cylindrical polar coordinates

$$\tilde{\Phi}_{l\lambda}(\rho,\varphi,k) = \tilde{\Phi}_{l\lambda}(\rho,0,k)e^{i\lambda\varphi}. \qquad (II.A.5)$$

Moreover, the bound state wavefunction $\Phi_{l\lambda} \to 0$ as $\rho \to \infty$. From this follows that

$$\tilde{\Phi}_{l\lambda}(\rho, \varphi, k) \to 0 \quad as \quad \rho \to \infty. \tag{II.A.6}$$

Since in *eq.* (*II*.15) the Fourier transforms $\tilde{\Phi}_1$ and $\tilde{\Phi}_2$ are only required on the surface Σ, which is supposed to be outside the range of the potentials V_1 and V_2 during the whole collision, the function $\Phi_{l\lambda}$ in *eq.* (*II*.*A*.1) is the solution of the free-particle Schrödinger equation

$$-(\hbar^2/2m)\nabla^2\Phi_{l\lambda}(\mathbf{r}) = \varepsilon\Phi_{l\lambda}(\mathbf{r})$$

or

$$\left(\nabla^2 - \gamma^2\right)\Phi_{l\lambda} = 0, \tag{II.A.7}$$

where γ is related to the bound state energy ε by $\varepsilon = -\hbar^2\gamma^2/(2m)$. As a consequence, the function $\tilde{\Phi}_{l\lambda}$ satisfies the two-dimensional equation

$$\left(\frac{\partial^2}{\partial x^2} + \frac{\partial^2}{\partial y^2} - \eta^2\right)\tilde{\Phi}_{l\lambda} = 0, \tag{II.A.8}$$

where

$$\eta = \sqrt{k^2 + \gamma^2}. \tag{II.A.9}$$

The solution of *eq.* (*II*.*A*.8) which tends to zero as $\rho \to \infty$ is given by (Abramowitz and Stegun 1970 p. 374)

$$\tilde{\Phi}_{l\lambda}(\rho, \varphi, k) = D_{l\lambda}(k)K_\lambda(\eta\rho)e^{i\lambda\varphi}, \tag{II.A.10}$$

where the coefficient $D_{l\lambda}(k)$ has to be determined and K_λ is a modified Bessel function.

There are several ways of calculating the coefficient $D_{l\lambda}(k)$ and it is interesting to compare them.

i) *saddle point method.* This is the simplest derivation (Lo Monaco and Brink, 1985). Though based on an approximate formula, *eq.* $(II.A.16)$ below, it gives the same result as the rigorous derivations which follow. The solution of *eq.* $(II.A.7)$ is

$$\Phi_{l\lambda}(r,\theta,\varphi) = C_l \gamma \chi_l(\gamma r) Y_{l\lambda}(\theta,\varphi), \qquad (II.A.11)$$

where

$$\chi_l(\gamma r) = -i^l h_l^{(1)}(i\gamma r). \qquad (II.A.12)$$

The function $h_l^{(1)}$ in *eq.* $(II.A.12)$ is a spherical Bessel function of the third kind (Abramowitz and Stegun 1970 p. 437). To evaluate $D_{l\lambda}$ we calculate the integral $(II.A.1)$ when ρ and r are large. Then $\chi_l(\gamma r)$ and $K_\lambda(\eta\rho)$ can be replaced by their asymptotic forms valid for large arguments (Abramowitz and Stegun 1970 p. 364, 378)

$$\chi_l(\gamma r) \sim \frac{e^{-\gamma r}}{\gamma r}, \qquad K_\lambda(\eta\rho) \sim \sqrt{\frac{\pi}{2\eta\rho}}\, e^{-\eta\rho} \qquad (II.A.13)$$

and *eqs.* $(II.A.11)$, $(II.A.1)$ and $(II.A.10)$ give

$$\tilde{\Phi}_{l\lambda}(\rho,\varphi,k) \sim C_l e^{i\lambda\varphi} \int_{-\infty}^{+\infty} \frac{\exp(-ikz-\gamma r)}{r} Y_{l\lambda}(\theta,0)\,dz \sim D_{l\lambda}(k) \sqrt{\frac{\pi}{2\eta\rho}}\, e^{-\eta\rho} e^{i\lambda\varphi} \qquad (II.A.14)$$

Therefore

$$D_{l\lambda}(k) = C_l \sqrt{\frac{2\eta\rho}{\pi}}\, e^{\eta\rho} \int_{-\infty}^{+\infty} \frac{\exp(-ikz-\gamma r)}{r} Y_{l\lambda}(\theta,0)\,dz \qquad (II.A.15)$$

We calculate the integral in *eq.* $(II.A.15)$ by the saddle-point formula (e.g. Brink 1985, p. 194):

$$\int_{-\infty}^{+\infty} g(z) e^{if(z)}\,dz \sim g(z_0) \left[\frac{2\pi}{|f''(z_0)|}\right]^{1/2} e^{i[f(z_0)-\chi]}, \qquad (II.A.16)$$

where z_0 is the saddle point given by $f'(z_0) = 0$ and the phase $\chi = 1/2[\arg f''(z_0) - \pi/2]$. *Eq.* $(II.A.16)$ can be used when $g(z)$ is slowly varying, that is $g(z)$ should not change much in the range $|z - z_0| \lesssim \Delta z$, where

$$\Delta z = [f''(z_0)]^{-1/2} \qquad (II.A.17)$$

is a measure of the width of the saddle region. To use the formula $(II.A.16)$ in the integral $(II.A.15)$ we put

$$f(z) = -kz + i\gamma r, \qquad g(z) = \frac{Y_{l\lambda}(\theta, 0)}{r} \qquad (II.A.18)$$

The saddle point z_0 is determined by

$$f'(z_0) = -k + i\frac{\gamma z_0}{r_0} = 0, \qquad (II.A.19)$$

where

$$r_0 = \sqrt{\rho^2 + z_0^2}$$

Eq. $(II.A.19)$ can be solved in terms of r_0 to give

$$r_0 = \frac{\gamma\rho}{\eta} \qquad (II.A.20)$$

where η is given by *eq.* $(II.A.9)$. Then follows

$$z_0 = -i\,\frac{kr_o}{\gamma} = -i\,\frac{k\rho}{\eta}, \qquad (II.A.21)$$

The stationary angle θ_0 is given in terms of z_0 and r_0 by the relations $(II.A.3)$ and $(II.A.4)$

$$\cos\theta_0 = \frac{z_0}{r_0} = -i\frac{k}{\gamma}, \qquad \sin\theta_0 = \frac{\rho}{r_0} = \frac{\eta}{\gamma}. \qquad (II.A.22)$$

In order to evaluate (II.A.15) we also need

$$f(z_0) = -kz_0 + i\gamma r_0 = ik^2\frac{\rho}{\eta} + i\gamma^2\frac{\rho}{\eta} = i\eta\rho \qquad (II.A.23)$$

and

$$f''(z_0) = i\frac{\gamma\rho^2}{r_0^3} = i\frac{\eta^3}{\gamma^2\rho} \implies \chi = 0. \qquad (II.A.24)$$

Substituting $(II.A.18)$, $(II.A.22)$, $(II.A.20)$, $(II.A.23)$ and $(II.A.24)$ into $(II.A.16)$ we find

$$\int_{-\infty}^{+\infty} \frac{\exp(-ikz-\gamma r)}{r} Y_{l\lambda}(\theta,0)dz = \frac{Y_{l\lambda}(\theta_0,0)}{r_0}\ \frac{\gamma\sqrt{2\pi\rho}}{\eta^{3/2}}\ e^{-\eta\rho}$$
$$= Y_{l\lambda}(\theta_0,0)\ \sqrt{\frac{2\pi}{\eta\rho}}\ e^{-\eta\rho},$$

so that *eqs.* $(II.A.15)$ and $(II.A.10)$ give

$$D_{l\lambda}(k) = 2\ C_l\ Y_{l\lambda}(\theta_0,0), \qquad (II.A.25)$$

$$\tilde{\Phi}_{l\lambda}(\rho,\varphi,k) = 2\ C_l\ Y_{l\lambda}(\theta_0,0)\ K_\lambda(\eta\rho)\ e^{i\lambda\varphi} = 2\ C_l\ Y_{l\lambda}(\theta_0,\varphi)\ K_\lambda(\eta\rho), \qquad (II.A.26)$$

where (ρ,φ) are related to (x,y) in *eq.* $(II.A.1)$ by $(II.A.3)$ and $(II.A.4)$. We should check the assumption that $g(z)$ defined in *eq.* $(II.A.18)$ does not vary significantly for z within the range Δz of z_0, where Δz is given by *eqs.* $(II.A.17)$ and $(II.A.24)$. The variation of $g(z)$ is

$$\Delta g(z) = \left[\frac{1}{r}\ \frac{dY_{l\lambda}(\theta,0)}{d\theta}\ \frac{d\theta}{dz} - \frac{1}{r^2}\ Y_{l\lambda}(\theta,0)\right]_{z=z_0} \Delta z$$
$$= -\frac{\eta^{1/2}}{\gamma\rho^{3/2}}\ \left\{\frac{\eta}{\gamma}\left[\frac{dY_{l\lambda}(\theta,0)}{d\theta}\right]_{\theta=\theta_0} + Y_{l\lambda}(\theta_0,0)\right\}.$$

Then Δg can be made smaller and smaller by choosing ρ bigger and bigger.

ii) *generating function method.* Consider the expansion (Abramowitz and Stegun 1970, pp. 440 and 437)

$$\frac{e^{-\gamma|\mathbf{r}-\mathbf{a}|}}{\gamma|\mathbf{r}-\mathbf{a}|} = -4\pi\sum_{l=0}^{\infty}\sum_{\lambda=l}^{l} j_l(i\gamma a)\ h_l^{(1)}(i\gamma r)\ Y_{l\lambda}^*(\hat{a})\ Y_{l\lambda}(\hat{r}), \qquad (II.A.27)$$

where $\mathbf{a}$ is a vector with modulus $a < r$ and direction $\hat{a} \equiv (\theta_a, \phi_a)$, j_l is a spherical Bessel function of the first kind and $Y_{l\lambda}$ is a spherical harmonic. By inserting *eqs.* $(II.A.12)$ and $(II.A.11)$ into the definition $(II.A.1)$ we have

$$\tilde{\Phi}_{l\lambda}(x,y,k) = -C_l\ \gamma\ i^l \int_{-\infty}^{+\infty} e^{-ikz}\ h_l^{(1)}(i\gamma r)\ Y_{l\lambda}(\theta,\varphi)\ dz. \qquad (II.A.28)$$

Multiplying *eq.* $(II.A.27)$ by $C_l\gamma e^{-ikz}$ and integrating over z we get

$$C_l \int_{-\infty}^{+\infty} e^{-ikz}\ \frac{e^{-\gamma|\mathbf{r}-\mathbf{a}|}}{|\mathbf{r}-\mathbf{a}|} dz = 4\pi \sum_{l\lambda} j_l(i\gamma a)\ Y_{l\lambda}^*(\hat{a})\ \tilde{\Phi}_{l\lambda}(\theta,\varphi,k)\ i^{-l}. \qquad (II.A.29)$$

Let ρ and $\mathbf{a}_\perp$ be the projections of $\mathbf{r}$ and $\mathbf{a}$ onto the $x-y$ plane. Then

$$|\mathbf{r}-\mathbf{a}| = \sqrt{|\rho - \mathbf{a}_\perp|^2 + (z-a_z)^2},$$

where $a_z = a\cos\theta_a$. By changing the integration variable from z to $z - a_z$ and using the integral representation

$$K_0(c\sqrt{b^2+d^2}) = \frac{1}{2}\int_{-\infty}^{+\infty} e^{-ibx}\ \frac{\exp(-d\sqrt{c^2+x^2})}{\sqrt{c^2+x^2}}\ dx \qquad (II.A.30)$$

for the modified Bessel function of order zero, the *l.h.s.* of *eq.* $(II.A.29)$ can be calculated and we obtain

$$2C_l e^{-ika_z} K_0(\eta|\rho - \mathbf{a}_\perp|) = 4\pi \sum_{l\lambda} j_l(i\gamma a) Y_{l\lambda}^*(\hat{a}) D_{l\lambda}(k) K_\lambda(\eta\rho) e^{i\lambda\varphi} i^{-l}, \qquad (II.A.31)$$

where we introduced *eq.* $(II.A.10)$ in the *r.h.s.*. Now consider an addition theorem for Bessel functions (Abramowitz and Stegun 1970)

$$K_0(w) = \sum_{n=-\infty}^{\infty} K_n(u) I_n(v) e^{in\alpha}, \qquad (II.A.32)$$

where $w = (u^2+v^2-2uv\cos\alpha)^{1/2}$. This relation is valid for any u, v, α, w complex, provided $|ve^{i\alpha}| < u$. Then we have

$$K_0(\eta|\rho - \mathbf{a}_\perp|) = \sum_{n=-\infty}^{\infty} K_n(\eta\rho) I_n(\eta a_\perp) e^{in(\varphi-\phi_a)}.$$

By substituting this result into the *l.h.s.* of *eq.* $(II.A.31)$ and writing the sum in the *r.h.s.* as $\sum_{\lambda=-\infty}^{\infty}\sum_{l=|\lambda|}^{\infty}$ we get for any λ

$$2C_l e^{-ika_z} I_\lambda(\eta a_\perp) = 4\pi \sum_{l=|\lambda|}^{\infty} j_l(i\gamma a)\ Y^*_{l\lambda}(\theta_a, 0)\ D_{l\lambda}(k)\ i^{-l}$$

By summing over λ from $-\infty$ to $+\infty$ and using the expansion (Abramowitz and Stegun 1970)

$$e^z = \sum_{k=-\infty}^{\infty} I_k(z)$$

in the *l.h.s.* we have

$$2C_l \exp(-ika_z + \eta a_\perp) = 4\pi \sum_{l\lambda} j_l(i\gamma a) Y^*_{l\lambda}(\theta_a, 0) D_{l\lambda}(k)(-i)^l. \qquad (II.A.33)$$

The argument of the exponential in *eq.* $(II.A.33)$ can be written as

$$\gamma a(-i\frac{k}{\gamma}\cos\theta_a + \frac{\eta}{\gamma}\sin\theta_a)$$

Consider the expansion of the exponential in terms of spherical Bessel functions (Abramowitz and Stegun 1970)

$$e^{z\cos\theta} = \sum_{n=-\infty}^{\infty} (2n+1) i^n (-)^n j_n(iz) P_n(\cos\theta)$$

valid for any z and θ complex. Then, from *eq.* $(II.A.33)$,

$$2C_l \sum_{n=-\infty}^{\infty} (2n+1) P_n(-i\frac{k}{\gamma}\cos\theta_a + \frac{\eta}{\gamma}\sin\theta_a) = 4\pi \sum_{l\lambda} Y^*_{l\lambda}(\theta_a, 0) D_{l\lambda}(k). \qquad (II.A.34)$$

If we define

$$\cos\beta = -i\frac{k}{\gamma}, \qquad \sin\beta = \frac{\eta}{\gamma}$$

and use the addition theorem (for complex angles)

$$P_n(\cos\beta\cos\theta_a + \sin\beta\sin\theta_a) = \frac{4\pi}{2n+1}\sum_{\lambda=-n}^{n} Y_{n\lambda}(\beta,0)Y^*_{n\lambda}(\theta_a,0)$$

we get

$$2C_l 4\pi \sum_{l\lambda} Y_{l\lambda}(\beta,0)Y^*_{l\lambda}(\theta_a,0) = 4\pi \sum_{l\lambda} Y^*_{l\lambda}(\theta_a,0)D_{l\lambda}(k).$$

from this follows

$$D_{l\lambda}(k) = 2\ C_l\ Y_{l\lambda}(\beta,0). \qquad (II.A.25)$$

The above results can also be obtained with a third method which uses raising and lowering angular momentum operators.

Appendix II.B Calculation of a two-dimensional Fourier transform.

We evaluate the coefficient $B(k_y, k_z)$ in *eqs.* $(II.56)$ and $(II.57)$ in a way very similar to the method i) employed in Appendix II.A. For large values of $|x|$ we substitute *eq.* $(II.20)$ into *eq.* $(II.50)$ and obtain

$$\tilde{\tilde{\Phi}}_{l\lambda}(x, k_y, k_z) \sim C_l \int_{-\infty}^{+\infty} dy \int_{-\infty}^{+\infty} dz \ \exp(-ik_y y - ik_z z - \gamma r) \ \frac{Y_{l\lambda}(\theta, \varphi)}{r} = B(k_y, k_z) e^{-\xi|x|}, \tag{II.B.1}$$

where we used *eq.* $(II.56)$. Now we calculate the integral in *eq.* $(II.B.1)$ by the saddle point formula in two dimensions (e.g. Brink 1985, Appendix B, § 4)

$$\int_{-\infty}^{+\infty} dy \int_{-\infty}^{+\infty} dz \ g(y,z) \ e^{if(y,z)} \sim g(y_0, z_0) \ \frac{2\pi}{|\det \ f_{jk}(y_0, z_0)|^{1/2}} \ e^{i[f(y_0,z_0) - \chi]}, \tag{II.B.2}$$

where j, k stand for y or z, the stationary point (if there is only one) $P_0 \equiv (y_0, z_0)$ is given by the condition that the derivatives

$$f_y(P_0) = f_z(P_0) = 0 \tag{II.B.3}$$

and the phase

$$\chi = (m-1)\frac{\pi}{2}, \tag{II.B.4}$$

where m is the number of negative eigenvalues of the matrix $\{f_{jk}(P_0)\}$. In *eq.* $(II.B.1)$ we put

$$\begin{aligned} f(y,z) &= i\gamma r - (k_y y + k_z z), \\ g(y,z) &= \frac{Y_{l\lambda}(\theta, \varphi)}{r}. \end{aligned} \tag{II.B.5}$$

Then P_0 is determined by

$$f_y(P_0) = i\gamma \frac{y_0}{r_0} - k_y = 0 = f_z(P_0) = i\gamma \frac{z_0}{r_0} - k_z, \tag{II.B.6}$$

where $r_0 = \sqrt{x^2 + y_0^2 + z_0^2}$. *Eqs.* $(II.B.6)$ can be solved to give

$$\begin{aligned} r_0 &= \frac{\gamma|x|}{\xi}, \\ y_0 &= -ik_y \frac{r_0}{\gamma} = -i\frac{|x|k_y}{\xi}, \\ z_0 &= -ik_z \frac{r_0}{\gamma} = -i\frac{|x|k_z}{\xi}, \end{aligned} \qquad (II.B.7)$$

where ξ is defined in *eq.* $(II.55)$. *Eqs.* $(II.B.7)$ show that in our case the stationary point is unique. Therefore

$$g(P_0) = \frac{Y_{l\lambda}(\theta_0, \varphi_0)}{r_0}, \qquad (II.B.8)$$

where

$$\cos\theta_0 = \frac{z_0}{r_0} = -i\frac{k_z}{\gamma}, \quad \sin\theta_0 = \frac{\sqrt{x^2 + y_0^2}}{r_0} = \frac{\sqrt{\gamma^2 + k_z^2}}{\gamma} = \frac{\eta}{\gamma} \qquad (II.B.9)$$

and

$$\cos\varphi_0 = \frac{x}{r_0 \sin\theta_0} = \pm\frac{\xi}{\eta}, \quad \sin\varphi_0 = \frac{y_0}{r_0 \sin\theta_0} = -i\frac{k_y}{\eta}. \qquad (II.B.10)$$

Eq. $(II.B.9)$ gives the same stationary (complex) angle θ_0 as *eq.*$(II.A.22)$. In *eq.* $(II.B.10)$ $\cos\varphi_0$ has the same sign as x. Substituting *eqs.* $(II.B.7)$ into *eq.*$(II.B.5)$ we also get

$$if(P_0) = -\left(\frac{\gamma^2|x|}{\xi} + \frac{k_y^2|x|}{\xi} + \frac{k_z^2|x|}{\xi}\right) = -\xi|x|. \qquad (II.B.11)$$

We also need the second derivatives

$$f_{yy}(P_0) = i\gamma\frac{x^2 + z_0^2}{r_0^3}, \quad f_{yz}(P_0) = -i\gamma\frac{y_0 z_0^2}{r_0^3} = f_{zy}(P_0), \quad f_{zz}(P_0) = i\gamma\frac{x^2 + y_0^2}{r_0^3},$$

so that

$$\det\{f_{jk}(P_0)\} = -\left(\frac{\gamma x}{r_0^2}\right)^2. \qquad (II.B.12)$$

The matrix $\{f_{jk}(P_0)\}$ has no negative eigenvalues. Therefore, from *eq.* $(II.B.4)$,

$$\chi = -\frac{\pi}{2}. \qquad (II.B.13)$$

Collecting the various terms for *eq.* $(II.B.2)$ we find

$$\int_{-\infty}^{+\infty} dy \int_{-\infty}^{+\infty} dz \ \exp(-ik_y y - ik_z z - \gamma r) \ \frac{Y_{l\lambda}(\theta,\varphi)}{r} = 2\pi i Y_{l\lambda}(\theta_0,\varphi_0)\frac{e^{-\xi|x|}}{\xi} \qquad (II.B.14)$$

and then, from $(II.B.1)$,

$$B(k_y,k_z) = 2\pi i \ C_l \ \frac{Y_{l\lambda}(\theta_0,\varphi_0)}{\xi}. \qquad (II.B.15)$$

Chapter III. Angular Distributions.

III.1 Classical cross section and transfer probability.

The simplest way to calculate the transfer cross section is to multiply the elastic cross section by a transfer probability

$$\sigma_{tr}(\theta) = \sigma_{el}(\theta) P_{tr}(\theta). \qquad (III.1)$$

If σ_{el} is the exact elastic cross section *eq.* $(III.1)$ can be taken as a definition of the transfer probability for the scattering angle θ. For instance $\sigma_{el}(\theta)$ could be the measured angular distribution or one calculated with an optical potential which fits the elastic scattering. The transfer probability will be calculated from our semiclassical amplitude along definite trajectories specified by the impact parameter b or the relative angular momentum Λ. Then one has to relate trajectories to scattering angles. In the classical description one solves the equations of motion in a ion-ion potential and determines the deflection function $\theta(b)$ or $\theta(\Lambda)$. Once this is known *eq.* $(III.1)$ reads

$$\sigma_{tr}(\theta) = \sigma_{el}(\theta) P_{tr}[\Lambda(\theta)]. \qquad (III.2)$$

A further approximation is that the elastic cross section is given by the product of the classical cross section

$$\left(\frac{d\sigma}{d\Omega}\right)_{clas} = \frac{b}{\sin\theta}\left|\frac{db}{d\theta}\right| \qquad (III.3)$$

times a reflection coefficient

$$|S_{\Lambda(\theta)}|^2 = \exp(-4Im\delta_L). \qquad (III.4)$$

In these formulæ the classical angular momentum Λ is related to the angular momentum quantum number L of relative motion by

$$\Lambda = \left(L + \frac{1}{2}\right)\hbar.$$

In a rearrangement reaction the deflection function in the final channel is different from that in the initial channel because of the transferred energy, angular momentum and mass. To take this into account one can use the geometric average between the two cross sections,

$$\frac{d\sigma}{d\Omega} = \sqrt{\left(\frac{d\sigma}{d\Omega}\right)_{in.}\left(\frac{d\sigma}{d\Omega}\right)_{fin.}},$$

but for this discussion we limit ourselves to the simpler formula $(VII.2)$. The reflection coefficient $|S|^2$ in *eq.* $(III.4)$ gives the probability that the system escapes absorption into other inelastic channels. It is expressed in terms of the imaginary part of elastic scattering phase shifts $\delta_L = \delta_L^C + \delta_L^N$, where δ_L^C are the Coulomb phase shifts and δ_L^N are the nuclear phase shifts. The latter can be obtained either by numerical solution of the Schrödinger equation with a complex potential $U = U_C + U_N$ or by first order WKB approximation. Considering the whole nuclear potential U_N as a perturbation one obtains for the nuclear part of the phase shifts (e.g. Brink 1978, p. 13)

$$\delta_L^N \approx -\frac{1}{2\hbar}\int_{-\infty}^{\infty} U_N[r_C(\Lambda, t)]\, dt, \qquad (III.5)$$

where the integral is taken along the Coulomb orbit corresponding to classical angular momentum $\Lambda = (L + 1/2)\hbar$. Alternatively, one can parametrize the nuclear part of the radial S-matrix $S_N(L) \equiv \exp(2i\delta_L^N)$ and study, for example, the energy dependence of the cross section without the intermediate step of an optical potential, as it is done in chapter VII.

For large impact parameters one has a Coulomb trajectory and the deflection function is given by

$$L + \frac{1}{2} = n \cot\left(\frac{\theta}{2}\right), \qquad (III.6)$$

where $n = \frac{Z_1 Z_2 e^2}{\hbar v_\infty}$ is the Sommerfeld parameter and v_∞ the asymptotic relative velocity. The classical elastic cross section is given by the Rutherford formula

$$\left(\frac{d\sigma}{d\Omega}\right)_{clas} = \left(\frac{d\sigma}{d\Omega}\right)_R = \frac{1}{4} \frac{a_C^2}{\left(\sin\frac{\theta}{2}\right)^4}, \qquad (III.7)$$

where $a_C = Z_1 Z_2 e^2/(2E_{c.m.})$ is half the distance of closest approach in a Coulomb head-on collision. For smaller impact parameters, where the distance of closest approach is within the range of the ion-ion nuclear potential, the deflection function is bent forward and there is a singularity at $\frac{d\theta}{db} = 0$ (rainbow angle). In general two or more impact parameters $b_i(\theta)$ contribute to the same scattering angle and *eq.* $(III.3)$ should be modified into a sum over $b_i(\theta)$. However, for small impact parameters more nuclear reactions take place and absorb flux from the elastic channel. Absorption is accounted for by the factor $|S|^2$, eq. (III.4). Therefore trajectories with small impact parameters, for which the deflection function differs appreciably from the Rutherford, are strongly absorbed and do not contribute to the quasi-elastic process we are considering here. As a result one can still use the simple forms $(III.3)$ and $(III.7)$. In this case *eq.* $(III.1)$ becomes

$$\sigma_{tr}(\theta) = \sigma_R(\theta)|S_{\Lambda(\theta)}|^2 P_{tr}[\Lambda(\theta)]. \qquad (III.8)$$

The effect of the nuclear potential on the Coulomb trajectory can give a shift in the peak of the angular distribution predicted by *eq.* $(III.8)$. This shift, θ_N, can be calculated as a perturbation to the Rutherford scattering angle θ_R. Let

$$\theta = \theta_R + \theta_N \qquad (III.9)$$

be the total scattering angle. We use the well known relation between the phase shift and the classical deflection function (e.g. Broglia and Winther, 1981, p. 131-132)

$$\theta_N = \hbar 2 \frac{\partial \delta_N}{\partial \Lambda} = \hbar \frac{\partial d}{\partial \Lambda} \frac{\partial 2\delta_N}{\partial d}, \qquad (III.10)$$

where d is the distance of closest approach for a Rutherford trajectory. d is related to the classical angular momentum Λ by

$$kd = n + \sqrt{n^2 + \left(\frac{\Lambda}{\hbar}\right)^2}, \qquad (III.11)$$

where k is the asymptotic wave number of relative motion. Then we have

$$\frac{\partial d}{\partial \Lambda} = \frac{1}{\hbar} \frac{\sqrt{d(d-2a_C)}}{k(d-a_C)}. \qquad (III.12)$$

Here $a_C = n/k$ is half the distance of closest approach in a Coulomb head-on collision. Approximating the ion-ion real potential U_N in *eq.* $(III.5)$ by an exponential (e.g. Brink 1978, p. 11-15 - also cf. chapter VII where the same approximation is used to relate a parametrization of the phase shifts to the imaginary part of the optical potential) we find

$$2\delta_N \simeq \frac{\sqrt{2\pi a d}}{\hbar v_d} U_N(d), \qquad (III.13)$$

where a is the diffuseness of U_N and v_d is the tangential velocity at the distance of closest approach d. v_d is related to the asymptotic velocity v_∞ by

$$v_d = v_\infty \sqrt{\frac{d-2a_C}{d}}. \qquad (III.14)$$

From eq. (III.13) we have

$$\frac{\partial 2\delta_N}{\partial d} = -\frac{\sqrt{2\pi a}}{\hbar v_\infty} \frac{U_N(d)}{\sqrt{d-2a_C}} \left[\frac{1}{2} - \frac{a_C}{d-2a_c} - \frac{d}{a} \frac{1}{\exp\left(\frac{R-d}{a}\right)+1}\right], \qquad (III.15)$$

where R is the radius of U_N and a its diffuseness. Substitution of eqs. (III.15) and (III.12) into (III.10) gives

$$\theta_N = -\frac{\sqrt{\pi a d}}{2}\,\frac{1}{d-a_C}\,\frac{U_N(d)}{E_{c.m.}}\left[\frac{1}{2}-\frac{a_C}{d-2a_c}-\frac{d}{a}\,\frac{1}{\exp\left(\frac{R-d}{a}\right)+1}\right]. \qquad (III.16)$$

This is the correction to be applied to the Coulomb scattering angle θ_R given by eq. (III.6). As an example, for the reaction $^{208}Pb(^{16}O,^{15}O)^{209}Pb_{(g.s.)}$ at $E_{lab} = 139$ MeV, the formula (III.8) gives a maximum cross section at $\theta_R = 49.1°$ and eq. (III.16) produces a correction $\theta_N = -5.1°$, which shifts the peak forward and brings it closer to the experimental result.

The transfer probability on the *r.h.s.* of *eq.* $(III.1)$ or $(III.8)$ depends on the quantum numbers α that specify the initial and final states. In a more general form the classical expression $(III.8)$ is:

$$\left[\frac{d\sigma(\theta)}{d\Omega}\right]_\alpha = \left[\frac{d\sigma(\theta)}{d\Omega}\right]_{cl} |S_{L(\theta)}|^2 P^{tr}_{L(\theta)}(\alpha). \qquad (III.17)$$

The simplest case is transfer between single particle states specified by their orbital angular momenta ℓ_1 and ℓ_2. The expression for the transfer probability is obtained by summing over the final magnetic substates and averaging over the initial ones:

$$P_{tr}(\ell_2,\ell_1) = \frac{1}{2\ell_1+1}\sum_{\lambda_1\lambda_2} |A(\ell_2\lambda_2,\ell_1\lambda_1)|^2, \qquad (III.18)$$

where A is the semiclassical amplitude given by the formula $(II.28)$ for neutron transfer. However, one is usually interested in the single particle angular momentum $\mathbf{j} = \ell + \mathbf{s}$, where $\mathbf{s}$ is the spin of the transferred particle. Therefore the transfer amplitude $A(\ell_2\lambda_2,\ell_1\lambda_1)$ needs to be re-coupled to j. This can be obtained by redefining the transfer probability as

$$P_{tr}(j_2,j_1) = \frac{1}{2j_1+1}\sum_{m_1 m_2} |B(j_2 m_2, j_1 m_1)|^2, \qquad (III.19)$$

where B is related to the semiclassical transfer amplitude A by

$$B(j_2 m_2, j_1 m_1) = \sum_{\lambda_1 \lambda_2 m_s} < j_2 m_2 | \ell_2 \lambda_2 s m_s > A(\ell_2 \lambda_2, \ell_1 \lambda_1) < \ell_1 \lambda_1 s m_s | j_1 m_1 > . \quad (III.20)$$

Here m_s is the z-projection of the spin of the transferred particle which is not changed by the transfer process. If we consider the transfer of a particle x from the single particle state (ℓ_1, j_1) in nucleus $a_1 = c_1 + x$ to the single particle state (ℓ_2, j_2) in $a_2 = c_2 + x$, we have $\alpha = (I_{a_1}, I_{c_2} \rightarrow I_{c_1}, I_{a_2})$, where I_k is the spin of nucleus k, and the transfer probability is given by:

$$\begin{aligned} P_{tr}(I_{a_1}, I_{c_2} \rightarrow I_{c_1}, I_{a_2}) &= \frac{1}{(2I_{a_1}+1)(2I_{c_2}+1)} \sum_{M_{a_1} M_{c_2}} \sum_{M_{c_1} M_{a_2}} |C(M_{c_1} M_{a_2}, M_{a_1} M_{c_2})|^2 \\ &= \frac{2I_{a_2}+1}{(2I_{c_2}+1)(2j_2+1)} P_{tr}(j_2, j_1), \end{aligned} \quad (III.21)$$

where

$$\begin{aligned} C(M_{c_1} M_{a_2}, M_{a_1} M_{c_2}) = \sum_{m_1 m_2} & < I_{a_2} M_{a_2} | I_{c_2} M_{c_2} j_2 m_2 > B(j_2 m_2, j_1 m_1) \\ & < I_{c_1} M_{c_1} j_1 m_1 | I_{a_1} M_{a_1} > \end{aligned} \quad (III.22)$$

and $P_{tr}(j_2, j_1)$ is the single particle transfer probability defined in *eq.* $(III.19)$.

According to which angular momenta are considered, eqs. (III.18), (III.19) and (III.21) define transfer probabilities by summing over final states and averaging over initial states. In chapter IV we show some angular distributions calculated with eqs. (III.1)-(III.21) and compare the various approximations mentioned above. One obtains a bell-shaped angular distribution in qualitative agreement with the data. The peak at or near the grazing angle is explained as the result of absorption for small impact parameters (corresponding to large scattering angles) and the exponential decrease for larger impact parameters (corresponding to small scattering angles) of the transfer probability.

III.2 Semiclassical partial wave sum.

When diffraction effects are present (cf. Fig. I.12) *eq.* $(III.8)$ gives completely wrong angular distributions. One could try to improve the results by calculating $P_{tr}(\theta)$ in *eq.* $(III.1)$ as the modulus square of some partial wave sum over the relative angular momentum. In this way several waves (in particular near-side and far-side waves) could interfere and contribute to the same scattering angle θ. Also the elastic cross section should be calculated as a partial wave sum. Then there is no advantage in maintaning the approximate factorization $(III.8)$ but it is still possible to use the semiclassical transfer amplitude of chapter II in a partial wave formalism. A theory suitable for our discussion was developed by Hasan and Brink (1978). Starting from the DWBA full transition matrix they obtain a partial wave formula which contains the semiclassical transfer amplitude $(II.28)$ as one term of the sum. Here we give an outline of their method.

By making a WKB approximation for the distorted waves

$$\chi(\mathbf{r}) \simeq \chi(\mathbf{s})\ e^{\frac{i}{\hbar}(\mathbf{r}-\mathbf{s})\cdot\mathbf{p}(\mathbf{s})}, \qquad (III.23)$$

where $\mathbf{s}(t)$ is the classical trajectory of relative motion and $\mathbf{p}(\mathbf{s})$ is the local momentum, the six-dimensional DWBA transition amplitude can be written in terms of a form factor $G(\mathbf{s})$ which contains the bound state wavefunctions, the interaction potential and the momenta $\mathbf{p}_i$ and $\mathbf{p}_f$:

$$T = \int \chi_f^{(-)*}(\mathbf{s})\ G(\mathbf{s})\ \chi_i^{(+)}(\mathbf{s})\ d^3\mathbf{s}. \qquad (III.24)$$

By expanding $\chi^{(\pm)}_{i,f}(\mathrm{s})$ in partial waves, they have

$$T = \frac{(4\pi)^{3/2}}{\sqrt{k_i k_f}} \sum_{L_i L_f M_f} \sqrt{2L_i+1}\; e^{i[\delta_i(L_i)+\delta_f(L_f)]}\; i^{L_i-L_f} Y_{L_f M_f}(\theta,\varphi)\; I(L_i,L_f,M_f). \tag{III.25}$$

The z-axis of the coordinate system coincides with the direction of the incident momentum $\mathbf{k}_i$ while θ,φ are the polar angles of the final momentum $\mathbf{k}_f$. $\delta_{i,f}(L_i,L_f)$ is the sum of the Coulomb and nuclear phase shifts in the initial and final channel, respectively. The term

$$I(L_i,L_f,M_f) = \frac{1}{\sqrt{k_i k_f}} \int_0^\infty f_{L_f}(s)\; G^{M_f}_{L_i L_f}(s)\; f_{L_i}(s)\; ds, \tag{III.26}$$

where

$$G^{M_f}_{L_i L_f}(s) = \int_0^\pi \sin\theta_{\mathrm{s}} d\theta_{\mathrm{s}} \int_0^{2\pi} d\phi_{\mathrm{s}}\; Y^*_{L_f M_f}(\theta_{\mathrm{s}},\phi_{\mathrm{s}})\; G(s,\theta_{\mathrm{s}},\phi_{\mathrm{s}})\; Y_{L_i 0}(\theta_{\mathrm{s}},\phi_{\mathrm{s}}) \tag{III.27}$$

and $f_{L_{i,f}}$ are the radial parts of the expansions of $\chi^{(\pm)}_{i,f}(\mathrm{s})$. Then Hasan and Brink (1978) make the following approximations.

i) Large values of the angular momenta of relative motion $L_{i,f}$. This is justified for heavy-ion reactions because partial waves with small L's are strongly absorbed.

ii) Transferred angular momenta small compared to $L_{i,f}$.

iii) Semiclassical evaluation of $I(L_i,L_f,M_f)$, *eq.* (*III*.26), by using WKB wavefunctions for the radial functions $f_{L_{i,f}}$. This is similar to the approach of Landowne et al. (1976).

iv) The orbits are not too different in the initial and final channel, so that they expand about the final orbit.

v) For forward-angle scattering the component of $\mathbf{p}_f$ perpendicular to the incident direction is not very large, so that the dependence of $G(\mathbf{s})$ on the scattering angles θ and φ can be neglected.

The final approximate expression they obtain from the DWBA transition amplitude is:

$$T(\ell_2\lambda_2,\ell_1\lambda_1) = i^{\lambda_1-\lambda_2}\sum_{L=0}^{\infty}\sqrt{2L+1}\; e^{i[\delta_i(L)+\delta_f(L)]}\; A'_L(\ell_2\lambda_2,\ell_1\lambda_1)\; Y_{L,\lambda_1-\lambda_2}(\theta,0), \tag{III.28}$$

where we specified the orbital angular momentum quantum numbers $(\ell_1\lambda_1)$ and $(\ell_2\lambda_2)$ of the initial and final bound states ψ_1 and ψ_2. The amplitude $A'_L(\ell_2\lambda_2,\ell_1\lambda_1)$ in eq. (III.28) is related to the semiclassical transfer amplitude A calculated in chapter II by the rotation

$$A'(\ell_2\lambda'_2,\ell_1\lambda'_1) = \sum_{\lambda_1\lambda_2} d^{\ell_1}_{\lambda'_1\lambda_1}(\theta/2)\; d^{\ell_2}_{\lambda'_2\lambda_2}(\theta/2)\; A(\ell_2\lambda_2,\ell_1\lambda_1), \tag{III.29}$$

where $d^{\ell}_{\lambda'\lambda}$ is a reduced rotation matrix (Brink and Satchler 1971).

The differential cross section $\frac{d\sigma}{d\Omega}$ for the reaction

$$a_1 + c_2 \longrightarrow c_1 + a_2$$

or

$$(c_1 + x) + c_2 \longrightarrow c_1 + (c_2 + x)$$

is obtained by re-coupling the transition matrix (III.28) to the spins that define the initial and final states, in the same way we did for the transfer probabilities, eqs. (III.19)-(III.21). For transfer from a single-particle state with spin j_1 in nucleus a_1 to a single-particle state with spin j_2 in nucleus a_2 we have

$$\frac{d\sigma}{d\Omega} = \frac{\pi}{k^2}\,\frac{\mu_i}{\mu_f}\,\frac{2I_{a_2}+1}{(2I_{c_2}+1)(2j_1+1)(2j_2+1)}\sum_{m_1m_2}|T(j_2m_2,j_1m_1)|^2, \tag{III.30}$$

where

$$T(j_2m_2,j_1m_1) = \sum_{\lambda_1\lambda_2m_s} <\ell_1\lambda_1 s m_s|j_1m_1><\ell_2\lambda_2 s m_s|j_2m_2>\, T(\ell_2\lambda_2,\ell_1\lambda_1). \tag{III.31}$$

In eq. (III.30) k is the wave number of relative motion in the initial channel, $\mu_{i,f}$ are the reduced masses of the initial and final system, respectively, I_{a_2} and I_{c_2} are the spins of the final nucleus a_2 and of the core c_2. In eq. (III.31) s is the spin of the transferred particle and m_s its projection along the z-axis.

The formulæ (III.28)-(III.31), together with the semiclassical transfer amplitude of chapter 2, provide a simple way for calculating angular distributions. They are used in chapter IV and compared with experimental data. One merit of this formulation is that, alike the classical expressions (III.8) or (III.17), the various components of the transition matrix, eq. (III.28), are factorized and one can 'see' how the reaction is taking place physically. The elastic scattering is contained in the factor

$$e^{i2Re\delta(L)} \qquad (III.32)$$

and absorption in the factor

$$e^{-2Im\delta(L)}, \qquad (III.33)$$

where we put

$$2\delta(L) = \delta_i(L) + \delta_f(L) \quad \text{and} \quad \delta_{i,f} = Re\delta_{i,f} + iIm\delta_{i,f}; \qquad (III.34)$$

the transfer process is given by the amplitude $A'_L(\ell_2\lambda_2, \ell_1\lambda_1)$ and the rest are geometric factors.

At the same time trajectories with different relative angular momenta L can interfere in the sum (III.28) to produce scattering at the angle θ. This is a typical quantum feature. In fact eq. (III.28) has the form of the ansatz (I.2) but we do not need to parametrize the

partial wave amplitudes. With the notation of eq. (I.2), these are now given by the theory as

$$g_L = \sqrt{2L+1}\; e^{i[\delta_i(L)+\delta_f(L)]}\; A'_L(\ell_2\lambda_2, \ell_1\lambda_1).$$

The approximations made in the derivation of eqs. (III.28)-(III.31) seem reasonable for heavy-ion transfer reactions at incident energies above the Coulomb barrier, where angular distributions are peaked at forward angles (cf. chapter I). However, the range of applicability of these formulæ is restricted to well matched reactions, as this is a fundamental assumption in the derivation. We shall see in chapter IV that a change in the relation between the distance of closest approach and the angular momentum from the initial channel, $d_i(L)$, to the final channel, $d_f(L)$, alters the magnitude of the cross section but not the shape of the angular distribution.

Last, we note a property of the partial-wave formula (III.28) that simplifies the calculation of the total (=angle-integrated) transfer cross section. By integrating over $d\Omega$ either the classical formula

$$\left[\frac{d\sigma(\theta)}{d\Omega}\right]_\alpha = \frac{b}{\sin\theta}\left|\frac{db}{d\theta}\right| |S_{L(\theta)}|^2 P^{tr}_{L(\theta)}(\alpha) \qquad (III.35)$$

or the partial-wave angular distribution (III.30) we obtain (almost) the same total transfer cross section. This property originates from the form of the partial-wave sum (III.28) and does not depend on the coupling of the internal angular momenta. This means that in eq. (III.35) the index α can specify the transitions

$$a) \qquad \alpha = (\ell_1\lambda_1 \rightarrow \ell_2\lambda_2),$$

or

$$b) \qquad \alpha = (j_1 m_1 \rightarrow j_2 m_2),$$

or

$$c) \qquad \alpha = (I_{a_1}, I_{c_2} \rightarrow I_{c_1}, I_{a_2}),$$

with the meaning of the angular momentum quantum numbers indicated before. We shall prove the equality of the angle-integrated transfer cross sections for the case c). The integral of *eq.* (*III*.35) over the solid angle $d\Omega = \sin\theta d\theta d\varphi$ is

$$\sigma_\alpha = 2\pi \int_0^\pi b(\theta) \left|\frac{db}{d\theta}\right| \; P^{tr}_{L(\theta)}(\alpha) \; |S_{L(\theta)}|^2 \; d\theta.$$

We assume that the deflection function $\theta(b)$ is monotonically decreasing (as it is the case for Colulomb scattering where $\theta = 2\arctan\frac{Z_{c_2} Z_x e^2}{2Eb}$) and that $b(\theta = 0) = \infty$ (particles passing undeflected at large distances) while $b(\theta = \pi) = 0$ (particles turned back in a head-on collision). Then changing the integration variable from θ to b gives

$$\sigma_\alpha = 2\pi \int_0^\infty P^{tr}_{L(b)}(\alpha) |S_{L(b)}|^2 \; b \; db. \qquad (III.36)$$

Eq. (*III*.36) can be transformed into an integral over the classical angular momentum $\Lambda = L + 1/2$ by the change of variable $\Lambda = \sqrt{2\mu E}\; b/\hbar = kb$ (note that now we use the classical angular momentum in units of $\hbar$):

$$\sigma_\alpha = \frac{2\pi}{k^2} \int_0^\infty P^{tr}_{\Lambda-1/2}(\alpha) \; |S_{\Lambda-1/2}|^2 \; \Lambda \; d\Lambda \simeq \frac{\pi}{k^2} \sum_{L=0}^{\infty} (2L+1) P^{tr}_L(\alpha) \; |S_L|^2. \qquad (III.37)$$

The last form is useful to evaluate the angle-integrated transfer cross section if the reflection coefficients $|S_L|^2$ are calculated numerically for each value of L.

By integrating eq. (III.30) over $d\Omega$ we have

$$\sigma(I_{a_1}, I_{c_2} \to I_{c_1}, I_{a_2}) \equiv \int_{4\pi} d\Omega \, \frac{d\sigma}{d\Omega}$$

$$= C \, 2\pi \sum_{m_1 m_2} \sum_{\lambda_1 \lambda_2 m_s} \sum_{\lambda_1' \lambda_2' m_s'} < \ell_1 \lambda_1 s m_s | j_1 m_1 >$$

$$< \ell_2 \lambda_2 s m_s | j_2 m_2 >< \ell_1 \lambda_1' s m_s' | j_1 m_1 >< \ell_2 \lambda_2' s m_s' | j_2 m_2 >$$

$$\int_0^\pi T^*(\ell_2 \lambda_2', \ell_1 \lambda_1') \, T(\ell_2 \lambda_2, \ell_1 \lambda_1) \, \sin\theta \, d\theta, \qquad (III.38)$$

where we denoted by C the factor in front of the $\sum_{m_1 m_2}$ in eq. (III.30). By substituting the partial-wave sum (III.28) the integral over θ becomes

$$\int_0^\pi T^*(\ell_2 \lambda_2', \ell_1 \lambda_1') \, T(\ell_2 \lambda_2, \ell_1 \lambda_1) \, \sin\theta \, d\theta$$

$$= i^{\lambda_1 - \lambda_2 - \lambda_1' + \lambda_2'} \sum_{LL'} (2L+1)^{1/2} (2L'+1)^{1/2} \, e^{2i\delta_L} \left(e^{2i\delta_{L'}}\right)^*$$

$$\int_0^\pi A_{L'}'^*(\ell_2 \lambda_2', \ell_1 \lambda_1') \, A_L'(\ell_2 \lambda_2, \ell_1 \lambda_1) \, Y^*_{L', \lambda_1' - \lambda_2'}(\theta, 0) \, Y_{L, \lambda_1 - \lambda_2}(\theta, 0) \, \sin\theta \, d\theta, \qquad (III.39)$$

where we introduced δ_L defined by (III.34). From the Clebsch-Gordan coefficients in eq. (III.38) we have $\lambda_1' - \lambda_2' = \lambda_1 - \lambda_2$. Then, by neglecting the slow dependence of A' on θ, eq. (III.29), we put $A' \approx A$ and make use of the orthogonality of spherical harmonics in eq. (III.39) to get

$$\int_0^\pi T^*(\ell_2 \lambda_2', \ell_1 \lambda_1') \, T(\ell_2 \lambda_2, \ell_1 \lambda_1) \, \sin\theta \, d\theta$$

$$= \frac{1}{2\pi} \sum_L (2L+1) \, e^{-4Im\delta_L} \, A_L^*(\ell_2 \lambda_2', \ell_1 \lambda_1') \, A_L(\ell_2 \lambda_2, \ell_1 \lambda_1). \qquad (III.40)$$

Substitution of eq. (III.40) into (III.38) gives

$$\sigma(I_{a_1}, I_{c_2} \to I_{c_1}, I_{a_2}) = \frac{\pi}{k^2} \frac{\mu_i}{\mu_f} \sum_L (2L+1)\, e^{-4Im\delta_L} \frac{2I_{a_2}+1}{(2I_{c_2}+1)(2j_1+1)(2j_2+1)}$$

$$\sum_{m_1 m_2} |B_L(j_2 m_2, j_1 m_1)|^2, \qquad (III.41)$$

where we have made explicit the dependence of $B(j_2 m_2, j_1 m_1)$, defined by eq. (III.20), on the relative angular momentum L. Eq. (III.41) is the same as eq. (III.37) (but for the factor μ_i/μ_f) because $e^{-4Im\delta_L} = |S_L|^2$ [cf. eq. (III.33)] and $\frac{2I_{a_2}+1}{(2I_{c_2}+1)(2j_1+1)(2j_2+1)}$ $\sum_{m_1 m_2} |B_L(j_2 m_2, j_1 m_1)|^2 = P_{tr}(I_{a_1}, I_{c_2} \to I_{c_1}, I_{a_2})$ [cf. eqs. (III.21) and (III.19)]. The ratio of the reduced masses μ_i/μ_f that enters in the cross section (III.30) is neglected in the classical formula (III.35). For the transfer reaction $a_1(= c_1 + x) + c_2 \to c_1 + a_2(= c_2 + x)$ it amounts to

$$\frac{\mu_i}{\mu_f} = \frac{a_1 c_2}{c_1 a_2} = \frac{c_1 c_2 + x c_2}{c_1 c_2 + x c_1},$$

where we indicated with the same symbols the nuclei and their mass numbers.

$$\text{If} \quad c_1 \approx c_2, \quad \text{then} \quad \frac{\mu_i}{\mu_f} \approx 1$$

For nucleon transfer (x=1),

$$\text{if} \quad c_1 \gg c_2, \quad \text{then} \quad \frac{\mu_i}{\mu_f} \approx \frac{c_2}{c_2+1},$$

$$\text{if} \quad c_2 \gg c_1, \quad \text{then} \quad \frac{\mu_i}{\mu_f} \approx \frac{c_1}{c_1+1}.$$

Several properties of transfer reactions can be studied by considering the total cross section instead of the angular distribution. The spin- and energy-dependence of σ_{tr}, discussed in chapter VII, are an example. Therefore one can use the simpler classical formulæ (III.36) or (III.37) instead of the full partial-wave expansion (III.28).

Chapter IV. Neutron Transfer calculations

IV.1 Transfer amplitudes, normalization and phase shifts.

In this section we present some examples of the semiclassical transfer amplitude A of chapter II and the elastic scattering matrix elements S_L mentioned in chapter III. These are the 'ingredients' we need in §§ IV.2 and IV.3 to calculate angular distributions. We also discuss possible parametrizations of A and S_L.

Fig. IV.1 shows a typical exponential decrease of the semiclassical transfer amplitude, A, as a function of the relative angular momentum quantum number, L, for the reaction $^{208}Pb(^{16}O,^{15}O)^{209}Pb$ at an incident energy $E_{lab} = 139$ MeV. Fig. IV.2 shows several components of $|A_L|$ for the transition $p_{1/2} \rightarrow d_{3/2}$ in $^{26}Mg(^{11}B,^{10}B)^{27}Mg$ at 114 MeV. Both figures are obtained by using the formula (II.28). Hasan (1976) reduced the amplitude A, eq. (II.5), to a one-dimensional integral to be computed numerically. With that method, in particular, transfer amplitudes for the reaction $^{26}Mg(^{11}B,^{10}B)^{27}Mg$ at 114 MeV were calculated with the same results as Fig. IV.2.

The transfer amplitudes in figs. IV.1 and IV.2 are very similar, although the angular distributions for these reactions are completely different (see §§ IV.2 and IV.3). We note that the slope of the curves does not depend on the particular transition, specified by the z-projection of the orbital angular momentum quantum numbers, λ_1 and λ_2, of the initial and final bound states. These calculations suggest a simple exponential parametrization for the modulus of the amplitude:

$$|A_L(\ell_2\lambda_2,\ell_1\lambda_1)| = G(\ell_2\lambda_2,\ell_1\lambda_1)e^{\frac{L_0-L}{\Delta}}. \qquad (IV.1)$$

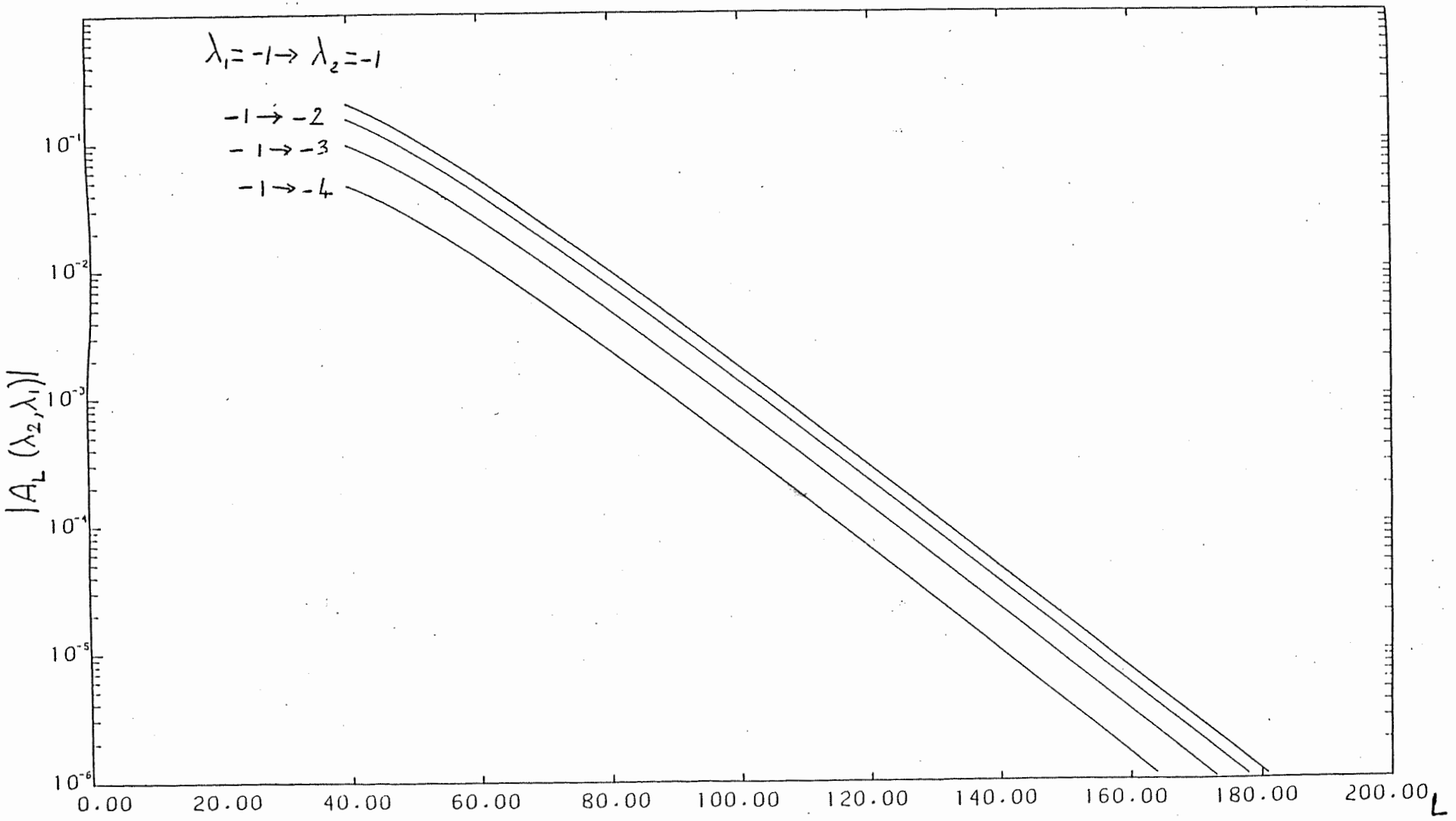

Fig.IV.1 Modulus of the semiclassical transfer amplitude for the reaction $^{208}Pb(^{16}O,^{15}O)^{209}Pb_{(g_{9/2},g.s.)}$ at E_{Lab}=139 Mev. The values of $|A|$ calculated by eq.(II.28), are shown as a function of the relative angular momentum L. λ_1 and λ_2 are the z-projections of the orbital angular momentum in the initial and final bound states, $\ell_1 = 1$ and $\ell_2 = 4$.

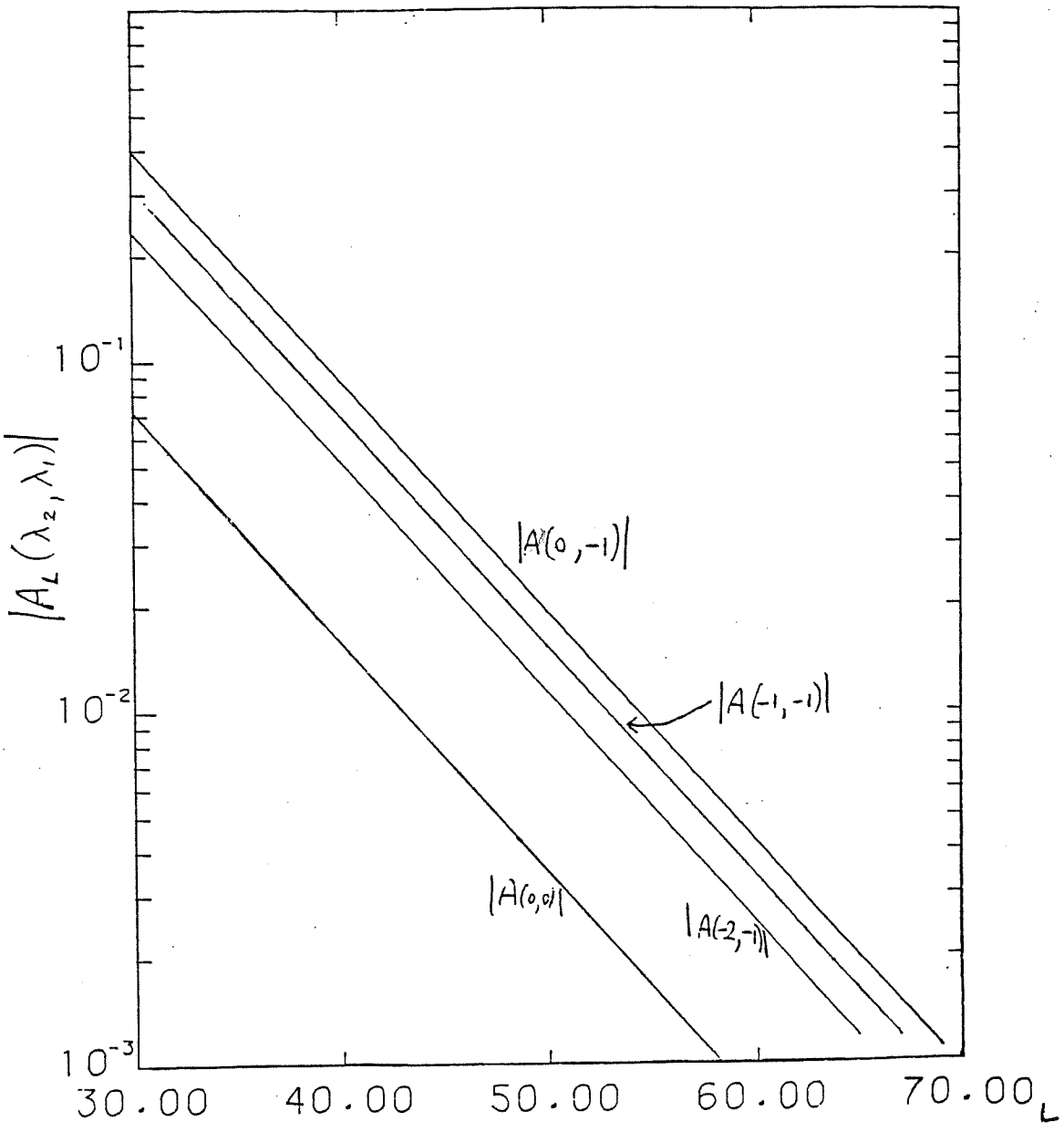

Fig.IV.2 The same as fig.IV.1 but for the reaction $^{24}Mg(^{11}B,^{10}B)^{25}Mg_{(d3/2,0.98\,MeV)}$ at E_{Lab}=114 MeV.

Eq. (IV.1) was used by Hasan (1976) to interpolate numerically-calculated amplitudes. We can find the constants G, L_0 and Δ from the analytical formula (II.29). For heavy-ion reactions at energies well above the Coulomb barrier, the relative angular momenta that contribute to quasi-elastic transfer satisfy

$$L \gg n,$$

where n is the Sommerfeld parameter. The distance of closest approach d for a Coulomb trajectory, given by eq. (III.11), can then be approximated by

$$d \simeq \frac{n+L}{k}. \qquad (IV.2)$$

With this approximation eq. (II.29) becomes

$$A(\ell_2\lambda_2,\ell_1\lambda_1) \approx -4\pi i \frac{\hbar}{mv}\, C_{\ell_1} C_{\ell_2}\, (-1)^{\lambda_1}\, Y_{\ell_1\lambda_1}(\hat{k}_1)\, Y^*_{\ell_2\lambda_2}(\hat{k}_2)$$

$$\sqrt{\frac{\pi}{2\eta d}}\, e^{-\eta a_C}\, e^{-\frac{\eta}{k}L}, \qquad (IV.3)$$

where $a_c = n/k$ and k is the asymptotic wave number. Eq. (IV.3) is of the form (IV.1), but for the L-dependent factor $d^{-1/2}$. However, this L-dependence is negligible when compared to that in the exponential factor and d *in eq.* (*IV*.3) can be considered as a constant, e.g. the strong absorption radius R_{sa}. By equating eq. (IV.3) to (IV.1) we find

$$G(\ell_2\lambda_2,\ell_1\lambda_1)\, e^{\frac{L_0}{\Delta}} = 4\pi \frac{\hbar}{mv}\, C_{\ell_1} C_{\ell_2}\, |Y_{\ell_1\lambda_1}(\hat{k}_1)\, Y_{\ell_2\lambda_2}(\hat{k}_2)| \sqrt{\frac{\pi}{2\eta R_{sa}}}\, e^{-\eta a_C}, \qquad (IV.4a)$$

and

$$\Delta = k/\eta. \qquad (IV.4b)$$

As an example, for the g.s. transition $^{26}Mg(^{11}B,^{10}B)^{27}Mg$ at 114 MeV, Hasan (1976) finds numerically $\Delta = 7.44$. From eqs. (II.30-31) we have $\eta = 0.77\ fm^{-1}$ and $\frac{k}{\eta} = 7.14$. The amplitude $A(\ell_2\lambda_2, \ell_1\lambda_1)$, given by eq. (II.28), is either real or purely imaginary.

The normalization constants C_{ℓ_1} and C_{ℓ_2} in eqs. (II.28) and (II.19) are given by the ratio between the solution of the radial Schrödinger equation for the neutron bound in the potential V_1 or V_2 and the function $\gamma\chi_l(\gamma r)$, which is related to a Hankel function by *eqs.* (*II.A.*12). Fig. IV.3 compares an exact (numerically computed) radial wave function to the Hankel function form. The actual wavefunction oscillates in the nuclear interior and assumes the same *form* as $\gamma\chi_l(\gamma r)$ outside the nuclear surface, with an asymptotic exponential decay. The normalization ratio C_ℓ takes into account properties of the nuclear interior, while the semiclassical transfer amplitude calculated in chapter II depends only on the 'tails' of the bound-state wavefunctions. These normalization constants can also be approximated by an analytical formula based on the WKB expression of the radial wavefunction. Stancu and Brink (1985) obtain a formula which agrees quite well with the numerically calculated C_ℓ for energy levels which are not too deep. Such a formula is useful when an exact solution of the Schrödinger equation for the bound states is not known. For example, normalizations C_ℓ for experimental single-particle levels can be calculated by using a standard potential.

To calculate angular distributions one also needs elastic scattering phase shifts δ_L. The classical formulæ of § III.1 contain only their imaginary part in the absorption factor $|S_L|^2 = \exp(-4Im\delta_L)$, while the formulæ of § III.2 contain the complete phase shifts δ_L (real and imaginary parts, initial and final channel) in the term $S_L = e^{2i\delta_L}$ of the

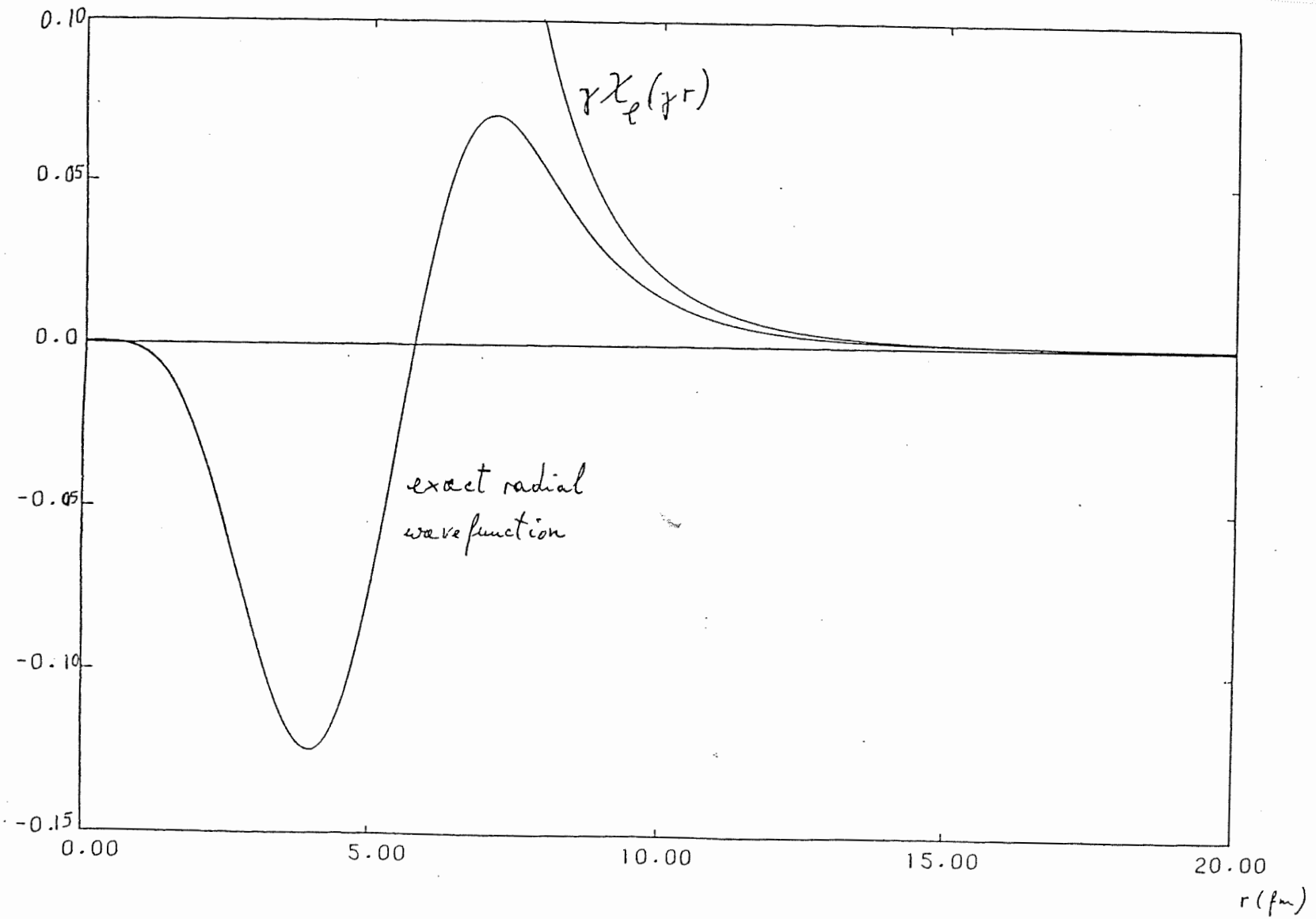

Fig. IV.3. Comparison between exact (numerically computed) radial wave function and Hankel function form $\gamma\chi_\ell(\gamma r)$ for a neutron bound in the $2g_{9/2}$ ground state of ^{209}Pb. Relevant parameters for this calculation are given in the last line of table IV.2.

partial-wave sum (III.28). Fig. IV.4 shows that the inclusion of the real part of δ_L in this formula can produce a shift in the peak of the angular distribution. To obtain accurate angular distributions and compare with experimental data, we determined the phase shifts by numerically solving the Schrödinger equation with optical potentials that give a good fit to elastic scattering. However, throughout this work, we also used some semiclassical formulæ and parametrizations for δ_L and S_L. We already mentioned the expression (III.5), which is derived by considering the nuclear potential U_N as a perturbation to the Coulomb potential U_C. Then eq. (III.5) or (III.13) can be used when U_N is weak, but also when $W \equiv Im\ U_N$ is very large, as it is usually the case for heavy ion reactions. This is because the absorption is so strong for orbits with small impact parameters that errors are not very important, while for large impact parameters the potential that enters in eq. (III.5) is small.

We now show some comparisons between exact values of $|S_L|$ and the semiclassical forms. Fig. IV.5 shows a comparison between $|S_L|^2 = \exp(-4Im\delta_L)$ calculated numerically and by using eq. (III.13) for $Im\delta_L$. The partial-wave angular distributions of § III.2 depend on the product between S_L and transfer amplitude A_L; the classical formulæ of § III.1 depend on the product $|S_L|^2 P_{tr}(j_2, j_1)$, where P_{tr} is related to the modulus of the transfer amplitude A_L by eq. (III.19). Fig. IV.5 also shows that $|S|^2 P_{tr}$ is peaked in L-space around L_{gr} such that $|S_{L_{gr}}|^2 = 1/2$. This entails the localization of classical angular distributions around trajectories with scattering angles $\theta \simeq \theta(L_{gr})$. According to the semiclassical formula (III.5), $Re\ \delta_L$ depends on $Re\ U_N$ only while $Im\ \delta_L$ depends on $Im\ U_N$ only. In an exact solution of the Schrödinger equation, however, the addition of an imaginary part

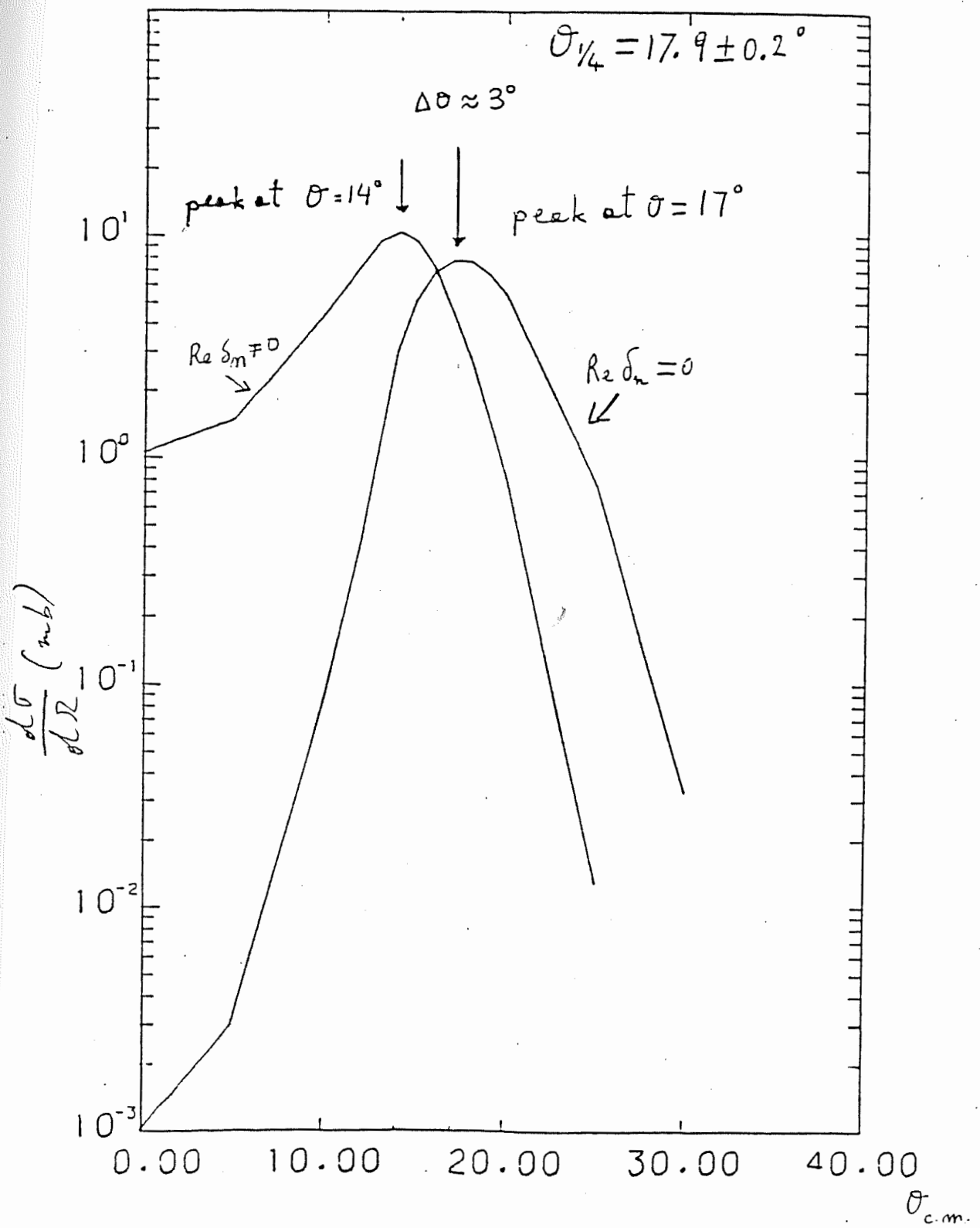

Fig. IV.4. The effect of the real part of the nuclear phase shifts, δ_n, on a bell-shaped angular distribution for the reaction $^{208}Pb(^{16}O,^{15}O)^{209}Pb_{(g.s.)}$ at 312.6 MeV incident energy. The angular distribution is obtained from the partial-wave formula (III.28) by using semiclassical phase shifts, eq. (III.5), calculated with the optical potential in the second line of table IV.1.

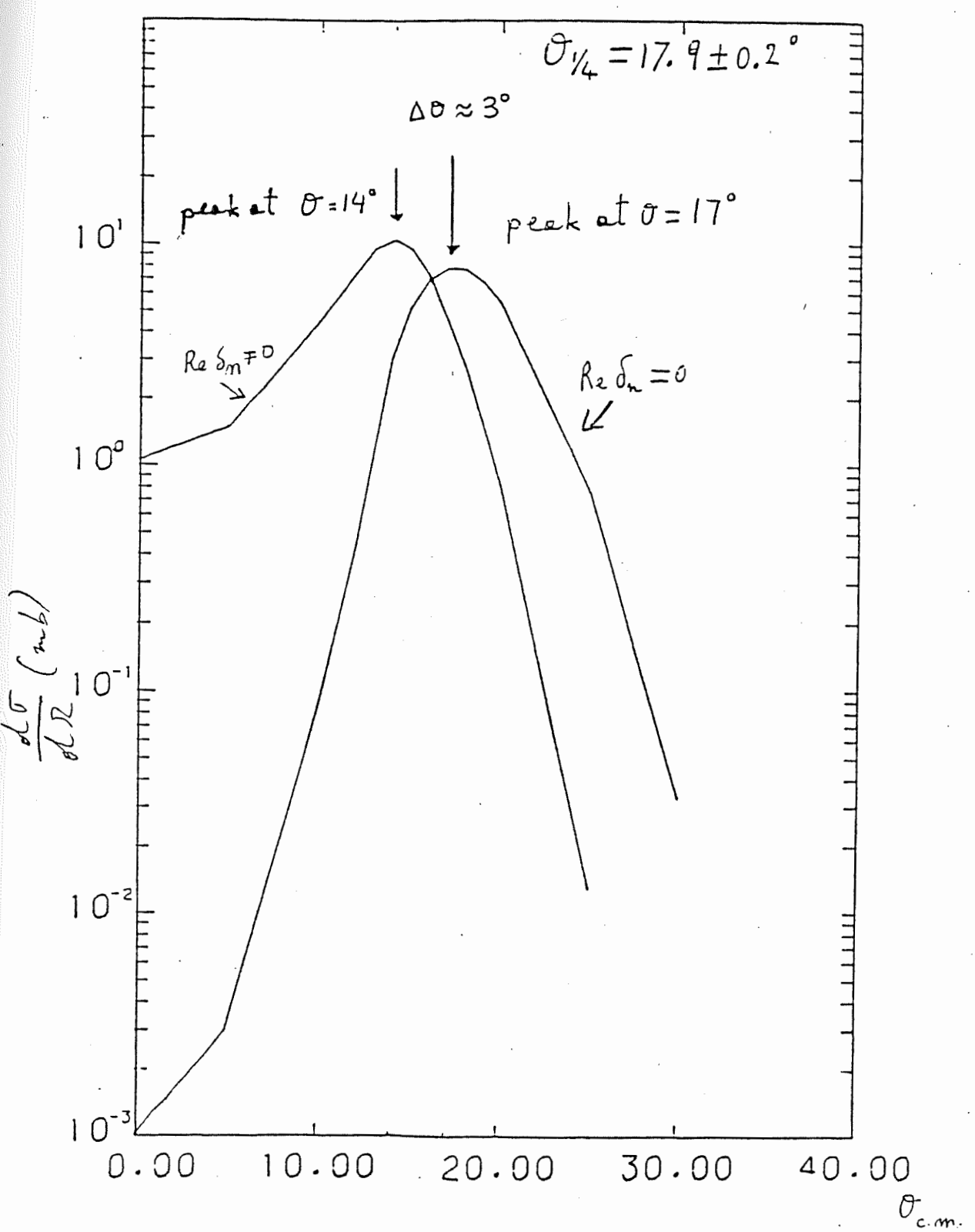

Fig. IV.4. The effect of the real part of the nuclear phase shifts, δ_n, on a bell-shaped angular distribution for the reaction $^{208}Pb(^{16}O,^{15}O)^{209}Pb_{(g.s.)}$ at 312.6 MeV incident energy. The angular distribution is obtained from the partial-wave formula (III.28) by using semiclassical phase shifts, eq. (III.5), calculated with the optical potential in the second line of table IV.1.

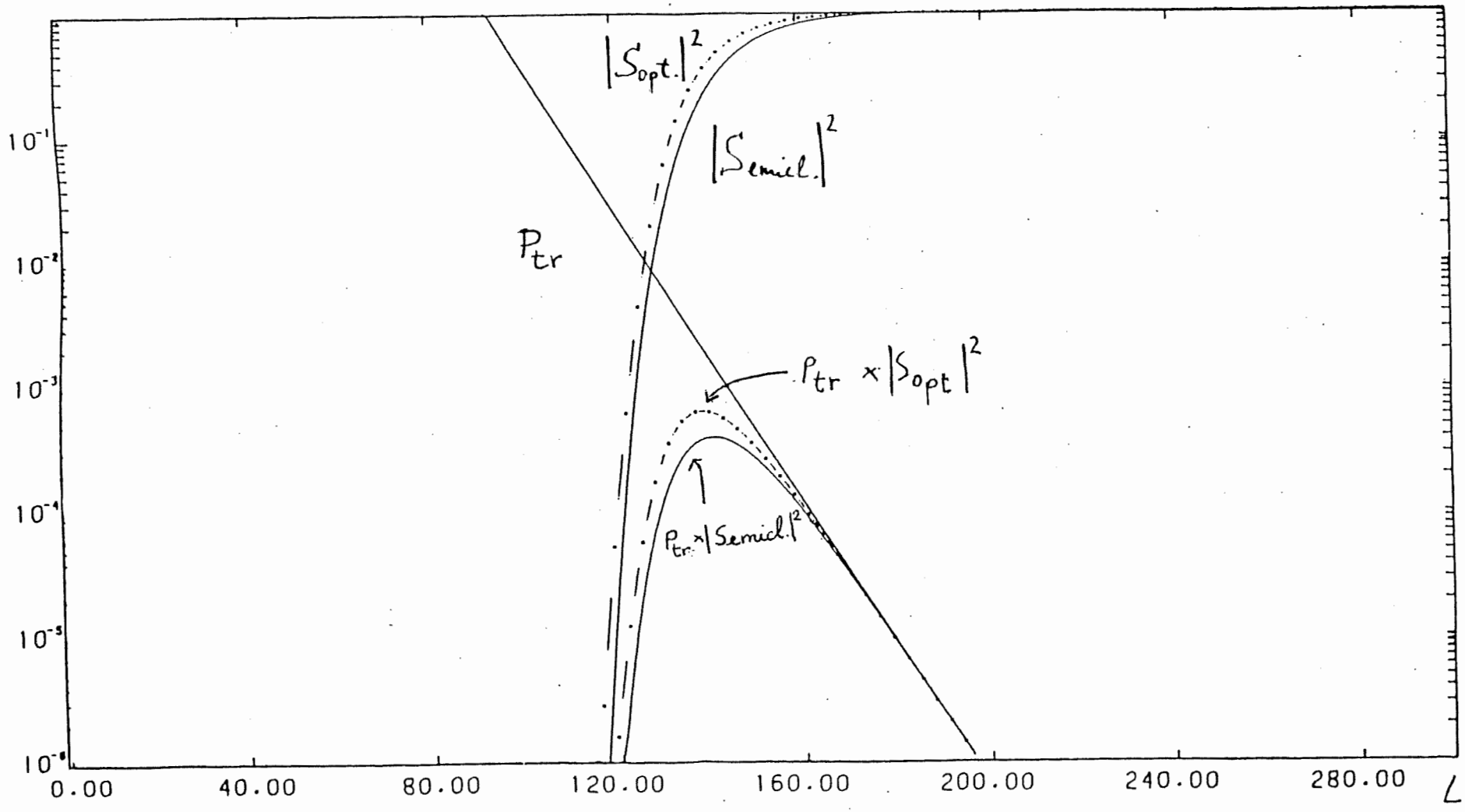

Fig.IV.5 Reflection coefficients and transfer probability for $^{16}O(312.6\ MeV)+^{209}Pb \rightarrow ^{15}O+^{209}Pb$ g.s.. The transition is $j1=p_{1/2} \longrightarrow j2=g_{9/2}$. The transfer probability $P_{tr}(j1,j2)$ is related to $|A_L(l_2,\lambda_2,l_1,\lambda_1)|$ by eq.(III.19); S_{opt} was calculated numerically with the optical potential in table IV.1, $|Semicl|$ was calculated with the same imaginary potential by using eq.(III.13) for $Im\delta_L$.

to the ion-ion potential affects also $Re\ \delta_L$ and $Im\ \delta_L$ depends on $Re\ U_N$ too.

A simple way to study the effect of elastic scattering phase shifts on the angular distribution is to parametrize the matrix elements

$$S_L = e^{2i\delta_L} = e^{2i(\delta_L^C + \delta_L^N)} = e^{2i\delta_L^C}\ S_L^N, \qquad (IV.5)$$

where the superscript C stands for 'Coulomb' and N for 'Nuclear'. A widely used parametrization is due to Ericson (1966). By introducing the classical angular momentum $\hbar\Lambda = (L + 1/2)\hbar$, one writes

$$S^N(\Lambda) = \{1 + \exp[(\Lambda - \Lambda_0)/\Delta]\}^{-1}, \qquad (IV.6)$$

with $\Lambda = \Lambda_R - i\Lambda_I$ and $0 \leq \Lambda_I \leq \frac{\pi}{2}\Delta$. With this form $|S^N| \to 0$ for small Λ's and $|S^N| \to 1$ for large Λ's, in agreement with the numerical result. The parameters Λ_R, Λ_I and Δ in eq. (IV.6) can be approximatively related to those of an optical potential with a Saxon-Woods form (see Brink 1978, p. 15).

Alternatively, one can parametrize the product $g_L = S_L A_L$ [cf. eq. (I.2) and chapter III, p. 61]. A possible form, related to eq. (IV.3), is (Brink 1978, p. 46)

$$g(\Lambda) = g_{\Lambda_0}\ \frac{\exp \alpha(\Lambda - \Lambda_0)}{1 + \exp[(\Lambda - \Lambda_0)/\Delta]}\ \exp[i\theta_0(\Lambda - \Lambda_0)]. \qquad (IV.7)$$

Fig. IV.6a shows that sometimes the absorption given by the semiclassical phase shifts, eqs. (III.5) and (III.13), is not strong enough for small angular momenta, so that the product $|S_L A_L|$ rises significantly from zero because of the exponential form (II.28) of A_L and gives wrong angular distributions. This is avoided if one uses exact phase shifts computed with an optical model code (fig. IV.6b). The parametrization (IV.7) can reproduce this

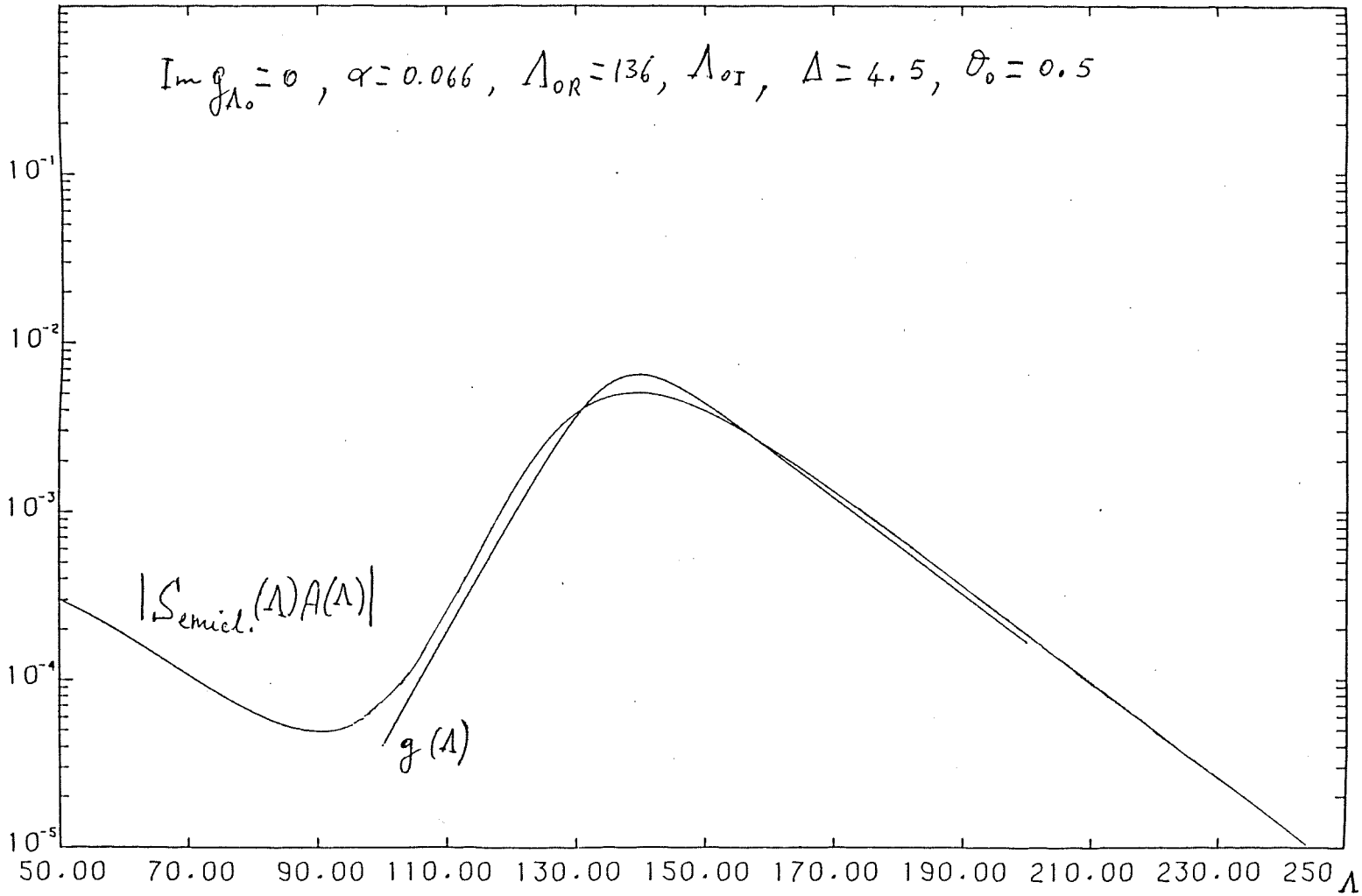

Fig.IV.6a Parametrization of the form factor |SA| by eq.(IV.7) for $^{16}O(312.6\,MeV)+^{208}Pb \longrightarrow ^{16}O+^{208}Pb$. Parameters are given in the figure. |Semicl(Λ)| has the same meaning as in Fig.IV.5. Λ is calcutated by the formula (II.28). Λ=L+1/2 is the relative angular momentum.

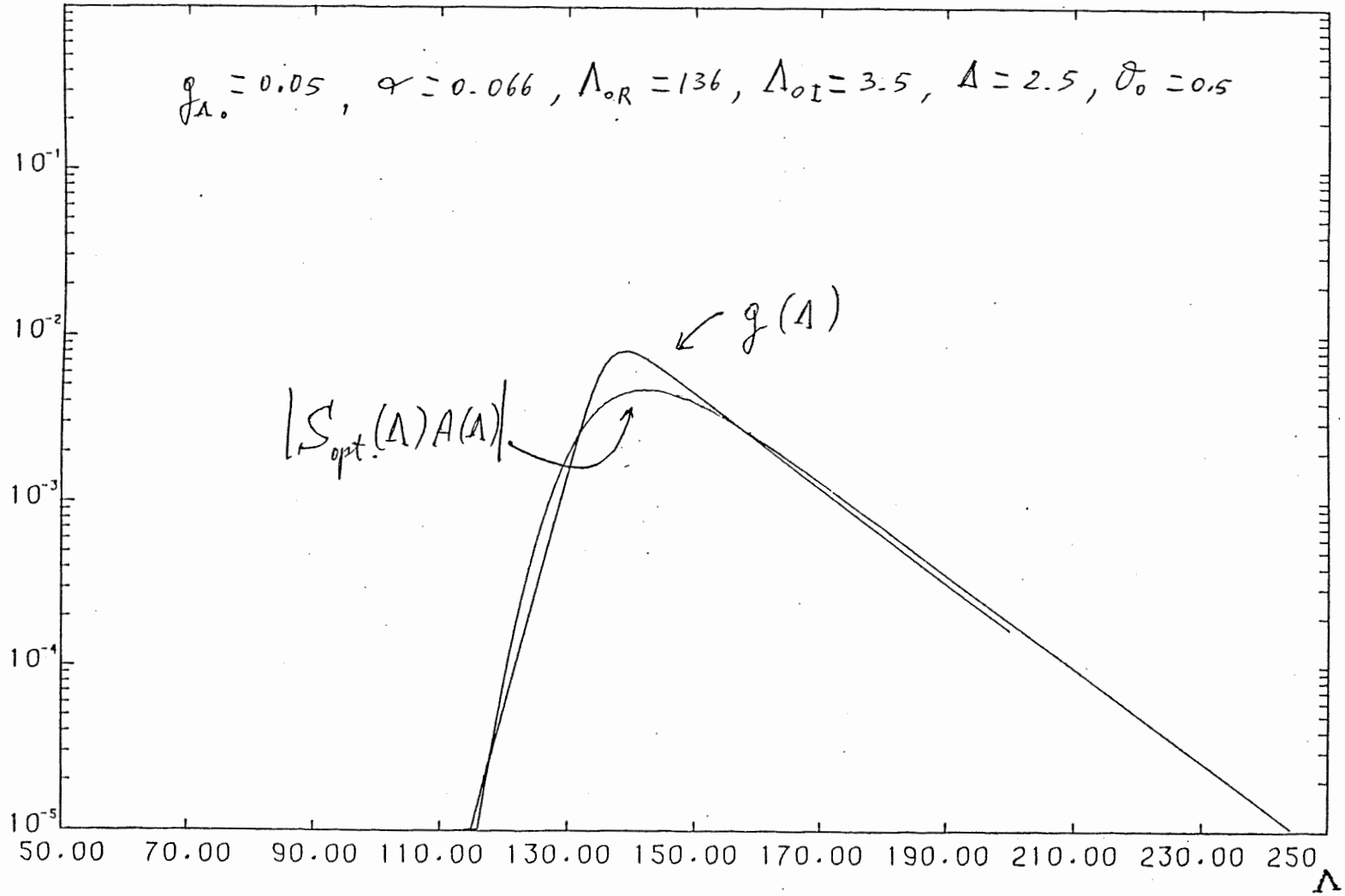

Fig.IV.6b Similar to Fig.IV.6a but with exact matrix elements Sopt(Λ).Parameters for calculating S are in the tableIV.1.

trend and can be used for calculating angular distributions. In chapter VII, where we study the energy dependence of the angle-integrated cross section, we use another exponential parametrization of δ_L and relate its parameters to the imaginary part of the optical potential.

IV.2 Angular distributions calculated as a product of probabilities.

Here we show a few examples of cross sections calculated with the classical formula (III.17). Fig. IV.7 shows an angular distribution for the reaction $^{208}Pb(^{16}O,^{15}O)^{209}Pb_{g.s.}$ at 312.6 MeV. For the same reaction, fig. IV.8 shows the effect of using semiclassical phase shifts, eq. (III.5), for the factor $|S_L|^2$ on the cross section. It should be compared with fig. IV.5. Fig. IV.9 shows the classical angular distribution for the reaction $^{208}Pb(^{16}O,^{15}O)^{209}Pb_{0.78\ \mathrm{MeV}}$ at 139 MeV incident energy. The classical formula (III.17) always predicts bell-shaped angular distributions. The calculated angle of the maximum is usually slightly larger than the experimental one and the peak is too narrow. This formula neglects deflection by the real part of the nuclear potential. As we saw in chapter III, p.53-55, these can be accounted for in an approximate way and one obtains a correction for the position of the peak. But eq. (III.17) also neglects diffraction effects, so it cannot give a correct angular distribution for, e.g., $^{26}Mg(^{11}B,^{10}B)^{27}Mg$ (see § IV.3) which shows nearside-farside interference oscillations. A more accurate cross section can be obtained by using the transfer amplitude (II.28) in the partial-wave formalism of § III.2, as we discuss in the next section.

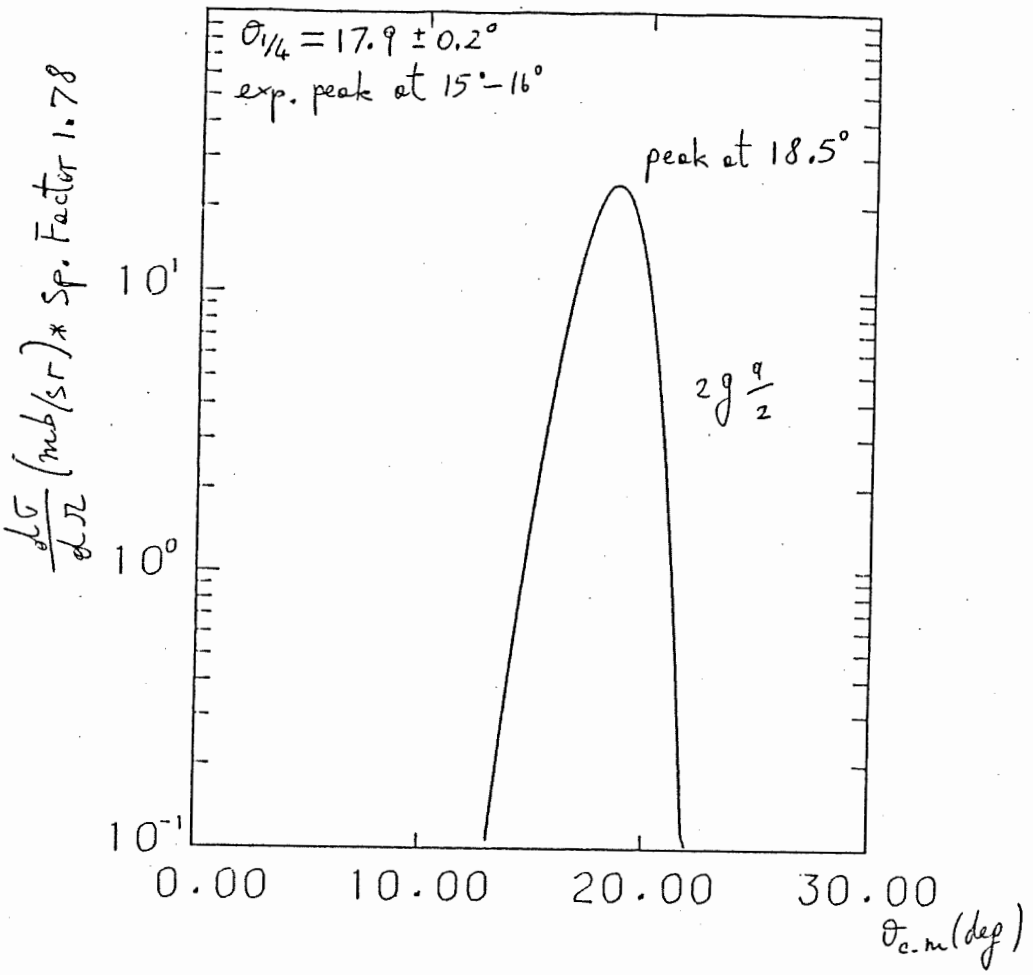

Fig. IV.7 Classical angular distribution for the reaction $^{208}Pb(^{16}O, ^{15}O)^{209}Pb_{g.s.}$ at 312.6 MeV. We used the classical formula (III.17) with the transfer probability $P_{tr}(l_2, l_1)$, where $l_{1(2)}$ is the orbital angular momentum of the initial (final) bound state.

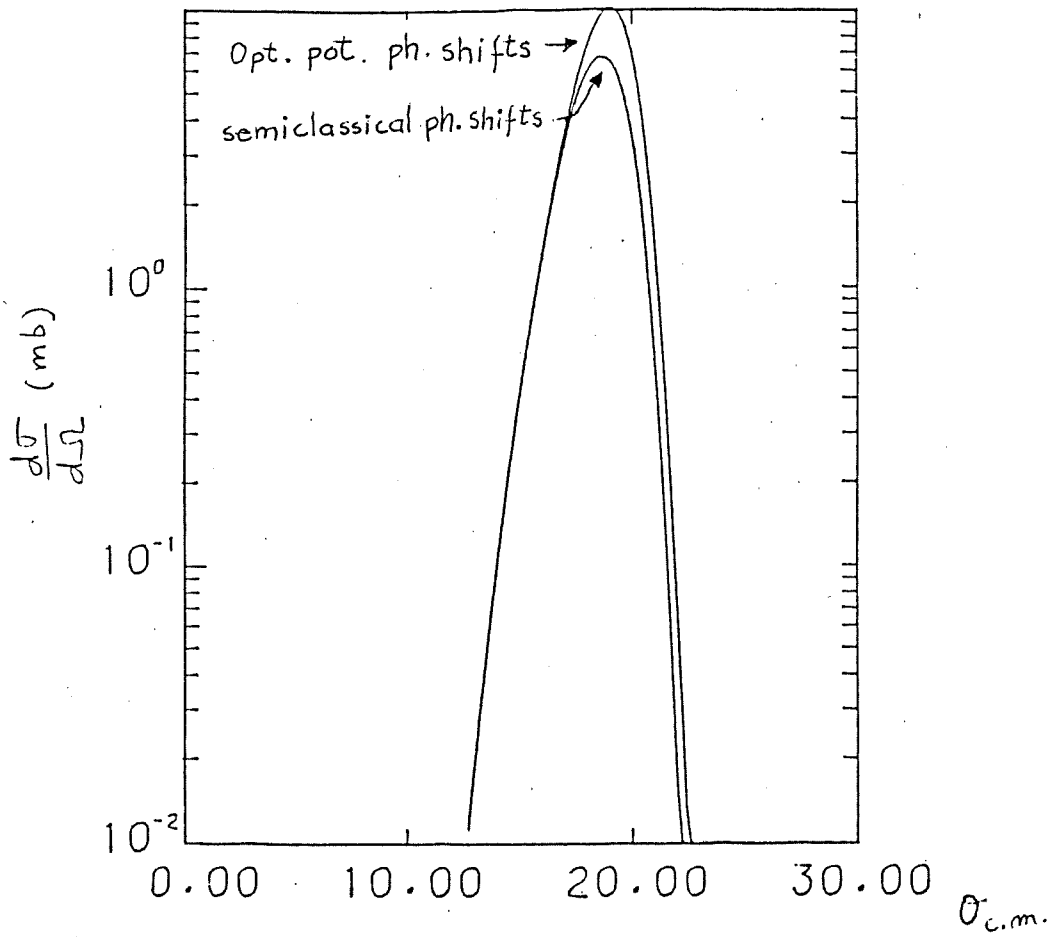

Fig.IV.8 The same as Fig.IV.7 but with $P_{tr}(j_1,j_2)$. This takes into account the spin $\underset{\sim}{s}$ of the transferred neutron by coupling to $\underset{\sim}{j}=\underset{\sim}{l}+\underset{\sim}{s}$. Angular distributions with exact and semiclassical phase shifts are compared.

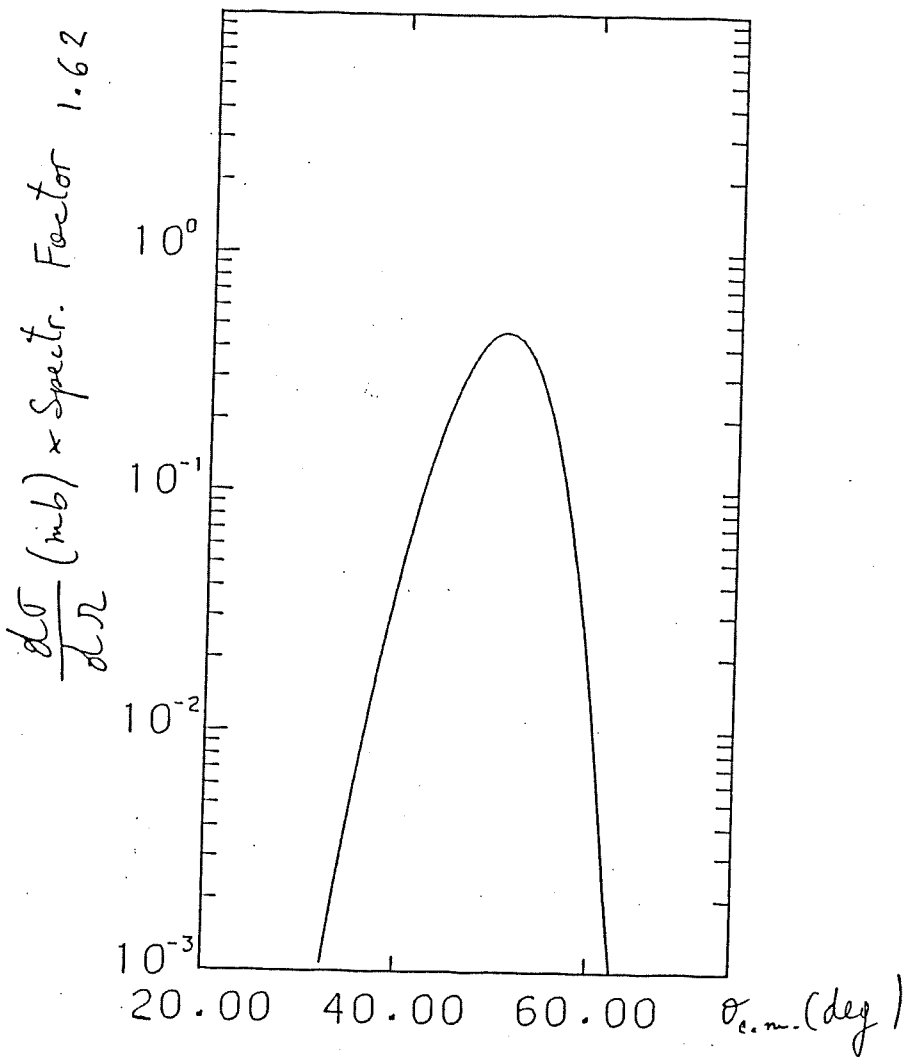

Fig. IV.9 Classical angular distributions for $^{208}Pb(^{16}O,^{15}O)$ $^{209}Pb\{i_{11/2}, 0.78\,MeV\}$ at E_{lab}=139 MeV. The transfer probability $P_{tr}(j_1, j_2)$ includes the spin of the transferred neutron.

IV.3 Angular distributions calculated from partial-wave formula.

In this section we apply the formulæ of Chapter II and Chapter III to the reactions $^{208}Pb(^{16}O,^{15}O)^{209}Pb$ at 139 and 312.6 MeV laboratory energy (Olmer et al. 1978) and $^{26}Mg(^{11}B,^{10}B)^{27}Mg$ at 114 MeV (Paschopoulos et al. 1975). These reactions (Lo Monaco and Brink 1978) have been chosen as typical: the first of bell-shaped angular distributions and the second of diffractive ones. We also show an example of neutron transfer between medium-mass nuclei, namely the reaction $^{34}S(^{32}S,^{33}S)^{33}S$.

The elastic scattering phase shifts in the transition matrix (III.28) were determined by numerically solving the Schrödinger equation with optical potentials having a Saxon-Woods form for both the real and imaginary parts. We used the parameters in table IV.1 which give a good fit to elastic scattering. The potentials in the final channel differ only by the radius $R_{R(I)}$. The normalization constants C_{ℓ_1} and C_{ℓ_2} in *eqs.* $(II.28)$ and $(II.19)$ are given by the ratio between the exact (numerically determined) solution of the radial Schrödinger equation for the neutron bound in nucleus 1 or 2 and the function $\gamma\chi_l(\gamma r)$ of *eqs.* $(II.19)$ and $(II.20)$. To determine the bound-state wavefunctions we used the Saxon-Woods potentials in table IV.2. The depth of the potential well was adjusted in each case to give the experimental neutron separation energy. In the case of $^{209}Pb(^{16}O,^{15}O)^{208}Pb$, following Olmer et al. (1978), we added a spin-orbit potential of the form

$$U_{so} = -\frac{4V_{so}}{a_{so}r}\ \frac{\mathbf{L}\cdot\mathbf{S}}{1+\exp\left[\left(R_{so}-r\right)/a_{so}\right]}.$$

The transfer amplitude in *eq.* $(II.28)$ depends on the relative angular momentum quantum number L through the distance of closest approach d. For peripheral collisions we approximate the orbit by a Coulomb trajectory. Then d is given by *eq.*$(III.11)$. For the

Table IV.1 Optical potential parameters used to determine elastic scattering phase shifts. $V_{R(I)}$, $a_{R(I)}$ and $R_{R(I)}$ are the potential depth, diffusivity and radius for the real (imaginary) part of the potential. The radius parameter r_0 is related to R by $R_{R(I)} = r_{0R(I)}(A_1^{1/3} + A_2^{1/3})$, where A_1 and A_2 are the mass numbers of the two nuclei.

Entrance channel	V_R (MeV)	a_R (fm)	r_{0R} (fm)	V_I (MeV)	a_I (fm)	r_{0I} (fm)
^{16}O(139 MeV) + ^{208}Pb†	50	0.612	1.221	50	0.612	1.194
^{16}O(312.6 MeV) + ^{208}Pb‡	50	0.682	1.181	50	0.682	1.145
^{11}B(114 MeV) + ^{26}Mg§	35	0.8	1.066	25	0.62	1.216

† From Pieper *et al* (1978).
‡ From Olmer *et al* (1978).
§ From Paschopoulos *et al* (1975).

Table IV.2 Parameters of the bound-state potentials. Radii are related to the radius parameters by $R = r_0 A^{1/3}$, where A is the mass number of the core. The last column gives the ratio of the potential slope $1/a$ to the quantity γ.

System	r_0 (fm)	a (fm)	V_{so} (MeV)	r_{so} (fm)	a_{so} (fm)	Ground-state binding energy (MeV)	$(a\gamma)^{-1}$
^{10}B + n†	1.2	0.65	0			−11.46	2.0
^{26}Mg + n†	1.2	0.65	0			−6.4	2.77
^{15}O + n‡	1.2	0.65	7	1.2	0.65	−15.7	1.77
^{208}Pb + n‡	1.25	0.63	7	1.1	0.5	−3.94	3.53

† From Paschopoulos *et al* (1975).
‡ From Olmer *et al* (1978).

calculations presented in this section we took d to be the distance of closest approach for the initial channel, assuming no change in the angular momentum L. The velocity v at the point of closest approach is then given by

$$v = \frac{\hbar L}{\mu d}, \qquad (IV.8)$$

where μ is the reduced mass in the initial channel. The transfer amplitude A_L was calculated from *eq.* $(II.28)$ and the angular distributions from *eqs.* $(III.28)-(III.31)$. The results for $^{208}Pb(^{16}O,^{15}O)^{209}Pb$ at 139 and 312.6 MeV laboratory energy are reported in figs. IV.10 and IV.11 respectively. The experimental data and DWBA calculations of Olmer et al. (1978) are shown in the same figures.

Fig. IV.12 shows angular distributions for the reaction $^{26}Mg(^{11}B,^{10}B)^{27}Mg$ at 114 MeV, together with experimental data and DWBA calculations of Paschopoulos et al.(1975). For this reaction our results are very similar to those obtained by Hasan and Brink (1978) by reducing the amplitude (II.5) to a one-dimensional integral which is evaluated numerically.

In all cases our cross-sections are normalized by the same spectroscopic factors used for the DWBA calculations. Relevant values of the Coulomb barrier E_{CB} and Sommerfeld parameter n are indicated in the figures.

It can be seen that the shapes of the angular distributions agree quite well with experimental data and DWBA calculations. However, there are some discrepancies in magnitude when compared with DWBA. Our calculated cross section for the lower states in Pb is too large at 312.6 MeV while it is too small for the highest state at 139 MeV. For the $^{26}Mg(^{11}B,^{10}B)$ reaction our calculated cross sections are a bit too large.

We studied the dependence of the results on the choice of the distance of closest

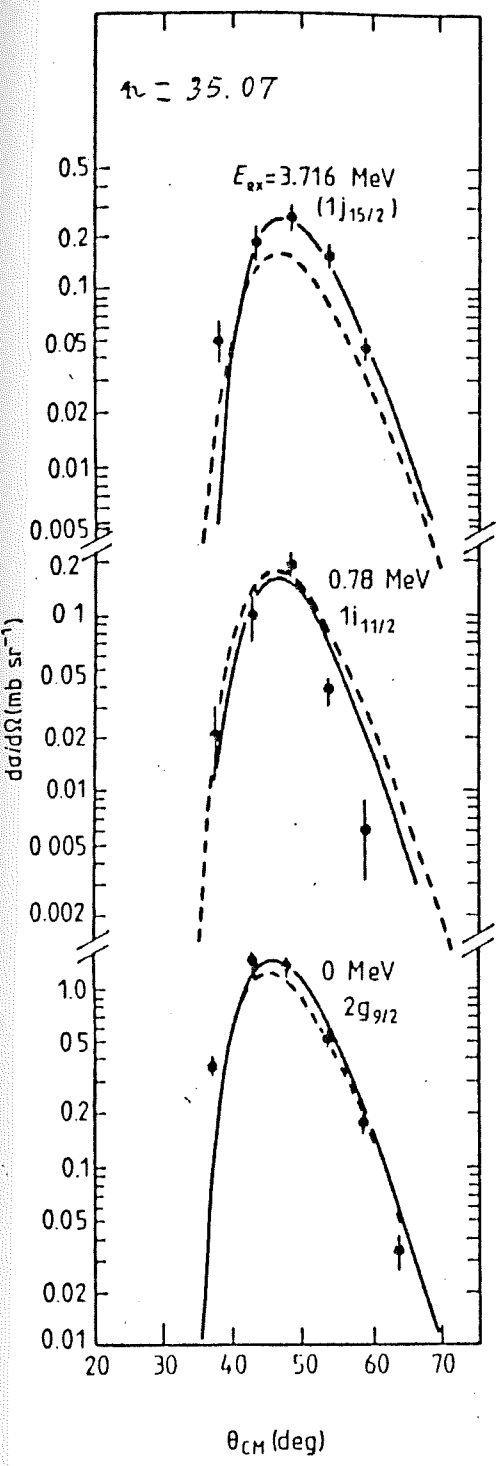

Figure *IV .10* Angular distributions for the ^{208}Pb(^{16}O, ^{15}O)^{209}Pb reaction at 139 MeV. The full curves represent DWBA calculations of Olmer *et al* (1978) while the broken curves are obtained using our formulae.

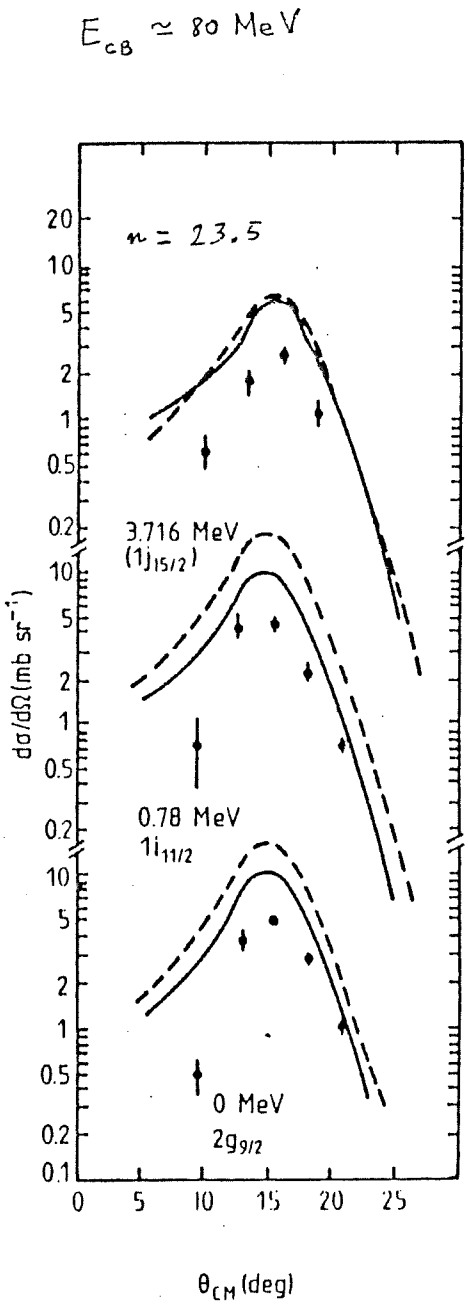

Figure *IV.11* Angular distributions for the ^{208}Pb(^{16}O, ^{15}O)^{209}Pb reaction at 312.6 MeV. The full curves represent DWBA calculations. The broken curves indicate our predictions.

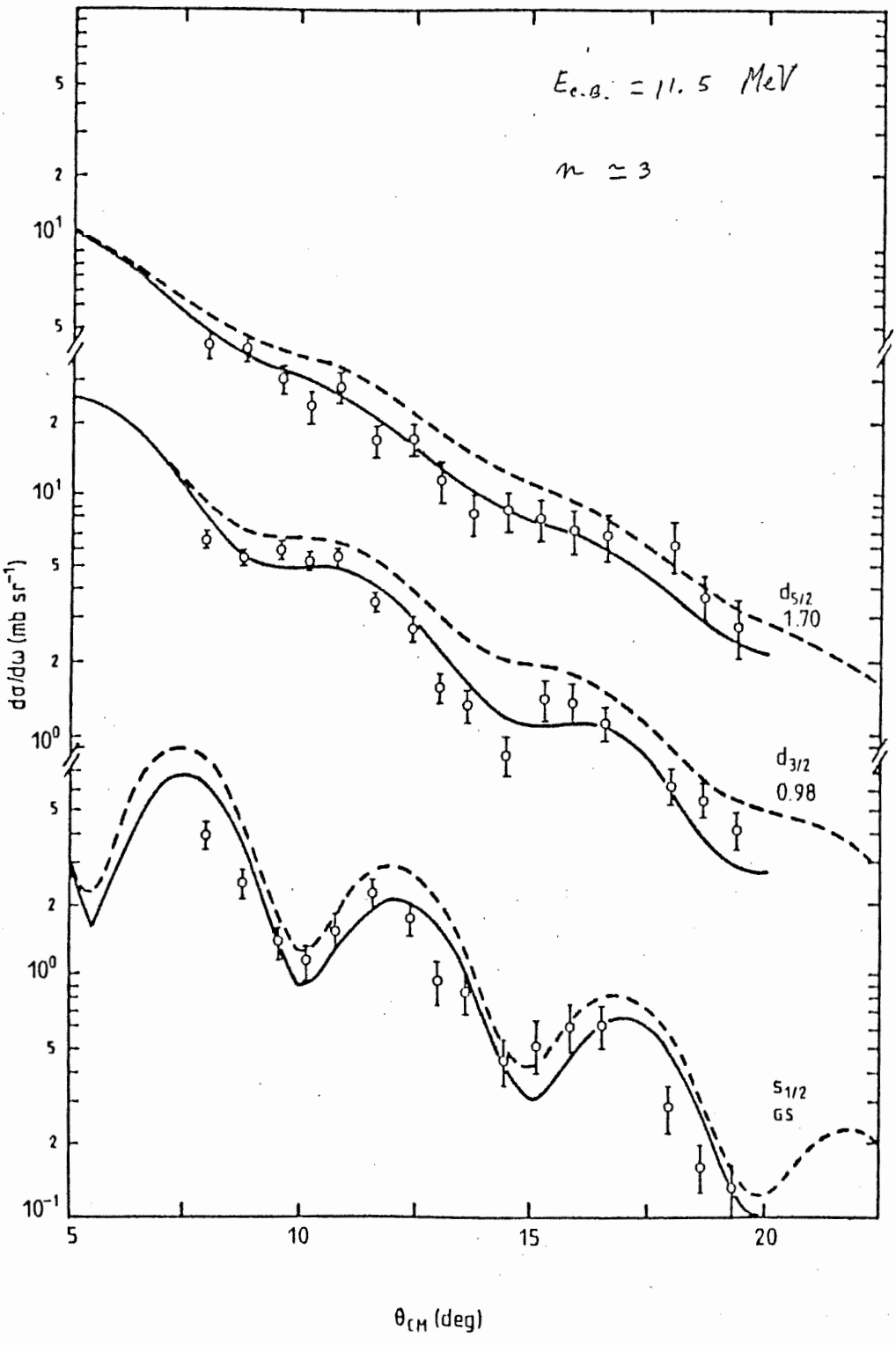

Figure IV.2 Differential cross sections for the $^{26}Mg(^{11}B, ^{10}B)^{27}Mg$ reaction at 114 MeV. The DWBA calculations of Paschopoulos *et al* (1975) are indicated by full curves. The broken curves correspond to the present calculation.

approach d. The results in figs. (IV.10-12) correspond to choosing d to be the distance of closest approach in the initial channel. We also made calculations by choosing d as the average of the distances of closest approach in the initial and final channel. The shapes of the angular distributions are not affected, but the magnitude is changed. some results for the peak cross sections for the ground-state transitions are shown in table IV.3. The effect of the different choice can be quite large, especially at the lowest incident energy for $^{16}O + ^{208}Pb$. This is because the distance of closest approach jumps from its value d_i for the initial channel to a larger value d_f in the final channel, because the energy of relative motion is diminished by the negative Q-value and because the reduced mass changes. If the change in angular momentum L of relative motion were taken into account it could allow the distance of closest approach to vary smoothly from the initial to the final channel.

In fig. IV.13 we show our results for the pick-up reaction $^{34}S(^{32}S,^{33}S)^{33}S_{d3/2\ g.s.}$ at E_{lab}=97.09 MeV. The experimental data are from Bilwes et al. (1983). Also shown are these authors' calculations obtained by an approximate DWBA treatment. This includes a parametrization of the elastic scattering matrix similar to eqs. (IV.6-7). We only calculated the forward-angle part of the angular distribution, which is symmetrical due to the identity of the final nuclei. We used the Saxon-Woods potential parameters given by Bilwes et al. (1985) for the elastic scattering of the initial system $^{32}S + ^{34}S$ at 97.09 MeV (V_R=29.8 MeV, a_R=0.65 fm, r_{0R}=1.25 fm, V_I=14.6 MeV, a_I=0.464 fm, r_{0I}=1.35 fm) to compute the phase shifts numerically. The potential in the final channel, $^{33}S + ^{33}S$, differs only by the radius. The normalization was obtained with a standard bound-state potential (without spin-orbit term) with radius parameter r_0=1.25 fm and diffuseness a=0.65 fm.

Table IV.3 Distances of closest approach and peak cross sections for the ground-state transitions in the three reactions considered. $d_{i(f)}$ is the distance of closest approach for a Coulomb trajectory in the initial (final) channel with angular momentum L_g. This is defined by the condition that the reflection coefficient $|S_{L_g}|^2 = \frac{1}{2}$. The last four lines show the values of the cross sections at the main maximum. σ_{expt}, σ_{DWBA} and σ_{d_i} correspond to the values in figures 2, 3 and 4, σ_{d_i} being our calculated cross section. In the last line $\sigma_{\bar{d}}$ is the cross section obtained by choosing d as the average between the distances of closest approach in the initial and final channels.

	$^{208}Pb(^{16}O, ^{15}O)^{209}Pb$		$^{26}Mg(^{11}B, ^{10}B)^{27}Mg$
	$E_{Lab} = 139$ MeV	$E_{Lab} = 312.6$ MeV	$E_{Lab} = 114$ MeV
L_g	74	143	39
d_i(fm)	12.18	11.68	7.7
$(d_f - d_i)$(fm)	1.08	0.59	0.49
σ_{expt}(mb)	1.47	5.0	$\geqslant 4.0$
σ_{DWBA}(mb)	1.47	10.0	7.2
σ_{d_i}(mb)	1.25	16.6	9.0
$\sigma_{\bar{d}}$(mb)	0.36	9.24	6.0

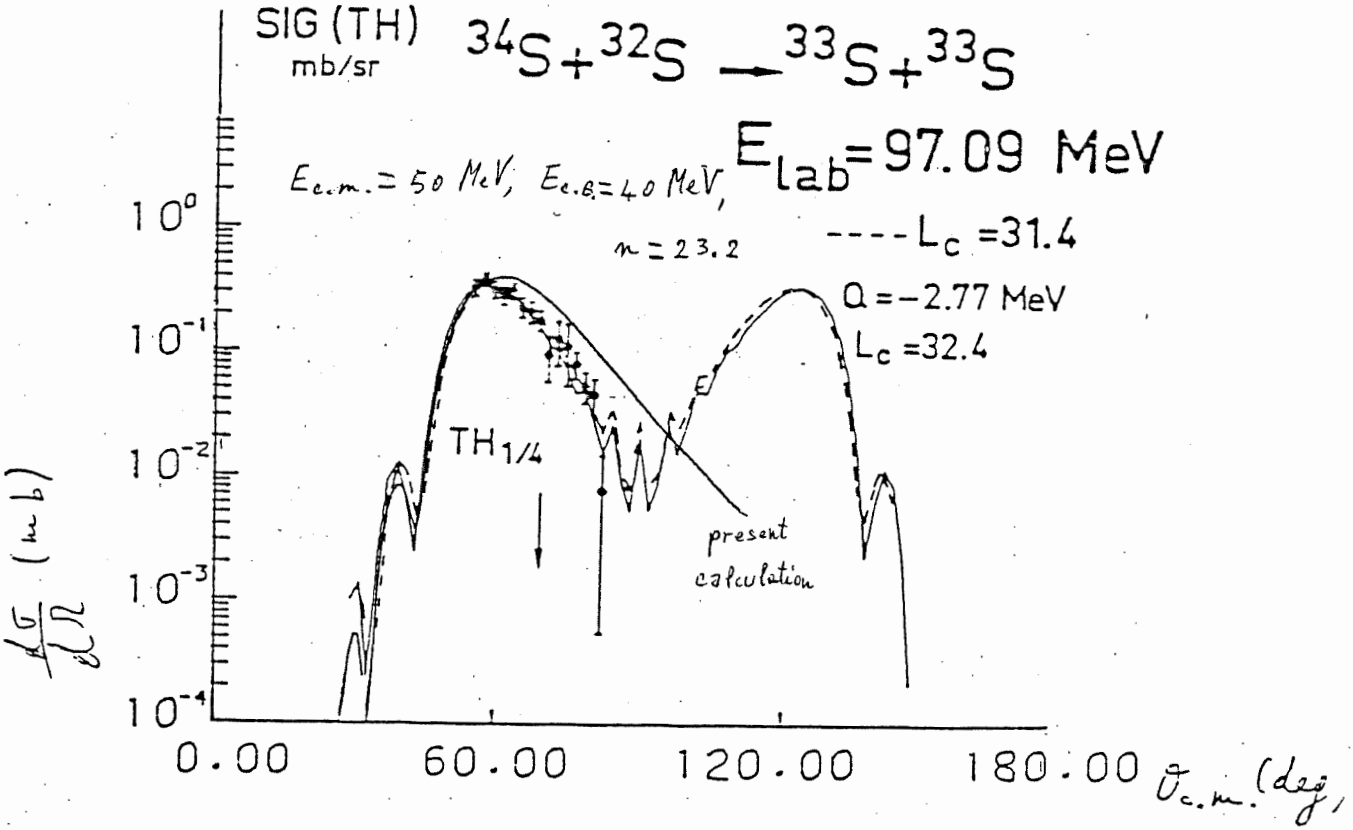

Fig.IV.13 Angular distribution for $^{34}S(^{32}S,^{33}S)^{33}Sd_{3/2}$ at E_{lab}=97.09 MeV. Our calculation is indicated in the figure. Experimental data and approximate DWBA calculations of Bilwes et al.(1983) are drawn on the experimental data. They computed the broken curve by using S-parameters deduced from elastic scattering data while the full curve was obtained by fitting the transfer experimental data.

The distance of closest approach (d.c.a.) d that enters in the transfer amplitude (II.28) was taken as the average

$$\bar{d}(L) = \frac{d_i(L) + d_f(L)}{2},$$

where $d_{i(f)}(L)$ is the d.c.a. in the initial (final) channel as a function of the relative angular momentum L of the partial-wave sum (III.28). Our calculation at forward angle is very close to that of Bilwes et al.

Chapter V. Proton Transfer Amplitude

V.1 Modification of the Amplitude by Coulomb Potentials.

In this chapter we extend the formalism of Chapter II to the analytical calculation of the amplitude $(II.5)$ for proton transfer. *A priori,* one would expect that both the perturbation approach and the surface integral approximation, *eq.*$(II.9)$, are not accurate enough because of the long range of the Coulomb potential. In fact the potential of one nucleus affects the proton wave funcion in the other even before transfer. By using a method similar to that employed by Hasan (1976), we shall take this into account in an approximate way. Then the analytical calculation proceeds in a parallel way to the method developed in § II.5 for neutron transfer.

The transfer amplitude for the reaction

$$a_1 + c_2 \longrightarrow c_1 + a_2$$

or

$$(c_1 + p) + c_2 \longrightarrow c_1 + (c_2 + p)$$

is still defined as in *eq.* $(II.3)$:

$$A(2,1) = < \Psi_2 | \Psi >_{t=\infty} .$$

Now the initial and final states of the proton bound in the nucleus a_1 or a_2 satisfy the following time-dependent Schrödinger equations:

$$i\hbar \frac{\partial \Psi_1(\mathbf{r},t)}{\partial t} = [T + V_1(\mathbf{r},t) + V_2^C(\mathbf{r},t)]\Psi_1(\mathbf{r},t), \qquad (V.1)$$

$$i\hbar\frac{\partial\Psi_2(\mathbf{r},t)}{\partial t} = [T + V_2(\mathbf{r},t) + V_1^C(\mathbf{r},t)]\Psi_2(\mathbf{r},t), \qquad (V.2)$$

where, for $\alpha = 1, 2$,

$$V_\alpha(\mathbf{r}_\alpha) = V_\alpha^N(\mathbf{r}_\alpha) + V_\alpha^C(\mathbf{r}_\alpha), \qquad (V.3)$$

In *eq.* $(V.1)$ the term $V_2^C(\mathbf{r},t)$ represents the effect of the Coulomb potential of nucleus a_2 on the proton when it is bound in nucleus a_1 and viceversa for $V_1^C(\mathbf{r},t)$ in *eq.* $(V.2)$. V_1 and V_2 are the potentials of the isolated cores c_1 and c_2, respectively. They consist of a short-range nuclear part and a long-range Coulomb term. The nuclear potential can have a Saxon-Woods form

$$V_\alpha^N(\mathbf{r}_\alpha) = \frac{-V_{0\alpha}}{1 + \exp\left(\frac{r_\alpha - R_\alpha}{a_\alpha}\right)} \qquad (V.3')$$

and the Coulomb potential can be that of two point charges

$$V_\alpha^C(\mathbf{r}_\alpha) = \frac{Z_{c_\alpha}e^2}{r_\alpha} \qquad (V.3'')$$

for the proton outside the nuclear surface or that of a particle in a charged sphere.

The wave function $\Psi(\mathbf{r},t)$ of the proton interacting with both nuclei is the solution of the Schrödinger equation:

$$i\hbar\frac{\partial\Psi}{\partial t} = (T + V_1 + V_2)\Psi, \qquad (V.4)$$

with the initial condition that $\Psi \to \Psi_1$ when $t \to -\infty$.

From *eqs.* $(V.2)$ and $(V.4)$ we have

$$i\hbar\frac{\partial}{\partial t} < \Psi_2|\Psi > = < \Psi_2|V_1 - V_1^C|\Psi > = < \Psi_2|V_1^N|\Psi > . \qquad (V.5)$$

Integrating *eq.* $(V.5)$ over time between $-\infty$ and $+\infty$ we find

$$A(2,1) \equiv < \Psi_2|\Psi >_{t=\infty} = \frac{1}{i\hbar}\int_{-\infty}^{+\infty} < \Psi_2|V_1^N|\Psi > \; dt. \qquad (V.6)$$

Eq. $(V.6)$ is an exact expression for the proton transfer amplitude. Since it contains a matrix element of the nuclear potential it is non-zero only in the region where $V_1^N \neq 0$. In this region the nuclear potential $V_2^N \simeq 0$ but the Coulomb potential V_2^C is still present. Then we approximate the wave function Ψ by Ψ_1 [cf. *eqs.* $(V.1)$ and $(V.4)$] and we get

$$A(2,1) = \frac{1}{i\hbar}\int_{-\infty}^{+\infty} < \Psi_2|V_1^N|\Psi_1 > \; dt \qquad (V.7a)$$

$$= \frac{1}{i\hbar}\int_{-\infty}^{+\infty} < \Psi_2|V_2^N|\Psi_1 > \; dt \qquad (V.7b)$$

We shall use the first form. Then, analogously to the neutron case, *eq.* $(V.7a)$ can be transformed (Appendix V.A) into

$$A(2,1) = \frac{\hbar}{2mi}\int_{-\infty}^{+\infty} dt \int_{\Sigma} d\mathbf{S}\cdot(\Psi_2^*\nabla\Psi_1 - \Psi_1\nabla\Psi_2^*)$$

$$+\frac{1}{i\hbar}\int_{-\infty}^{+\infty} dt\left[\int_{R_1}\Psi_2^* V_2^N \Psi_1 d^3\mathbf{r} + \int_{R_2}\Psi_2^* V_1^N \Psi_1 d^3\mathbf{r}\right]. \qquad (V.8)$$

This is similar to the expression for neutron transfer, *eq.* $(II.8)$, but now Ψ_α and V_α, $(\alpha = 1,2)$ are proton wave functions and potentials. The last term can be neglected, as we discussed in § II.4 for neutron transfer. Then the surface integral can be evaluated analytically as in the neutron case.

Eqs. $(V.1)$ and $(V.2)$ can be satisfied approximately by

$$\Psi_\alpha(\mathbf{r},t) \simeq \overline{\Psi}_\alpha(\mathbf{r},t)\; e^{-\frac{i}{\hbar}\phi_\alpha(\mathbf{r},t)}, \qquad (V.9)$$

where

$$i\hbar\frac{\partial\overline{\Psi}_\alpha(\mathbf{r},t)}{\partial t} = [T + V_\alpha(\mathbf{r},t)]\overline{\Psi}_\alpha(\mathbf{r},t), \qquad (V.10)$$

$$\left.\begin{aligned}\phi_1(\mathbf{r},t) &= \int_0^t V_2^C(\mathbf{r},t')\; dt' \\ \phi_2(\mathbf{r},t) &= \int_0^t V_1^C(\mathbf{r},t')\; dt'.\end{aligned}\right\} \qquad (V.11)$$

The functions $\overline{\Psi}_\alpha$ are solutions for the proton bound in nucleus α completely isolated, i.e. when the Coulomb interaction from the other nucleus is switched off. *Eqs.* (*V*.9) are solutions of (*V*.1) and (*V*.2) if one assumes that space derivatives of $\phi_\alpha(\mathbf{r},t)$ are small. This is reasonable since they contain potentials that go as $1/r$.

Hence, with the same system of reference and definitions as in Chapter II, we have

$$\overline{\Psi}_1(\mathbf{r},t) = \Phi_1\left(\mathbf{r}-\mathbf{s}(t)\right)\exp\left\{(i/\hbar)\left[m\mathbf{v}\cdot\mathbf{r}-\left(\varepsilon_1+\frac{1}{2}mv^2\right)t\right]\right\}, \qquad (V.12)$$

$$\overline{\Psi}_2(\mathbf{r},t) = \Phi_2(\mathbf{r})\exp(-i\varepsilon_2 t/\hbar), \qquad (V.13)$$

where the bound-state proton wavefunctions Φ_α satisfy the eigenvalue equations

$$[T+V_\alpha(\mathbf{r}_\alpha)]\Phi_\alpha(\mathbf{r}_\alpha) = \varepsilon_\alpha\Phi_\alpha(\mathbf{r}_\alpha), \qquad \alpha = 1,2. \qquad (V.14)$$

Here V_α are the proton static potentials and ε_α the corresponding binding energies. We assumed that V_2 is at rest while V_1 moves along the trajectory $\mathbf{s}(t)$. Since the biggest contribution to the integral over Σ comes from the point of closest approach (fig. II.1) we approximate $V_\alpha^C(r_\alpha)$ by their values at the point of closest approach given by the coordinates $x_\alpha, y=0, z=0$, where $x_1 = d_2 - d = -d_1$ and $x_2 = d_2$ (see fig. II.2). By doing so *eqs.* (*V*.11) give

$$\phi_1 \simeq V_2^C(d_2)\ t = \frac{Z_{c_2}e^2}{d_2}\ t, \qquad \phi_2 \simeq V_1^C(d_1)\ t = \frac{Z_{c_1}e^2}{d_1}\ t. \qquad (V.15)$$

Setting this into the first line of *eq.* (*V*.8) gives

$$A(2,1) = \frac{-\hbar}{2mi}\int_{-\infty}^{+\infty} dt \int_{-\infty}^{+\infty} dy \int_{-\infty}^{+\infty} dz \Bigg\{ \Phi_2^*(d_2,y,z)\frac{\partial}{\partial d_2}\Phi_1(d_2-d,y,z-vt)$$

$$-\Phi_1(d_2-d,y,z-vt)\frac{\partial}{\partial d_2}\Phi_2^*(d_2,y,z)$$

$$+\frac{i}{\hbar}t\Phi_1(d_2-d,y,z-vt)\Phi_2^*(d_2,y,z)\left(\frac{\partial}{\partial d_2}V_1^C(d_1)-\frac{\partial}{\partial d_2}V_2^C(d_2)\right)\Bigg\}$$

$$\exp\left\{\frac{i}{\hbar}\left[mvz+\left(\varepsilon_2-\varepsilon_1-\frac{1}{2}mv^2+V_1^C(d_1)-V_2^C(d_2)\right)t\right]\right\}, \qquad (V.16)$$

Henceforth we neglect the term containing derivatives of V_α^C. This is consistent with the approximation in *eq.* (*V*.9). With the change of variables $(z,t) \rightarrow (z, z_1 = z - vt)$ the argument of the exponential in *eq.* (*V*.16) becomes

$$\frac{i}{\hbar v}\left[\left(\frac{1}{2}mv^2 - Q_{eff}\right)z + \left(\frac{1}{2}mv^2 + Q_{eff}\right)z_1\right]$$

where

$$Q_{eff} = \varepsilon_1 - \varepsilon_2 - [V_1^C(d_1) - V_2^C(d_2)] = Q - [V_1^C(d_1) - V_2^C(d_2)] = \bar{\varepsilon}_1 - \bar{\varepsilon}_2. \qquad (V.17a)$$

with

$$\bar{\varepsilon}_\alpha = \varepsilon_\alpha - V_\alpha^C(d_\alpha) = \varepsilon_\alpha - \frac{Z_{c_\alpha}e^2}{d_\alpha}, \qquad \alpha = 1,2. \qquad (V.17b)$$

In *eq.* (*V*.17*b*) the Coulomb potential between the proton and the core c_α is that of two point charges. This form of the effective Q-value is different from the one used in other references. We discuss the difference at the end of this chapter. *Eq.* (*V*.16) gives

$$A(2,1) = -\frac{i\hbar}{2mv}\int_{-\infty}^{+\infty}[\tilde{\Phi}_2^*(d_2,y,k_{2z})\frac{\partial}{\partial d_2}\tilde{\Phi}_1(d_2-d,y,k_{1z})$$

$$-\tilde{\Phi}_1(d_2-d,y,k_{1z})\frac{\partial}{\partial d_2}\tilde{\Phi}_2^*(d_2,y,k_{2z})]dy, \qquad (V.18)$$

where the Fourier transform $\tilde{\Phi}(x,y,k)$ is defined in *eq.* $(II.16)$ but now

$$k_{1z} = -(Q_{eff} + \frac{1}{2}mv^2)/(\hbar v), \qquad k_{2z} = -(Q_{eff} - \frac{1}{2}mv^2)/(\hbar v), \qquad (V.19)$$

Therefore

$$k_{\alpha z}^{proton} = k_{\alpha z}^{neutron} + \frac{V_1^C(d_1) - V_2^C(d_2)}{\hbar v} = k_{\alpha z}^{neutron} + \frac{e^2}{\hbar v}\left(\frac{Z_{c_1}}{d_1} - \frac{Z_{c_2}}{d_2}\right), \qquad \alpha = 1,2.$$

V.2 Calculation of the Proton Transfer Amplitude.

In this section we calculate the amplitude $(V.18)$ analytically. We use the same method developed in § II.5 for neutron transfer. The final formula is very similar to eq. (II.28) but contains effective binding energies and normalization constants that account for the Coulomb effects. By introducing the double Fourier transform $\tilde{\tilde{\Phi}}(x,k_y,k_z)$, defined by *eq.* $(II.50)$, we find

$$A(2,1) = -\frac{i\hbar}{4\pi mv}\int_{-\infty}^{+\infty}[\tilde{\tilde{\Phi}}_2^*(d_2,k_y,k_{2z})\frac{\partial}{\partial d_2}\tilde{\tilde{\Phi}}_1(d_2-d,k_y,k_{1z})$$

$$-\tilde{\tilde{\Phi}}_1(d_2-d,k_y,k_{1z})\frac{\partial}{\partial d_2}\tilde{\tilde{\Phi}}_2^*(d_2,k_y,k_{2z})]dk_y, \qquad (V.20)$$

which is identical to *eq.* $(II.52)$. In the proton case, however, *eq.* $(II.53)$ will contain a Coulomb term from the potential V which does not vanish on the surface Σ. So, in place of *eq.* $(II.54)$, we have, for $\alpha = 1,2$,

$$\left(\frac{\partial^2}{\partial x_\alpha^2} - \xi^2\right)\tilde{\tilde{\Phi}}_\alpha(x_\alpha,k_y,k_{\alpha z}) = \frac{2m}{\hbar^2}\int_{-\infty}^{+\infty}\int_{-\infty}^{+\infty} e^{-i(k_y y + k_{\alpha z})}\, V_\alpha^C(|x_\alpha|,y,z)$$

$$\cdot\Phi_\alpha(x_\alpha,y,z)\; dydz, \qquad (V.21)$$

where $x_1 = d_2 - d = -d_1$ and $x_2 = d_2$ are the distances of the surface Σ from the two nuclei at closest approach *(see figs. II.1 and II.2)*.

One could try to solve *eq.* (*V*.21) by iteration, taking as a first approximation for Φ_α on the *r.h.s.* an Hankel function form which corresponds to the case of vanishing potential. The simplest thing to do, however, is to approximate the Coulomb potentials by their value at the point of closest approach given by the coordinates $|x_\alpha| \equiv d_\alpha, y = 0, z = 0$. Then *eq.* (*V*.21) gives

$$\left(\frac{\partial^2}{\partial x_\alpha^2} - \bar{\xi}_\alpha^2\right) \tilde{\tilde{\Phi}}_\alpha(x_\alpha, k_y, k_{\alpha z}) = 0, \tag{V.22}$$

where $\alpha = 1, 2$ and

$$\left.\begin{aligned} \bar{\xi}_\alpha &= \sqrt{\bar{\gamma}_\alpha^2 + k_y^2 + k_{\alpha z}^2}, \\ \bar{\gamma}_\alpha = \frac{1}{\hbar}\sqrt{-2m\bar{\varepsilon}_\alpha} &= \frac{1}{\hbar}\sqrt{-2m\left[\varepsilon_\alpha - V_\alpha^C(d_\alpha)\right]}. \end{aligned}\right\} \tag{V.23}$$

Notice that with these definitions $\bar{\xi}_1 = \bar{\xi}_2 \equiv \bar{\xi}$, which makes the analytical calculation feasible. The effective parameters $\bar{\gamma}_\alpha$ in *eq.* (*V*.23) can be written as

$$\bar{\gamma}_\alpha = \gamma_\alpha \sqrt{1 - \frac{\Delta\epsilon_\alpha}{\varepsilon_\alpha}}, \tag{V.24}$$

where γ_α are defined by *eq.* (*II*.21) in terms of the proton binding energies ε_α and

$$\Delta\epsilon_\alpha = V_\alpha^C(d_\alpha) = \frac{Z_{c_\alpha} e^2}{d_\alpha}. \tag{V.24'}$$

In *eq.* (*V*.24') we have explicitly inserted the Coulomb potential between the proton and the charge of the core c_α. If $\frac{\Delta\epsilon_\alpha}{\varepsilon_\alpha} \ll 1$ we can use the following approximation:

$$\bar{\gamma}_\alpha \simeq \gamma_\alpha - \frac{1}{2}\gamma_\alpha \frac{\Delta\epsilon_\alpha}{\varepsilon_\alpha} = \gamma_\alpha + \frac{m Z_{c_\alpha} e^2}{\hbar^2 d_\alpha \gamma_\alpha} = \gamma_\alpha + \frac{n_\alpha}{d_\alpha}, \tag{V.24''}$$

where

$$n_\alpha = \frac{m Z_{c_\alpha} e^2}{\hbar^2 \gamma_\alpha} \qquad (V.25)$$

are the Sommerfeld parameters for the initial and final bound states.

However, *eq.* $(V.24'')$ is not always a good approximation. For example, the reaction $^{208}Pb(^{16}O,^{15}N)^{209}Bi$ at 312.6 MeV has a grazing distance $d \approx 12\ fm = d_1 + d_2$. With the prescription of p. 28, $d_1/d_2 = A_1^{1/3}/A_2^{1/3}$, where A_1 and A_2 are the mass numbers of the two nuclei, we have $d_1 = 3.58\ fm$, $d_2 = 8.42\ fm$ and

$$\varepsilon_1 = -12.13\ Mev, \qquad \Delta\epsilon_1 = \frac{7 * 1.44}{3.58} = 2.82\ \text{MeV}$$

but

$$\varepsilon_2 = -3.8\ Mev, \qquad \Delta\epsilon_2 = \frac{82 * 1.44}{8.42} = 14\ \text{MeV}\,.$$

As a next step we need to approximate the radial proton wavefunction which enters in $\tilde{\tilde{\Phi}}$. We write the actual proton wavefunction (obtained by numerical integration of the Schrödinger equation with both nuclear and Coulomb potentials) as

$$\Phi^{proton}_{radial}(r) = \frac{\mathcal{R}_\ell(r)}{r}.$$

Then $\mathcal{R}_\ell$ satisfies the radial equation

$$\left[\frac{d^2}{dr^2} - \frac{l(l+1)}{r^2} - \frac{2m}{\hbar^2}V(r) - \gamma^2\right]\mathcal{R}_\ell = 0. \qquad (V.26)$$

At a distance greater than the nuclear potential range (as on the surface Σ where $r_\alpha = \sqrt{x_\alpha^2 + y^2 + z^2}$) the potential $V(r)$ reduces to its Coulomb part $\frac{Z_c e^2}{r}$ only. Dividing by $4\gamma^2$ and setting

$$k = -\frac{m Z_c e^2}{\hbar^2 \gamma} \equiv -n, \qquad \mu = \ell + \frac{1}{2}, \qquad z = 2\gamma r,$$

eq. $(V.26)$ can be cast in the form of the Whittaker equation (Abramowitz and Stegun, 1970, p.505)

$$\frac{d^2\mathcal{R}_\ell}{dz^2} + \left(-\frac{1}{4} + \frac{k}{z} + \frac{1/4 - \mu^2}{z^2}\right)\mathcal{R}_\ell = 0. \qquad (V.27)$$

The solution of *eq.* $(V.27)$ which vanishes at infinity (as a bound state must do) is given by the Whittaker function

$$\mathcal{R}_\ell = W_{-n,\ell+1/2}(2\gamma r).$$

Then the radial part of the proton wave function is given by

$$\Phi^{proton}_{radial}(r) = B_\ell \frac{1}{r} W_{-n,\ell+1/2}(2\gamma r), \qquad r \geq r_\alpha, \qquad (V.28)$$

where B_ℓ is a normalization constant which keeps into account the behaviour of the wave function inside the region of the nuclear potential. However, the form (V.28) is still too complicated for an analytical calculation of the transfer amplitude. Then we approximate the wavefunction by

$$\Phi^{proton}_{radial}(r) \simeq C^p_\ell \ \bar{\gamma}\ \chi_\ell(\bar{\gamma}r) \equiv \Phi_{approx}(r), \qquad (V.29)$$

where $\chi_\ell(\bar{\gamma}r)$ is the neutron wave function defined in $(II.19)$ and C^p_ℓ is a normalization constant that depends on r. We choose it such that

$$\Phi_{approx}(r_\Sigma) = \Phi_{exact}(r_\Sigma)$$

on the surface Σ where it is needed. With this we have for r very large

$$\Phi^{proton}_{radial}(r) \sim C^p_\ell \ \frac{e^{-\bar{\gamma}r}}{r}$$

For distances of the order of the distance of closest approach, d, eqs. $(V.28)$ and $(V.29)$ have a similar decay. Then we use the approximation $(V.29)$ to calculate the transfer amplitude

as in the neutron case, in particular from *eq.* $(II.53)$ to $(II.60)$. The result is

$$A(2,1) = -4\pi i \, \frac{\hbar}{m_p v} \, C^p_{\ell_1} C^p_{\ell_2} \, (-1)^{\lambda_1} \, Y_{\ell_1 \lambda_1}(\beta^p_1, 0) \, Y^*_{\ell_2 \lambda_2}(\beta^p_2, 0) \, K_{\lambda_1 - \lambda_2}(\bar{\eta} d), \qquad (V.36)$$

where

$$\cos \beta^p_\alpha = -i \, \frac{k_{\alpha z}}{\bar{\gamma}_\alpha}, \qquad \sin \beta^p_\alpha = \frac{\bar{\eta}}{\bar{\gamma}_\alpha}, \qquad \alpha = 1, 2, \qquad (V.37)$$

$k_{\alpha z}$ are given by *eq.* $(V.19)$ and

$$\bar{\eta} = \sqrt{k^2_{1z} + \bar{\gamma}^2_1} = \sqrt{k^2_{2z} + \bar{\gamma}^2_2} = \frac{1}{\hbar}\sqrt{-2m\bar{\varepsilon}}. \qquad (V.38)$$

Here

$$\bar{\varepsilon} = \frac{1}{2}(\bar{\varepsilon}_1 + \bar{\varepsilon}_2) - \frac{1}{4}\left(\frac{Q^2_{eff}}{\frac{1}{2} m_p v^2} + \frac{1}{2} m_p v^2 \right) \qquad (V.39)$$

is a kind of average bound-state energy for the proton.

The analytical formula (V.36) for proton transfer has the same form as eq. (II.28) for neutron transfer, but the quantities β and η are substituted by effective quantities, β^p and $\bar{\eta}$, eqs. (V.37)- (V.39), which take into account the Coulomb field. This results in a shift of the proton binding energies $\varepsilon_{1,2}$ by $\Delta\varepsilon_{1,2}$, *eqs.* $(V.24')$. Another difference is in the prescription $(V.29)$ for determining the normalization constants. Since the surface Σ on which the transfer amplitude is integrated lies between the two nuclei, a suitable choice is, for $\alpha = 1, 2$, to calculate C_{ℓ_α} at a distance d_α such that $d_1 + d_2 = d(L_{peak})$ and $d_1/d_2 = (A_1/A_2)^{1/3}$ Here $d(L_{peak})$ is the distance of closest approach for an orbit with L corresponding to the maximum of $|S_L A_L|$ and A_1 and A_2 are the mass numbers of the two nuclei.

V.3 Discussion of the effective Q-value.

As we mentioned in §V.2, our definition of the Q-value for proton transfer,

$$Q_{eff} = Q - \left(\frac{Z_{c_1}}{d_1} - \frac{Z_{c_2}}{d_2} \right) e^2 \qquad (V.17a)$$

is different from the one used elsewhere. In particular, a widely used definition is (Buttle and Goldfarb 197 i, Brink 1972, Broglia and Winther 1972)

$$Q^{(o)}_{eff} = Q - \frac{\left(Z^f_1 Z^f_2 - Z^i_1 Z^i_2 \right) e^2}{d}, \qquad (V.40)$$

where $Z^{i(f)}_{1,2}$ are the charges in the initial and final channels and d is the sum of the radii of the nuclei (neglecting differences between initial and final channel). To compare with our definition $(V.17a)$ we can put $d_1 + d_2 = d$. For proton transfer, in our notation (cf. beginning of this chapter), we have

$$Z^i_1 \equiv Z_{a_1} = Z_{c_1} + 1, \qquad Z^i_2 \equiv Z_{c_2};$$

$$Z^f_1 \equiv Z_{c_1} = Z^i_1 - 1, \qquad Z^i_2 \equiv Z_{a_2} = Z_{c_2} + 1 = Z^i_2 + 1.$$

Then

$$Q^{(o)}_{eff} = Q - \frac{\left(Z^i_1 - Z^f_2 \right) e^2}{d} = Q - \frac{\left(Z_{c_1} - Z_{c_2} \right) e^2}{d} \equiv Q + \Delta Q^{(o)}. \qquad (V.41)$$

If $d_1 = d_2 = d/2$ eq. (V.17a) gives

$$\Delta Q \equiv Q_{eff} - Q = 2 \frac{\left(Z_{c_2} - Z_{c_1} \right) e^2}{d} = 2 \Delta Q^{(o)}.$$

In general ΔQ and $\Delta Q^{(o)}$ are quite different. For example, in the case of the reaction $^{208}Pb(^{16}O,^{15}N)^{209}Bi$ at 312.6 MeV, with the values of d_1 and d_2 use at p. 82, we have

$$\Delta Q = \Delta \epsilon_2 - \Delta \epsilon_1 = 11.18\,\mathrm{MeV},$$

while eq. (V.41) gives

$$\Delta Q^{(o)} = 9\,\mathrm{MeV}\,.$$

Such a difference in Q_{eff} implies a different optimum kinetic energy for proton tranfer [cf. eq. (II.32)]

$$\frac{1}{2}m_p v^2 = |Q_{eff}|. \qquad (V.42)$$

The definition $(V.17a)$ of Q_{eff} follows in our calculation from the approximations (V.9) and (V.15) for the bound-state proton wavefunctions. One advantage of this definition is that the quantities $\bar{\xi}$, eq. (V.23), and $\bar{\eta}$, eq. (V.38), are the same for the initial and final state, as in the neutron case. This makes the analytical calculation of the transfer amplitude feasible. The new form (V.17a) of Q_{eff} may also be better than the old one, eq. (V.40), because it depends on the Coulomb potentials at the transfer point in the initial and final channel.

Appendix V.A Proton Transfer Amplitude as a Surface Integral

The matrix element in *eq.* $(V.7a)$ can be written as

$$< \Psi_2|V_1^N|\Psi_1 >= \int_{R_1} \Psi_2^* V_1^N \Psi_1 d^3\mathbf{r} + \int_{R_2} \Psi_2^* V_1^N \Psi_1 d^3\mathbf{r}. \qquad (V.A.1)$$

Eq. $(V.1a)$ gives

$$V_1^N \Psi_1 = (i\hbar\frac{\partial}{\partial t} + \frac{\hbar^2}{2m}\nabla^2 - V_1^C - V_2^C)\Psi_1, \qquad (V.A.2)$$

from which follows

$$\int_{R_1} \Psi_2^* V_1^N \Psi_1 d^3\mathbf{r} = \frac{\hbar^2}{2m}\int_\Sigma d\mathbf{S}\cdot(\Psi_2^*\nabla\Psi_1 - \Psi_1\nabla\Psi_2^*)$$

$$+\int_{R_1}\left(i\hbar\frac{\partial\Psi_2}{\partial t} + \frac{\hbar^2}{2m}\nabla^2\Psi_2\right)^*\Psi_1\ d^3\mathbf{r} + i\hbar\frac{\partial}{\partial t}\int_{R_1}\Psi_2^*\Psi_1 d^3\mathbf{r} - \int_{R_1}\Psi_2^*(V_1^C + V_2^C)\Psi_1\ d^3\mathbf{r}. \qquad (V.A.3)$$

Eq. $(V.2)$ gives

$$\left(i\hbar\frac{\partial\Psi_2}{\partial t} + \frac{\hbar^2}{2m}\nabla^2\Psi_2\right)^* = (V_2 + V_1^C)\Psi_2^*(\mathbf{r},t).$$

Then we substitute *eqs.* $(V.A.1)$ and $(V.A.3)$ into *eq.* $(V.7a)$. Integrating between $t=-\infty$ and $t=\infty$ the third term on the *r.h.s.* of *eq.* $(V.A.3)$ vanishes because there is no overlap between Ψ_1 and Ψ_2 long before and long after transfer. So we get

$$A(2,1) = \frac{\hbar}{2mi}\int_{-\infty}^{+\infty} dt \int_\Sigma d\mathbf{S}\cdot(\Psi_2^*\nabla\Psi_1 - \Psi_1\nabla\Psi_2^*)$$

$$+\frac{1}{i\hbar}\int_{-\infty}^{+\infty} dt\left[\int_{R_1}\Psi_2^* V_2^N\Psi_1 d^3\mathbf{r} + \int_{R_2}\Psi_2^* V_1^N\Psi_1 d^3\mathbf{r}\right] \qquad (V.A.4)$$

which is *eq.* $(V.8)$ of text.

Chapter VI. Proton Transfer Calculations

Here we show some results for the reaction $^{208}Pb(^{16}O,^{15}N)^{209}Bi$ at several incident energies and for various final states. The following angular distributions are obtained by using the analytical form (V.36) of the semiclassical transfer amplitude and the partial-wave formulæ (III.28)- (III.31) for the differential cross section. The phase shifts that enter in eq.(III.28) are calculated numerically for the initial channel only, i.e. we appoximate $\delta_L^i \simeq \delta_L^f$. In all cases we used the same optical potentials as for the DWBA calculations shown. The normalization constants C_ℓ^p that enter in the amplitude (V.36) are given by eq. (V.29). Following the discussion at the end of § V.2, p.84, we use

$$C^p_{\ell_\alpha}(d_\alpha) = \frac{\Phi_\alpha^{exact}(d_\alpha)}{\bar{\gamma}_\alpha \chi_{\ell_\alpha}(\bar{\gamma}_\alpha d_\alpha)}, \qquad \alpha = 1,2. \tag{VI.1}$$

In eq. (VI.1) $\chi_{\ell_\alpha}(\bar{\gamma}_\alpha r)$ is the Hankel function form (II.19),

$$\bar{\gamma}_\alpha^2 = -\frac{2m_p}{\hbar^2}\bar{\varepsilon}_\alpha, \tag{VI.2}$$

where

$$\bar{\varepsilon}_\alpha = \varepsilon_\alpha - \frac{Z_{c_\alpha}e^2}{d_\alpha} \tag{VI.3}$$

is the proton binding energy diminished by the Coulomb term. The distances d_α are such that $d_1 + d_2 = d(L_{peak}$ (cf. p. 84) in the initial channel.

Fig. VI.1 compares our angular distributions to the experimental data and DWBA calculations of Pieper et al. (1978) for the reaction $^{208}Pb(^{16}O,^{15}N)^{209}Bi$ at incident energies E_{lab} =138.5 and 216.6 MeV.

Fig. VI.2 shows our results for the same reaction at 312.6 MeV for several final states in ^{209}Bi. Experimental data and DWBa calculations (Olmer et al. 1978) are also shown.

Our cross sections are normalized by the spectroscopic factors given in the references cited. In all cases the shape of our angular distributions is very similar to the DWBA results. However, there are discrepancies in the magnitude of the cross section. At the highest incident energy, the transitions to the ground state ($h_{9/2}$) and to the excited state at 1.61 MeV ($i_{13/2}$) are well reproduced by our calculations. But the transfer to the $f_{7/2}$ state at 0.91 MeV excitation energy is underestimated, at variance with the DWBA prediction which is larger than the experimental data.

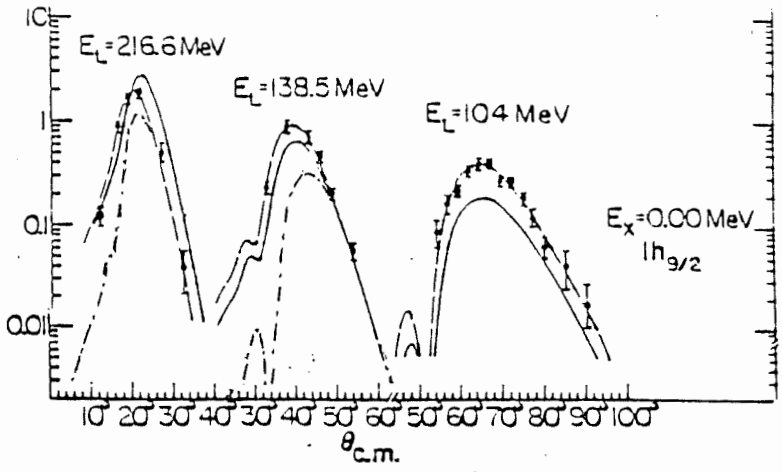

Fig.VI.1 Differential cross sections for the $^{208}Pb(^{16}O,^{15}N)^{209}Bi$ reaction. The solid curves are DWBA calculations, the dashed curves are those calculations shifted in angle and renormalized to best fit the data(Pieper et al. 1978).Our calculations are the dashed-dotted curves.The incident energy E_L is shown in the figure.

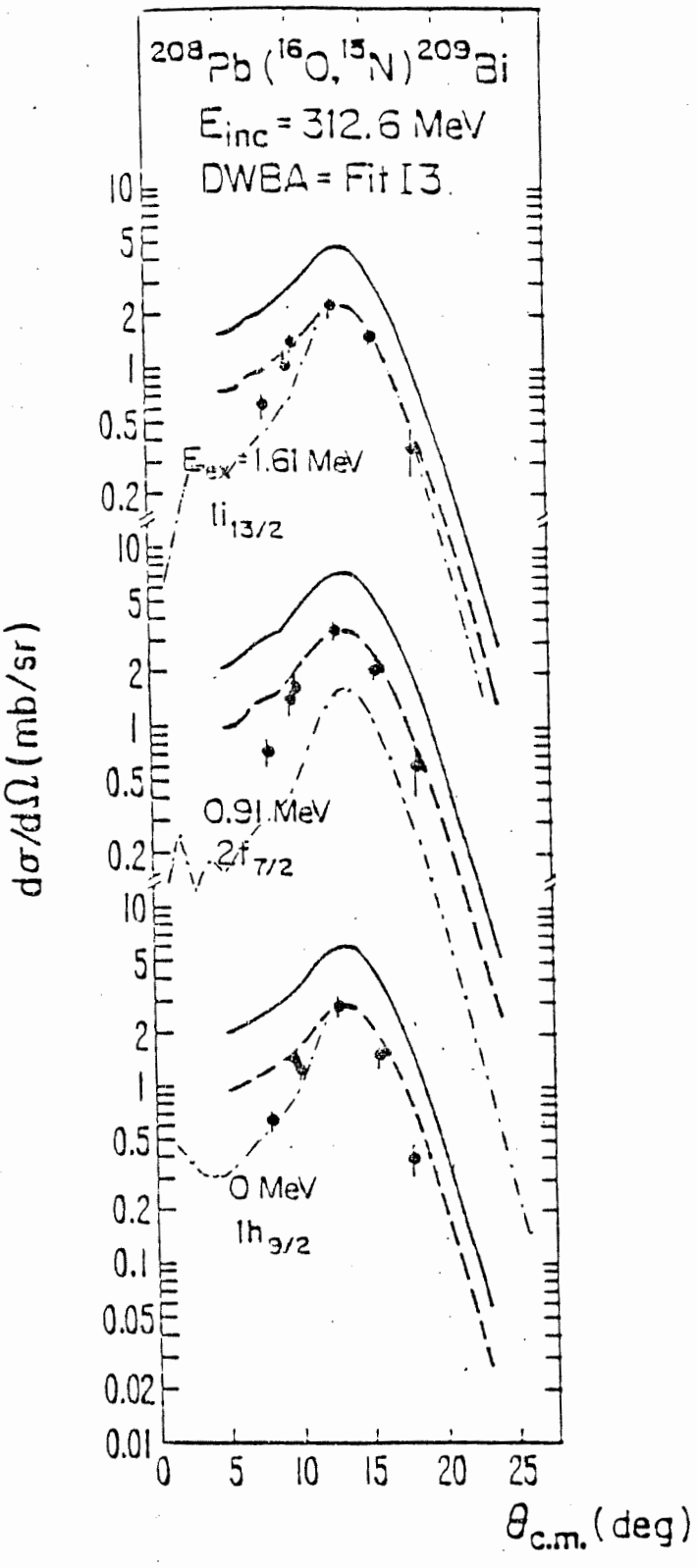

Fig.VI.2 The same as Fig.VI.1 but at higher incident energy. Experimental data and DWBA calculations are from Olmer et al.(1976).

Chapter VII. Uses of the Transfer Amplitude

VII.1 Spin Selectivity and Angular Momentum Transfer.

Information about the selectivity can be obtained by considering the transfer probability

$$P_L^{tr}(j_2, j_1) = \frac{1}{2j_1+1} \sum_{m_1 m_2} |B_L(j_2 m_2, j_1 m_1)|^2, \qquad (VII.1)$$

where B is related to the semiclassical transfer amplitude A (given by the formula $(II.28)$ for neutron transfer and $(V.36)$ for proton transfer) by

$$B_L(j_2 m_2, j_1 m_1) = \sum_{\lambda_1 \lambda_2 m_s} < j_2 m_2 | \ell_2 \lambda_2 s m_s > A_L(\ell_2 \lambda_2, \ell_1 \lambda_1) < \ell_1 \lambda_1 s m_s | j_1 m_1 > . \qquad (VII.2)$$

Here s is the spin of the transferred particle and m_s its z-projection, which is not changed by the transfer process. For example, by using eq. (VII.1) and the semiclassical formula (II.28), we calculated the relative population of all the transitions shown in fig. VII.0 (from Bond 1983). Our predictions qualitatively agree with the spectra shown. In particular they reproduce the enhancement of some final states in one reaction with respect to another. This effect is associated with the different Q-value of the three reactions considered.

Now we express the amplitude $(VII.2)$ in terms of the transferred angular momentum. For the reaction

$$a_1 + c_2 \longrightarrow c_1 + a_2$$

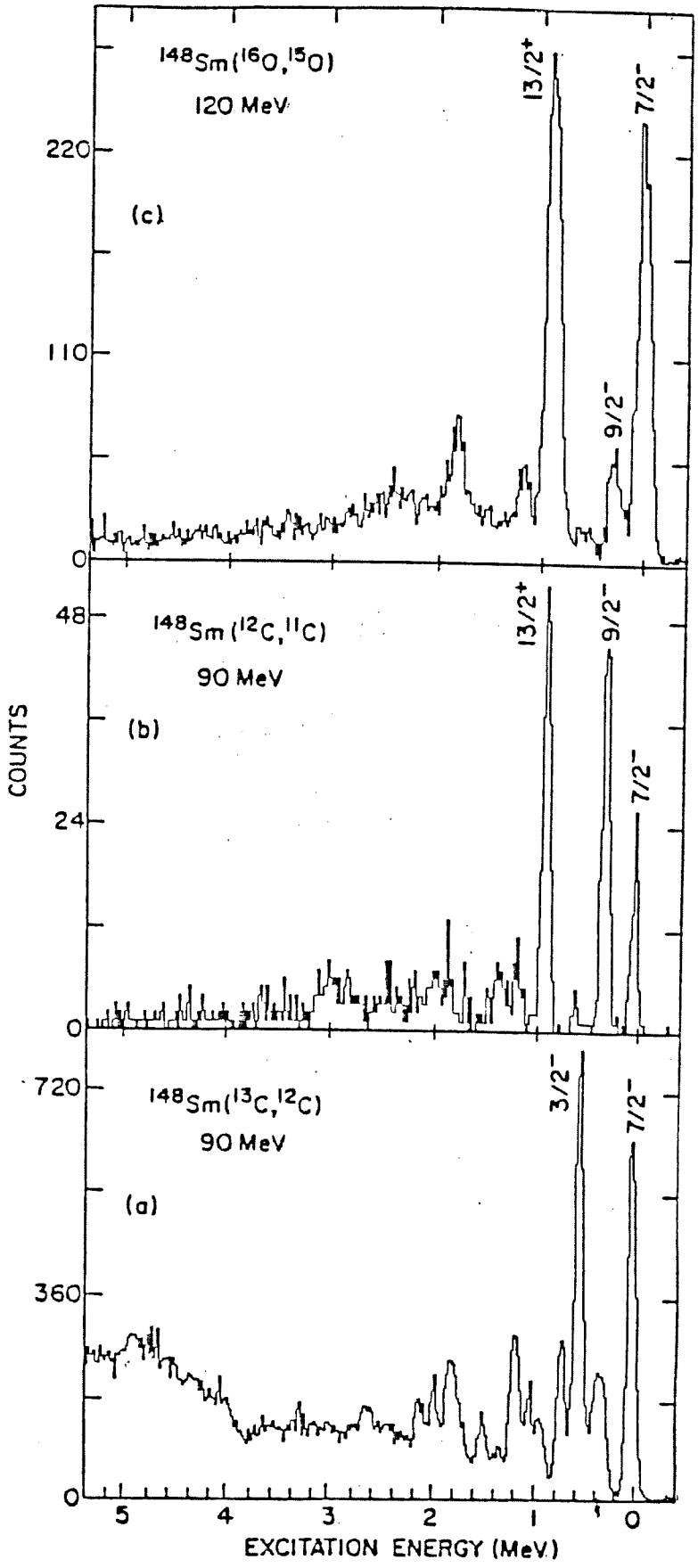

FIG.VII. 0 Single neutron transfer reactions for $^{148}Sm \rightarrow {}^{149}Sm$. Spectra were taken at the peaks of the bell-shaped angular distributions. Note the strong difference in the relative population of final states with (a) the (^{13}C, ^{12}C) reaction, (b) the (^{12}C, ^{11}C) reaction and (c) the (^{16}O, ^{15}O) reaction. (From Bond 1983)

or

$$(c_1 + x) + c_2 \longrightarrow c_1 + (c_2 + x)$$

the angular momentum transfer ℓ is defined as the difference between the total spin in the final and initial channel:

$$\ell = \mathbf{I}_{c_1} + \mathbf{I}_{a_2} - \mathbf{I}_{a_1} - \mathbf{I}_{c_2}.$$

From angular momentum conservation

$$\mathbf{L}_{in} + \mathbf{I}_{a_1} + \mathbf{I}_{c_2} = \mathbf{L}_{fin} + \mathbf{I}_{c_1} + \mathbf{I}_{a_2}$$

we find

$$\ell = \mathbf{L}_{in} - \mathbf{L}_{fin},$$

where $\mathbf{L}$ is the angular momentum of relative motion. The single particle angular momenta $\mathbf{j}_1$ and $\mathbf{j}_2$ relative to the cores c_1 and c_2 are defined by

$$\mathbf{I}_{a_1} = \mathbf{I}_{c_1} + \mathbf{j}_1, \qquad \mathbf{I}_{a_2} = \mathbf{I}_{c_2} + \mathbf{j}_2.$$

If the interaction is spin-independent $\mathbf{I}_{c_1}$ and $\mathbf{I}_{c_2}$ have the same orientation in the initial and final channel. Then

$$\ell = \mathbf{I}_{c_1} + (\mathbf{I}_{c_2} + \mathbf{j}_2) - (\mathbf{I}_{c_1} + \mathbf{j}_1) - \mathbf{I}_{c_2} = \mathbf{j}_2 - \mathbf{j}_1$$

and we have the selection rule

$$|j_1 - j_2| \leq \ell \leq j_1 + j_2, \qquad m_\ell = m_2 - m_1,$$

where m_ℓ is the z-projection of ℓ and m_α that of $\mathbf{j}_\alpha$ $(\alpha = 1, 2)$.

Since the spin orientation of the particle x is not changed by the transfer process we have

$$\mathbf{j}_1 = \ell_1 + \mathbf{s}, \qquad \mathbf{j}_2 = \ell_2 + \mathbf{s},$$

where ℓ_α is the single particle orbital angular momentum in the initial ($\alpha = 1$) and final ($\alpha = 2$) nucleus. Then

$$\ell = \ell_2 - \ell_1$$

and we have the selection rule

$$|\ell_1 - \ell_2| \leq \ell \leq \ell_1 + \ell_2, \qquad m_\ell = \lambda_2 - \lambda_1,$$

where λ_α is the z-projection of ℓ_α.

In order to decompose the matrix element $B(j_2 m_2, j_1 m_1)$ into terms corresponding to the angular momentum transfer ℓ we have to vector-couple its two states to a resultant that behaves under rotation of the coordinates like $< \ell m_\ell|$. To do so we must remember that $|j_1 m_1 >$ behaves under rotation like $(-)^{j_1 - m_1} < j_1 \ -m_1|$. Then we may write

$$B(j_2 m_2, j_1 m_1) = (-)^{j_1 - m_1} \sum_{\ell m_\ell} < j_2 m_2 j_1 - m_1 | \ell m_\ell > B(j_1 j_2; \ell m_\ell). \qquad (VII.3)$$

Substituting into *eq.* ($VII.1$) and using the orthogonality property of the Clebsch-Gordan coefficients it is easy to see that

$$P^{tr}(j_2, j_1) = \frac{1}{2j_1 + 1} \sum_{\ell m_\ell} |B(j_1 j_2; \ell m_\ell)|^2, \qquad (VII.4)$$

where we dropped the relative angular momentum subscript L for simplicity. The amplitude $B(j_1 j_2; \ell m_\ell)$ is given by the inverse of the relation ($VII.3$):

$$B(j_1 j_2; \ell m_\ell) = \sum_{m_1 m_2} (-)^{j_1 - m_1} < j_2 m_2 j_1 - m_1 | \ell m_\ell > B(j_2 m_2, j_1 m_1) = \sum_{\lambda_1 \lambda_2} A(\ell_2 \lambda_2, \ell_1 \lambda_1)$$

$$\cdot \sum_{m_1 m_2 m_s} (-)^{j_1 - m_1} < \ell_1 \lambda_1 s m_s | j_1 m_1 >< \ell_2 \lambda_2 s m_s | j_2 m_2 >< j_2 m_2 j_1 - m_1 | \ell m_\ell >, \quad (VII.5)$$

where we substituted the definition $(VII.2)$. The sum of Clebsch-Gordan coefficients in *eq.* $(VII.5)$ can be expressed in terms of a six-j symbol (e.g. Lawson 1980, p.472):

$$\sum_{m_1 m_2 m_s} (-)^{j_1 - m_1} < \ell_1 \lambda_1 s m_s | j_1 m_1 >< \ell_2 \lambda_2 s m_s | j_2 m_2 >< j_2 m_2 j_1 - m_1 | \ell m_\ell >$$

$$= (-)^{j_1 - j_2 + \ell_2 - \lambda_1} \sqrt{\frac{(2j_2+1)}{(2\ell_2+1)}} \sum_{m_1 m_2 m_s} < \ell_1 \lambda_1 s m_s | j_1 m_1 >< j_1 m_1 j_2 - m_2 | \ell - m_\ell >$$

$$\cdot < s m_s j_2 - m_2 | \ell_2 - \lambda_2 >= (-)^{j_1 + s + \ell_1 - \lambda_1 + \ell_2 + \ell} \sqrt{(2j_1+1)(2j_2+1)}$$

$$\cdot < \ell_1 \lambda_1 \ell_2 - \lambda_2 | \ell - m_\ell > \begin{Bmatrix} \ell_1 & s & j_1 \\ & & \\ j_2 & \ell & \ell_2 \end{Bmatrix}. \quad (VII.6)$$

This implies that each of the four sets of quantum numbers

$$(\ell_1 \; s \; j_1), \quad (\ell_1 \; \ell \; \ell_2), \quad (j_2 \; s \; \ell_2), \quad (j_2 \; \ell \; j_1)$$

must satisfy the triangular inequality, e.g. $|\ell_1 - s| \leq j_1 \leq \ell_1 + s$.

Using the geometric relation $(VII.6)$ into $(VII.5)$ we have

$$B(j_1 j_2; \ell m_\ell) = (-)^{j_1 + \ell_2 + s + \ell} \sqrt{(2j_1+1)(2j_2+1)} \begin{Bmatrix} \ell_1 & s & j_1 \\ & & \\ j_2 & \ell & \ell_2 \end{Bmatrix} A(\ell_1 \ell_2; \ell m_\ell), \quad (VII.7)$$

where

$$A(\ell_1 \ell_2; \ell m_\ell) = \sum_{\lambda_1 \lambda_2} (-)^{\ell_1 - \lambda_1} < \ell_2 \lambda_2 \ell_1 - \lambda_1 | \ell m_\ell > A(\ell_2 \lambda_2, \ell_1 \lambda_1). \quad (VII.8)$$

Substituting *eq.*$(VII.7)$ into $(VII.4)$ gives

$$P^{tr}(j_2, j_1) = (2j_2+1) \sum_{\ell} \begin{Bmatrix} \ell_1 & s & j_1 \\ & & \\ j_2 & \ell & \ell_2 \end{Bmatrix}^2 \sum_{m_\ell} |A(\ell_1 \ell_2; \ell m_\ell)|^2$$

$$\equiv \sum_{\ell} f_{\ell}(j_1, j_2)\ g_{\ell}(\ell_1, \ell_2, Q, E). \qquad (VII.9)$$

In this form the transfer probabilty is separated into a geometrical factor f which depends on the initial and final single particle angular momenta, j, and a dynamical factor g which depends on the other variables of the reaction, notably the incident energy and the reaction Q-value. In the case of nucleon transfer, for a given reaction specified by (ℓ_1, ℓ_2) this factor weighs the selectivity with respect to the four possible transfers

$$j_1 = \ell_1 - 1/2 \longrightarrow j_2 = \ell_2 - 1/2, \qquad j_1 = \ell_1 - 1/2 \longrightarrow j_2 = \ell_2 + 1/2,$$

$$j_1 = \ell_1 + 1/2 \longrightarrow j_2 = \ell_2 - 1/2, \qquad j_1 = \ell_1 + 1/2 \longrightarrow j_2 = \ell_2 + 1/2.$$

Table VII.1 and Fig VII.1 show the results obtained for the reaction $^{208}Pb(^{16}O, ^{15}O)^{209}Pb$ as an example.

Table VII.1 : geometric factors for the transfer probability eq. (VII.9)

$$f_{\ell}(j_1, j_2) = (2j_2 + 1) \begin{Bmatrix} \ell_1 & s & j_1 \\ j_2 & \ell & \ell_2 \end{Bmatrix}^2$$

$j_1 \rightarrow j_2$	$\ell = 3$	$\ell = 4$	$\ell = 5$
$1/2 \rightarrow 7/2$	$1/3$	$5/27$	0
$1/2 \rightarrow 9/2$	0	$4/27$	$1/3$
$3/2 \rightarrow 7/2$	$1/18$	$7/54$	$6/27$
$3/2 \rightarrow 9/2$	$5/18$	$11/54$	$1/9$

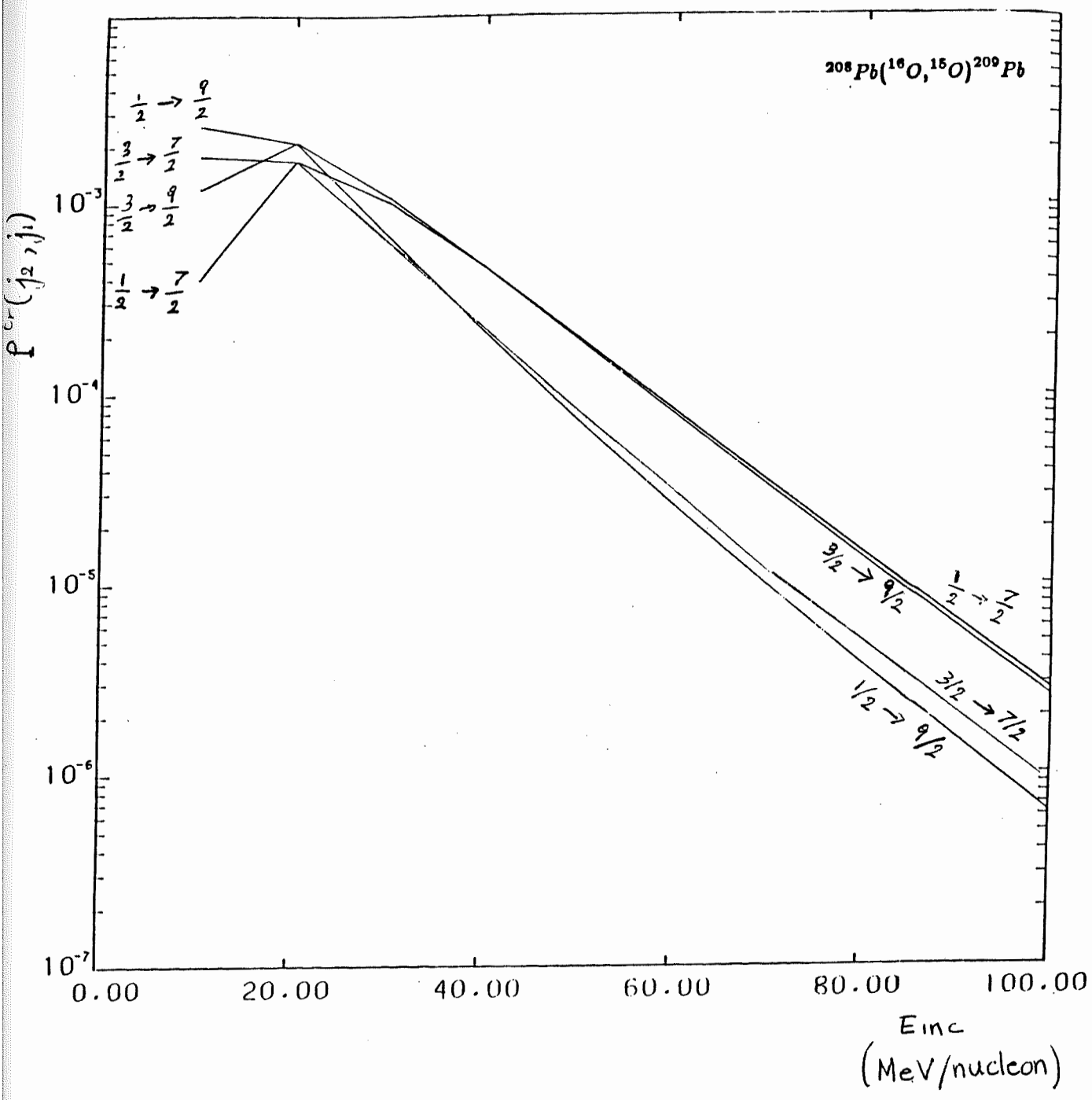

Fig. VII.1a. Transfer probabilities calculated from *eq.* $(VII.9)$ or *eq.* $(VII.17)$ for the reaction $^{208}Pb(^{16}O,^{15}O)^{209}Pb_{(g.s.)}$ as a function of incident energy. The four possible transitions from the initial p-state to the final g-state are indicated. The calculation is done for the relative angular momentum corresponding to the grazing orbit.

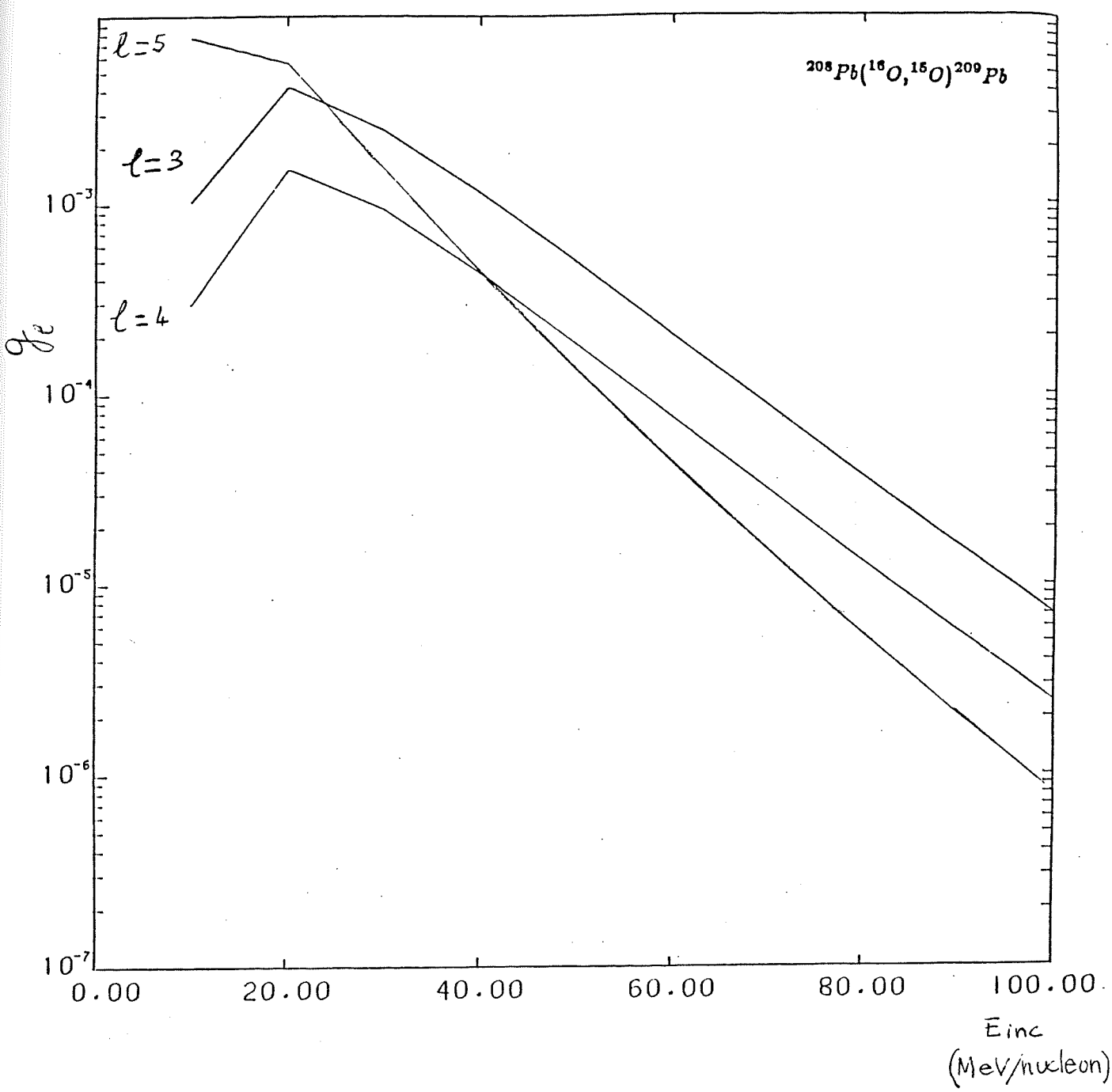

Fig. VII.1b. For the same reaction in fig. a, coefficients g_ℓ in the sum (VII.9) as a function of incident energy. The possible values of the transferred angular momentum ℓ are indicated.

The coefficients g and the transfer probabilities $P^{tr}(j_2, j_1)$ were calculated numerically from the analytical formula $(II.28)$ at a relative angular momentum L_0 such that the transmission coefficients $|S_{L_0}|^2 = 1/2$. L_0 was obtained from the optical potential of table $IV.1$ and extrapolated at higher energies with the parametrization $(VII.32)$.

VII.2 A new angular momentum coupling.

In this section we want to study the selectivity of the reaction with respect to the spin-flip of the transferred nucleon. Then we define new quantities F_0 and F_1 corresponding to antiparallel and parallel spins of the nucleon before and after transfer. Formally, this is done by expanding the coefficients g of the previous section in the following way:

$$g_\ell(\ell_1, \ell_2, Q, E) \equiv \sum_{m_\ell} |A(\ell_1 \ell_2; \ell m_\ell)|^2 = (-)^\ell (2\ell+1) \sum_J \begin{Bmatrix} \ell_1 & \ell_2 & \ell \\ \ell_2 & \ell_1 & J \end{Bmatrix} F_J, \qquad (VII.10)$$

where the sum runs over all (integral) values of J which satisfy the triangular inequality for the sets (ℓ_1, ℓ_1, J) and (ℓ_2, ℓ_2, J), i.e. $0 \leq J \leq 2\ell_1$ and $0 \leq J \leq 2\ell_2$. The F_J are given by the inverse relation of $(VII.10)$, namely

$$F_J = (2J+1) \sum_{\ell=|\ell_1-\ell_2|}^{\ell_1+\ell_2} (-)^\ell \begin{Bmatrix} \ell_1 & \ell_2 & \ell \\ \ell_2 & \ell_1 & J \end{Bmatrix} g_\ell. \qquad (VII.11)$$

Substituting *eq.* $(VII.10)$ into $(VII.9)$ and using the symmetry relations for the six-j symbols (e.g. Messiah, 1969, p. 914-915)

$$\sum_\ell (-)^\ell (2\ell+1) \begin{Bmatrix} \ell_1 & s & j_1 \\ j_2 & \ell & \ell_2 \end{Bmatrix}^2 \begin{Bmatrix} \ell_1 & \ell_2 & \ell \\ \ell_2 & \ell_1 & J \end{Bmatrix}$$

$$= (-)^{j_1+j_2+2s+J} \sum_\ell (-)^{\ell+j_1+j_2+2s+J} (2\ell+1) \begin{Bmatrix} \ell_1 & \ell_2 & \ell \\ j_2 & j_1 & s \end{Bmatrix} \begin{Bmatrix} j_2 & j_1 & \ell \\ \ell_1 & \ell_2 & s \end{Bmatrix} \begin{Bmatrix} \ell_1 & \ell_2 & \ell \\ \ell_2 & \ell_1 & J \end{Bmatrix}$$

$$= (-)^{j_1+j_2+2s+J} \begin{Bmatrix} s & s & J \\ \ell_1 & \ell_1 & j_1 \end{Bmatrix} \begin{Bmatrix} s & s & J \\ \ell_2 & \ell_2 & j_2 \end{Bmatrix}$$

we have for the transfer probability

$$P^{tr}(j_2, j_1) = (2j_2+1)(-)^{j_1+j_2+2s} \sum_J (-)^J \begin{Bmatrix} s & s & J \\ \ell_1 & \ell_1 & j_1 \end{Bmatrix} \begin{Bmatrix} s & s & J \\ \ell_2 & \ell_2 & j_2 \end{Bmatrix} F_J \quad (VII.12)$$

Because of the selection rules for the 6-j coefficients in the sum $(VII.12)$ J spans the range

$$0 \leq J \leq 2s, \quad 0 \leq J \leq 2\ell_1, \quad 0 \leq J \leq 2\ell_2,$$

that is J is an integer or zero whose maximum value is given by twice the $\min(s, \ell_1, \ell_2)$. Therefore if one of these quantities is zero only F_0 contributes to the sum $(VII.12)$.

By using *eq.* $(VII.1)$ or $(VII.4)$ or $(VII.12)$ it is straightforward to prove that the probability P satisfies the sum rule:

$$\sum_{j_2} P^{tr}(j_2, j_1) = \frac{1}{2\ell_1+1} \sum_{\lambda_1 \lambda_2} |A(\ell_2 \lambda_2, \ell_1 \lambda_1)|^2 \stackrel{\text{def}}{=} P^{tr}(\ell_2, \ell_1)$$

$$= \frac{1}{2\ell_1+1} \sum_{\ell m_\ell} |A(\ell_1 \ell_2; \ell m_\ell)|^2 = \frac{1}{2\ell_1+1} \sum_{\ell} g_\ell, \quad (VII.13)$$

where we introduced the probabilty of transfer from a single particle level with orbital angular momentum ℓ_1 in the initial nucleus to a single particle level with orbital angular momentum ℓ_2 in the final nucleus. Notice that the sum over the final single particle spins j_2 is independent of the initial spin j_1. In the case of nucleon transfer $s = 1/2$, then $J = 0, 1$ and *eq.* $(VII.12)$ becomes

$$P^{tr}(j_2, j_1) = (2j_2+1)(-)^{j_1+j_2+1} \begin{Bmatrix} 1/2 & 1/2 & 0 \\ \ell_1 & \ell_1 & j_1 \end{Bmatrix} \begin{Bmatrix} 1/2 & 1/2 & 0 \\ \ell_2 & \ell_2 & j_2 \end{Bmatrix} F_0$$

$$\cdot \left(1 - D_{j_1} D_{j_2} \frac{F_1}{F_0}\right), \quad (VII.14)$$

where (for $\alpha = 1, 2$)

$$D_{j_\alpha} = \frac{\begin{Bmatrix} 1/2 & 1/2 & 1 \\ \ell_\alpha & \ell_\alpha & j_\alpha \end{Bmatrix}}{\begin{Bmatrix} 1/2 & 1/2 & 0 \\ \ell_\alpha & \ell_\alpha & j_\alpha \end{Bmatrix}} = (-)^{\ell_\alpha + j_\alpha - 1/2} \sqrt{\frac{2\ell_\alpha + 1/2 - j_\alpha}{3(j_\alpha + 1/2)}}$$

$$= \begin{cases} -\sqrt{\frac{\ell_\alpha + 1}{3\ell_\alpha}} & \text{if } j_\alpha = \ell_\alpha - 1/2, \\ \sqrt{\frac{\ell_\alpha}{3(\ell_\alpha + 1)}} & \text{if } j_\alpha = \ell_\alpha + 1/2. \end{cases} \qquad (VII.15)$$

Now we calculate F_0 and F_1 from *eq.* $(VII.11)$.

$$F_0 = \frac{(-)^{\ell_1 + \ell_2}}{\sqrt{(2\ell_1 + 1)(2\ell_2 + 1)}} \sum_{\ell m_\ell} |A(\ell_1 \ell_2; \ell m_\ell)|^2 = (-)^{\ell_1 + \ell_2} \sqrt{\frac{2\ell_1 + 1}{2\ell_2 + 1}}\, P^{tr}(\ell_2, \ell_1), \qquad (VII.16a)$$

$$F_1 = \frac{3}{2} \frac{(-)^{\ell_1 + \ell_2 + 1}}{\sqrt{\ell_1(\ell_1 + 1)(2\ell_1 + 1)\ell_2(\ell_2 + 1)(2\ell_2 + 1)}}$$

$$\cdot \left\{ [\ell_1(\ell_1 + 1) + \ell_2(\ell_2 + 1)] \sum_\ell g_\ell - \sum_\ell \ell(\ell + 1) g_\ell \right\}, \qquad (VII.16b)$$

$$\frac{F_1}{F_0} = \frac{3}{2} \frac{1}{\sqrt{\ell_1(\ell_1 + 1)\ell_2(\ell_2 + 1)}} \left[\frac{\sum_\ell \ell(\ell + 1) g_\ell}{\sum_\ell g_\ell} - \ell_1(\ell_1 + 1) - \ell_2(\ell_2 + 1) \right]. \qquad (VII.16c)$$

Eq. $(VII.14)$ can be written as

$$P^{tr}(j_2, j_1) = \frac{1}{2} \frac{(2j_2 + 1)}{(2\ell_2 + 1)} \left(1 - D_{j_1} D_{j_2} \frac{F_1}{F_0} \right) P^{tr}(\ell_2, \ell_1) \qquad (VII.17)$$

Eq. (VII.17) gives the probability for transfer from $j_1 = \ell_1 \pm \frac{1}{2}$ to $j_2 = l_2 - \frac{1}{2}$ or $j_2 + \frac{1}{2}$ in terms of the simpler probability $P^{tr}(\ell_2, \ell_1)$, eq.(VII.13). The factor in front of $P^{tr}(\ell_2, \ell_1)$ is separated into a j-dependent part $D_{j_1} D_{j_2}$ and the energy-dependent ratio $R = F_1/F_0$. This ratio can change sign as a function of energy (fig. VII.2). This implies a change in the selectivity of the reaction as a function of incident energy. As it has been suggested by classical arguments, at low energy the 'spin-flip' transitions $j_1 = \ell_1 \pm \frac{1}{2} \rightarrow j_2 = \ell_2 \mp \frac{1}{2}$

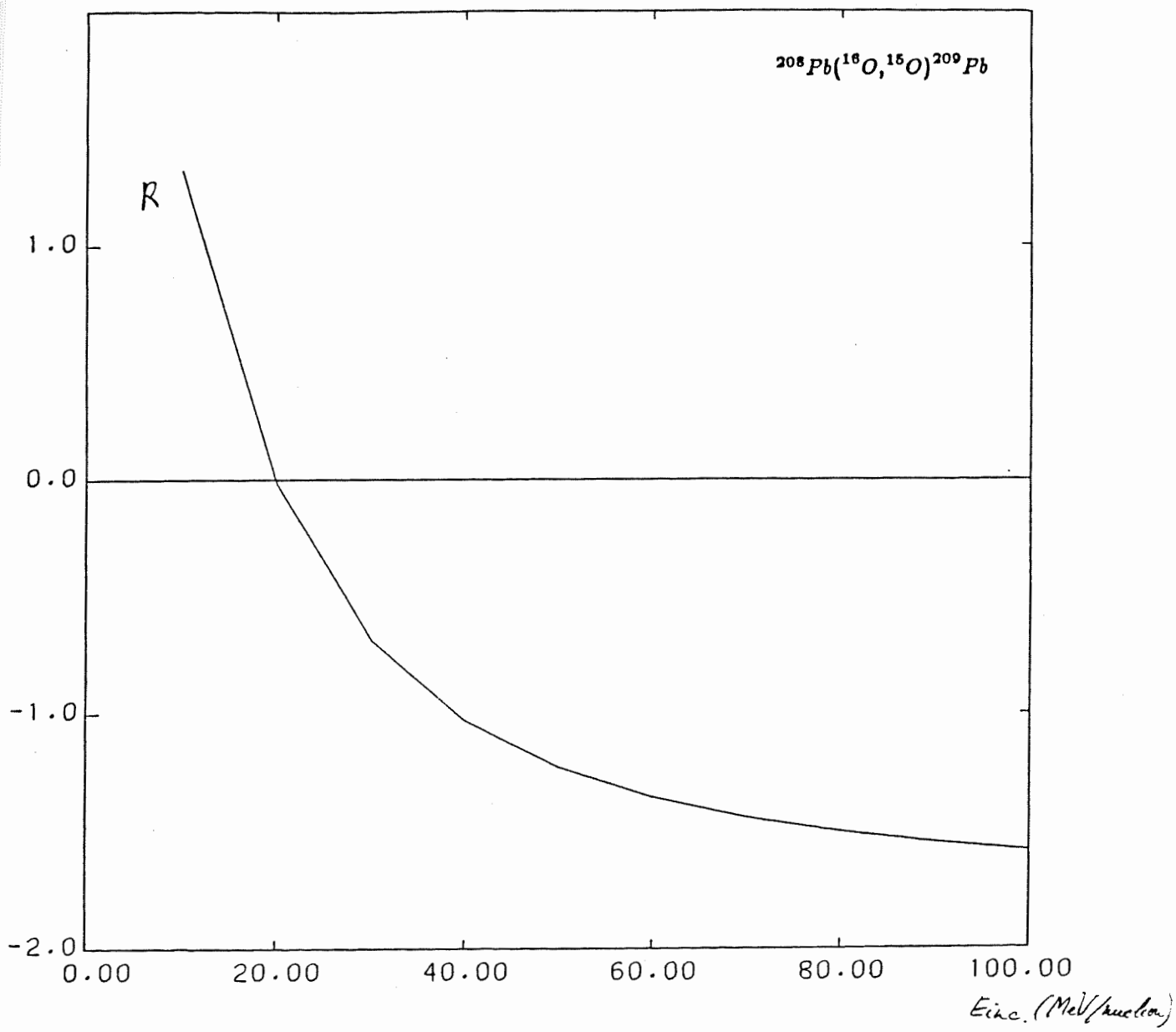

Fig. VII.2. Ratio $R \equiv F_1/F_0$ for the transfer probability eq. (VII.17) as a function of incident energy. Same reaction as fig. 1.

are favoured , while the opposite situation $j_1 = \ell_1 \pm \frac{1}{2} \rightarrow j_2 = \ell_2 \pm \frac{1}{2}$ occurs at higher energy. Our calculation suggests that this 'inversion' of selectivity occurs at an incident energy such that (cf. chapter II)

$$\frac{1}{2}mv_d^2 = |Q| = |\varepsilon_1 - \varepsilon_2|, \qquad (II.32)$$

where v_d is the relative velocity at the point of closest approach, d. This corresponds to an incident energy $E_{crit} \simeq 20$ Mev/nucleon for the reaction $^{208}Pb(^{16}O, ^{15}O)^{209}Pb$. This is the point where R in fig. VII.2 changes sign. As a result the factor $(1 - D_{j_1} D_{j_2} R)$ that enters in eq.(VII.17) crosses the value 1 at this energy (see fig.VII.3). The transfer probability $P^{tr}(\ell_2, \ell_1)$, eq. (VII.13), rises from low energy to a maximum at E_{crit}, then decays exponentially at higher energy (fig. VII.4). Due to the form of the transfer amplitude, eq.(II.29), the energy dependence of $P^{tr}(\ell_2, \ell_1)$ is governed by the quantity η (cf. p. 26). From the factors shown in figs. VII.2-VII.4 we obtain the transfer probability $P^{tr}(j_2, j_1)$, eq. (VII.17). Of course this is the same result obtained with the transferred angular momentum coupling, eq.(VII.9), shown in fig.(VII.1a). In a realistic calculation figs. VII.1 and VII.3 would be slightly modified because single-particle states with different spins in general have different binding energies. In particular the energy E_{crit} would be shifted by an amount $\Delta E_{crit} = \Delta|Q|$ [cf. *eqs.* $(II.32)$ and $(VII.25)$]. The analytical calculation of $P^{tr}(j_2, j_1)$ can be taken a step further by using an approximate formula of the type (II.29) for the transfer amplitude $A(\ell_2\lambda_2, \ell_1\lambda_1)$, where the rotational properties are contained only in the factor $Y_{\ell_1\lambda_1}(\hat{k}_1)\ Y^*_{\ell_2\lambda_2}(\hat{k}_2)$. Thus one can calculate analytically the ratio $R \equiv \frac{F_1}{F_0}$ which determines the spin dependence. The calculation of H. Hashim (private communication) shows that R changes sign when either k_{1z} or k_{2z}, defined by eq.(II.17), changes sign. This happens when the condition (II.32) is satisfied.

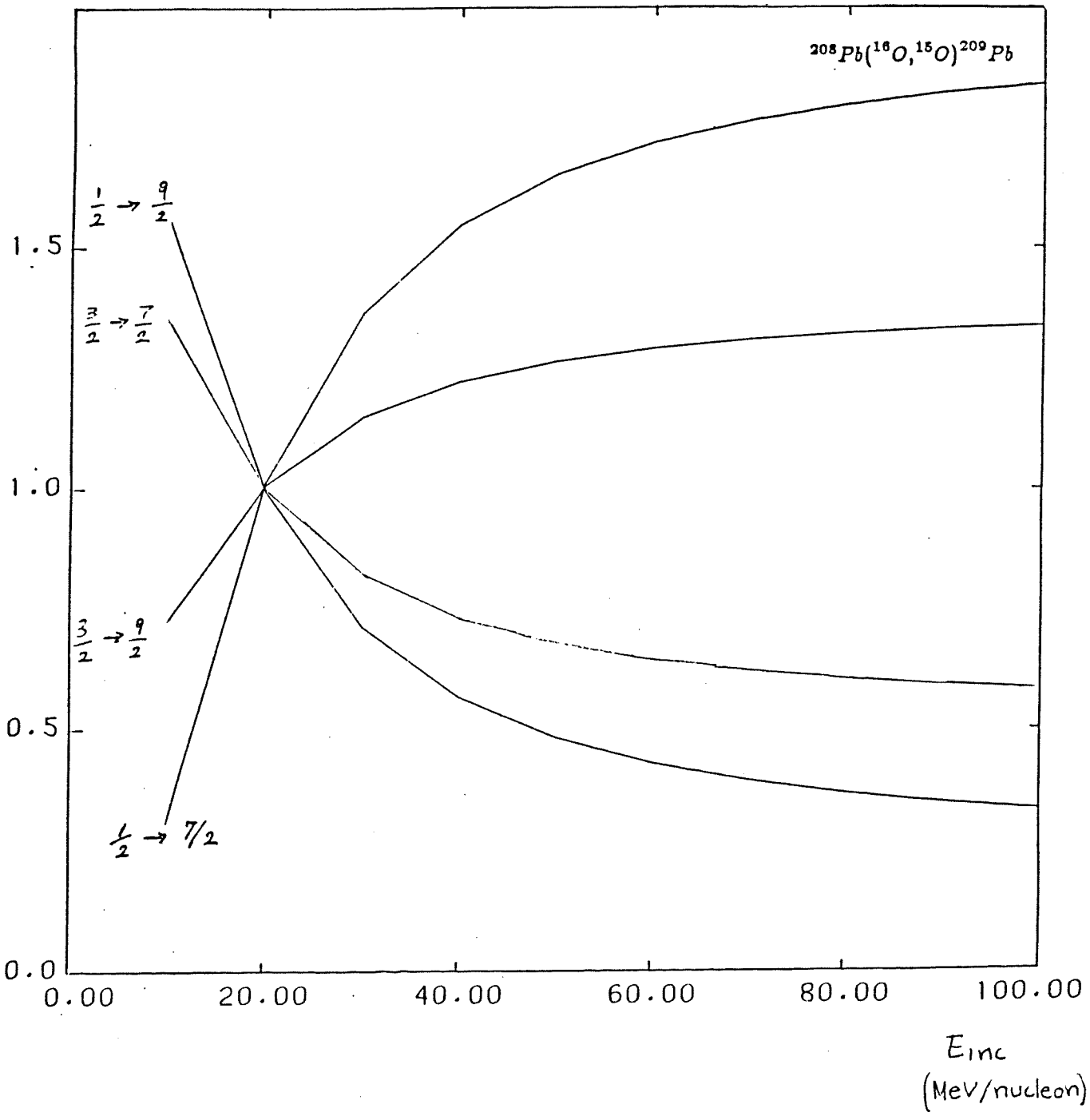

Fig. VII.3. The factor $(1 - D_{j_1} D_{j_2} \frac{F_1}{F_0})$ that enters in eq. (VII.17). The ratio $R \equiv F_1/F_0$ is given in fig. 2. The possible transitions $j_1 \rightarrow j_2$ are indicated (cf. fig. 1a)

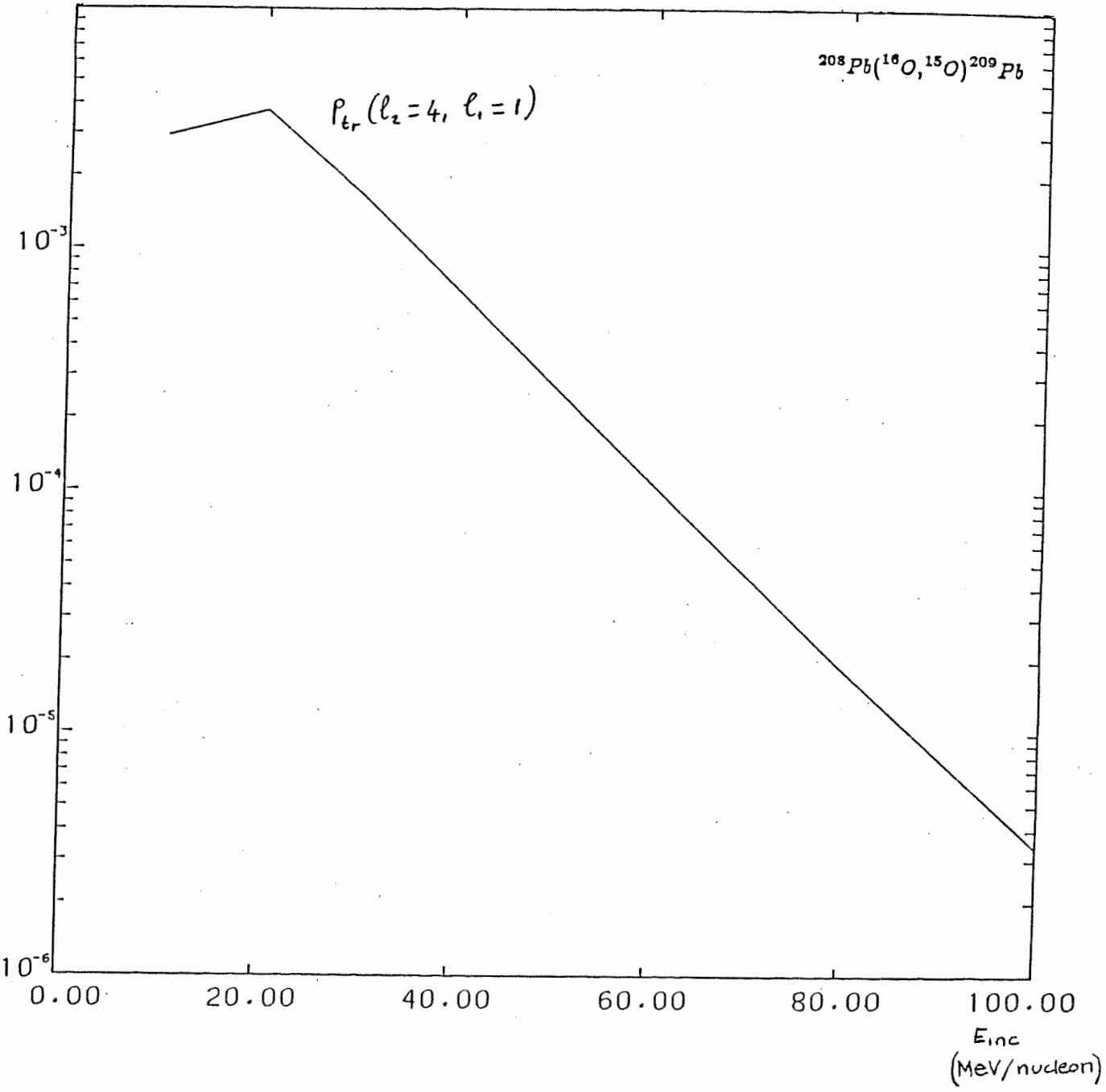

Fig. VII.4. Same reaction as fig. 1. Transfer probability, eq. (VII.13), as a function of incident energy. ℓ_1 and ℓ_2 are the orbital angular momenta of the initial and final single-particle states.

VII.3 Energy Dependence of the Transfer Cross Section.

In Chapters IV and VI we discussed mainly angular distributions and we saw that DWBA calculations as well as our model predict shapes which agree quite well with those observed for several one-nucleon transfer reactions. Both methods also reproduce the relative intensities of transitions to single-particle states. However, the DWBA cross sections increase more rapidly with energy than the measured cross sections (see fig. I.14). Fig. VII.5 shows that, after a rapid increase through the Coulomb barrier, the experimental cross sections level off at around 100 MeV and start to decrease steadily with incident energy. The DWBA cross sections, after reproducing the observed increase of about two orders of magnitude through the Coulomb barrier, remain almost constant with increasing energy and become clearly too large with respect to experimental data. In a region of considerably higher incident energy ($\gtrsim 20\,\mathrm{MeV}\,/nucleon$) one expects an exponential decrease of the transfer cross section due to the diminished overlap of the momentum distributions of the transferred nucleon in the initial and final state. This has been studied by Von Oertzen (1985) and is often referred to as TGV (Transfert à Grande Vitesse). In particular the reaction $^{12}C(^{13}C,^{12}C)^{13}C$ was calculated for an incident energy between 20 and 80 MeV/nucleon. The calculation clearly showed an exponential decrease with energy.

In this section we study the energy dependence of the cross section with our analytical formula for the semiclassical transfer amplitude in relation to the selectivity of the reaction. To do so it is better to consider the angle-integrated cross section. This eliminates the uncertainty in the angle (a prescription could be θ_{peak}) and the relative angular momentum at which the cross section is calculated. Another advantage is that both the

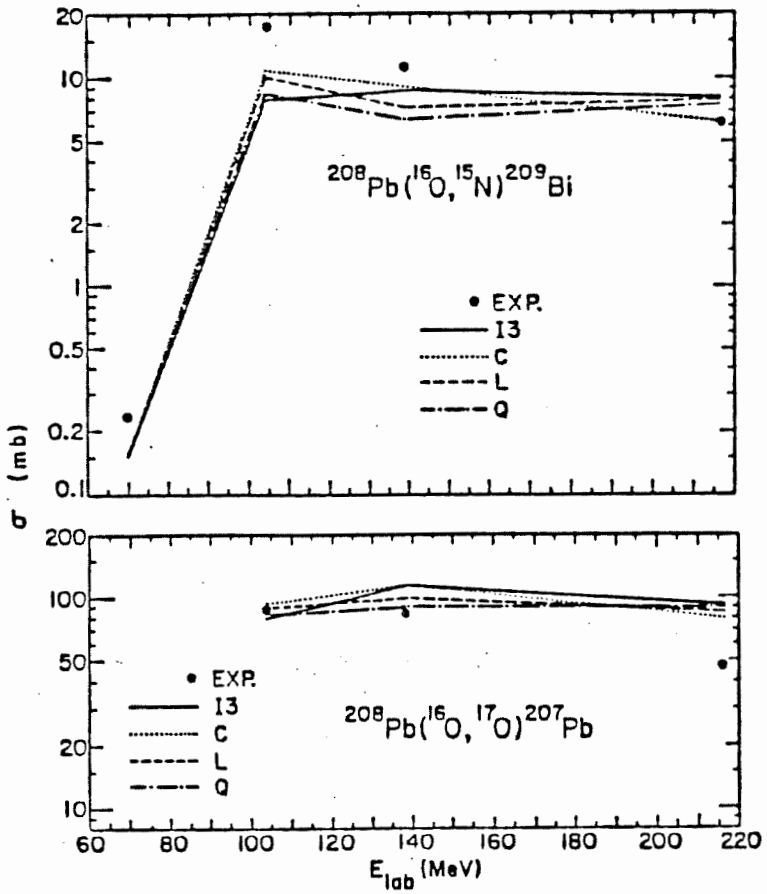

FIG. VII.5. Total ^{208}Pb(^{16}O, ^{15}N)^{209}Bi (top) and ^{208}Pb(^{16}O, ^{17}O)^{207}Pb (bottom) cross sections. The top section shows the angle-integrated cross sections for producing ^{15}N in its ground state and ^{209}Bi in any of its single-proton states. The bottom section shows the angle-integrated cross sections for ^{17}O in either its ground state or $2s_{1/2}$ (0.87 MeV) excited state and ^{207}Pb in any of its neutron-hole states. The dots are the experimental total cross sections; the errors are about the size of the dots. The curves are the results of DWBA calculations made with the indicated optical potentials. (From Pieper et al. 1978)

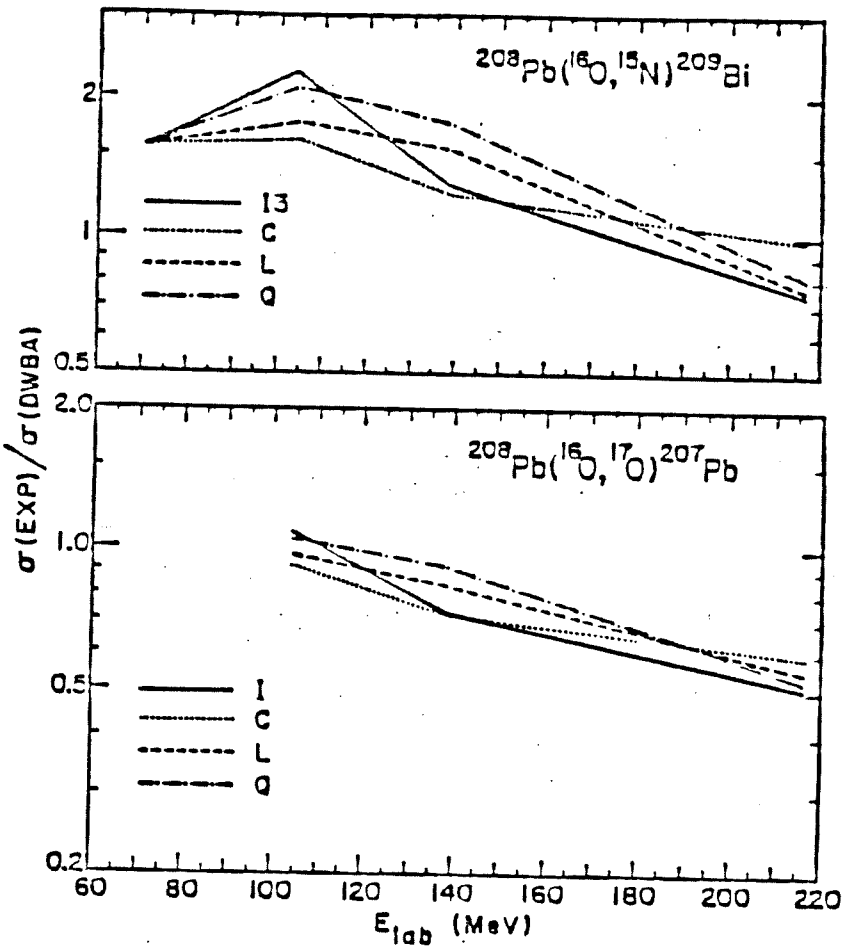

FIG. VII.5b Ratios of the $^{208}Pb(^{16}O, ^{15}N)^{209}Bi$ (top) and the $^{208}Pb(^{16}O, ^{17}O)^{207}Pb$ (bottom) cross sections. Shown are the ratios σ(exp)/σ(DWBA) of the cross sections given in Fig. VII.5a (From Pieper et al. 1978)

classical formula $(III.17)$ and the partial wave formula $(III.28)$ for the transfer angular distribution, once integrated over the solid angle $d\Omega$ give the same cross section, as we proved in §III.2. We recall the classical expression $(III.17)$:

$$\left[\frac{d\sigma(\theta)}{d\Omega}\right]_{\alpha} = \left[\frac{d\sigma(\theta)}{d\Omega}\right]_{cl} P^{tr}_{L(\theta)}(\alpha)|S_{L(\theta)}|^2, \qquad (VII.18)$$

where α stands for the quantum numbers describing the initial and final (single particle) states. This formula assumes that for a given scattering angle θ the contribution to the cross section comes from one orbit with classical angular momentum $\hbar\Lambda(\theta)$ or impact parameter $b(\theta)$. Λ is related to the angular momentum quantum number L by $\Lambda = L + 1/2$. In *eq.* $(VII.18)$

$$\left[\frac{d\sigma}{d\Omega}\right]_{cl} = \frac{b}{\sin\theta}\left|\frac{db}{d\theta}\right|$$

is the classical cross section for elastic scattering. If more impact parameters lead to the same scattering angle the classical cross section is given by the sum of the cross sections for each impact parameter. For our discussion we shall exclude this case.

$P^{tr}_L(\alpha)$ is the transfer probability for the transition specified by the quantum numbers α. The factor $|S_L|^2$ gives the probability that the system escapes absorption into other inelastic channels.

Integrating *eq.* $(VII.18)$ over the solid angle $d\Omega = \sin\theta d\theta d\varphi$ gives

$$\sigma_{\alpha} = 2\pi \int_0^{\pi} b(\theta)\left|\frac{db}{d\theta}\right| P^{tr}_{L(\theta)}(\alpha)\ |S_{L(\theta)}|^2\ d\theta.$$

We assume that the deflection function $\theta(b)$ is monotonically decreasing (as it is the case for Coulomb scattering where $\theta = 2\arctan\frac{Z_{c_2}Z_x e^2}{2Eb}$) and that $b(\theta = 0) = \infty$ (particles

passing undeflected at large distances) while $b(\theta = \pi) = 0$ (particles turned back in a head-on collision). Then changing the integration variable from θ to b gives

$$\sigma_\alpha = 2\pi \int_0^\infty P^{tr}_{L(b)}(\alpha) |S_{L(b)}|^2 \; b \; db. \qquad (VII.19)$$

Eq. $(VII.19)$, with the analytical expression for the transfer amplitude given before, was used by Bonaccorso, Brink and Lo Monaco (1985). In that work a sharp cut-off approximation for the transmission coefficient

$$|S_{L(b)}|^2 = \begin{cases} 0 & \text{for } b \leq b_0 \\ 1 & \text{for } b > b_0 \end{cases}$$

was used to derive an explicit formula for the cross section. This was applied to the reaction $^{12}C(^{13}C, ^{12}C)^{13}C$ studied by Von Oertzen (1985) (see fig. VII.7).

Here we derive a similar analytical formula for the cross section with a more realistic parametrization of $|S_L|^2$ and an explicit j-dependence in the transfer probability.

Eq. $(VII.19)$ can be transformed into an integral over the classical angular momentum $\Lambda = L + 1/2$ by the change of variable $\Lambda = \sqrt{2\mu E_{c.m.}}\; b/\hbar = kb$:

$$\sigma_\alpha = \frac{2\pi}{k^2} \int_0^\infty P^{tr}_{\Lambda-1/2}(\alpha) \; |S_{\Lambda-1/2}|^2 \; \Lambda \; d\Lambda. \qquad (VII.20)$$

Our strategy will be to identify which factors in the integrand of *eq.* $(VII.20)$ are slowly varying with Λ, approximate them at a fixed value $\bar{\Lambda}$ such that the integrand is maximum and then integrate analytically the factors which vary rapidly with Λ. We must specify the quantum numbers α in the transfer amplitude. If we consider the transfer of a particle x from the single particle state (ℓ_1, j_1) in nucleus $a_1 = c_1 + x$ to the single particle state (ℓ_2, j_2) in $a_2 = c_2 + x$, with the same notation of §VII.1, we have $\alpha = (I_{a_1}, I_{c_2} \rightarrow I_{c_1}, I_{a_2})$

and the transfer probability in *eq.* $(VII.20)$ is given by:

$$P_L^{tr}(I_{a_1}, I_{c_2} \to I_{c_1}, I_{a_2}) = \frac{2I_{a_2}+1}{(2I_{c_2}+1)(2j_2+1)}\, P^{tr}(j_2, j_1)$$

$$= \frac{1}{2}\frac{2I_{a_2}+1}{(2I_{c_2}+1)(2\ell_2+1)}\, (1 - D_{j_1} D_{j_2} R)\, P^{tr}(\ell_2, \ell_1) \qquad (VII.21)$$

where $P^{tr}(j_2, j_1)$ is the single particle transfer probability defined in *eq.* $(VII.1)$ and the factor in front takes into account the sum over final states and the average over initial states, as we discussed in §III.1. In the last step we used the result *eq.* $(VII.17)$, where the D_j's are given by *eq.* $(VII.15)$. The quantity $R \equiv \frac{F_1}{F_0}$, given by *eq.* $(VII.16c)$, is the ratio of quantities containing the modulus square of the semiclassical transfer amplitude. Therefore R varies slowly with the relative angular momentum Λ and will be substituted by the constant $R_0 \equiv R(\Lambda = \bar{\Lambda})$. By using the approximation

$$K_{\lambda_1 - \lambda_2}(\eta d) \sim K_0(\eta d) \simeq \sqrt{\frac{\pi}{2\eta d}}\, e^{-\eta d} \qquad (VII.22)$$

in the expression of the semiclassical transfer amplitude $A(\ell_2\lambda_2, \ell_1\lambda_1)$ [*eq.* $(II.28)$ for neutrons and $(V.36)$ for protons] we have (cf. Bonaccorso, Brink and Lo Monaco 1985)

$$P^{tr}_{\Lambda - 1/2}(\ell_2, \ell_1) = \frac{\pi}{4}(2\ell_2+1)\frac{(\hbar c\, C_{\ell_1} C_{\ell_2})^2}{mc^2\, E_d} P_{\ell_1}(\cos\omega_1) P_{\ell_2}(\cos\omega_2)\frac{e^{-2\eta d}}{\eta d}, \qquad (VII.23)$$

where $P_\ell(z)$ is a Legendre polynomial and

$$\cos\omega_\alpha \equiv 1 + 2\left(\frac{k_{\alpha z}}{\gamma_\alpha}\right)^2, \qquad \alpha = 1, 2,$$

$$\Rightarrow \quad \cos\omega_1 = 1 - \frac{(Q+E_d)^2}{2\varepsilon_1 E_d}, \quad \cos\omega_2 = 1 - \frac{(Q-E_d)^2}{2\varepsilon_2 E_d}. \qquad (VII.24)$$

In these formulæ E_d is the kinetic energy of the nucleon at the distance of closest approach d:

$$E_d = \frac{1}{2}mv_d^2 = \frac{m}{\mu}[E_{cm} - V(d)] = \frac{A_1 + A_2}{A_1 A_2}[E_{cm} - V(d)] = \frac{(\hbar\Lambda)^2}{2\mu d^2}, \qquad (VII.25)$$

where μ is the reduced mass, A_1 and A_2 are the mass numbers of the colliding nuclei (in the initial channel). The tangential relative velocity v_d of the nuclei at the distance of closest approach can be related to Λ and E_{cm} by using the angular momentum and energy conservation

$$\Lambda = \frac{\mu v_d}{\hbar} d = \frac{1}{\hbar}\sqrt{2\mu[E_{cm} - V(d)]}\; d \equiv k_d\, d \qquad (VII.26)$$

For Coulomb scattering we have

$$d = \frac{n + \sqrt{n^2 + \Lambda^2}}{k}, \qquad (VII.27)$$

where

$$n = \frac{Z_1 Z_2 e^2}{\hbar v} = \frac{Z_1 Z_2 e^2}{\hbar\sqrt{2E_{cm}/\mu}},$$

is the Sommerfeld parameter, and

$$E_d = \frac{A_1 + A_2}{A_1 A_2}\; E_{cm}\; \left(\frac{\Lambda}{n + \sqrt{n^2 + \Lambda^2}}\right)^2. \qquad (VII.28)$$

Then in *eq.* $(VII.23)$ a smooth Λ-dependence is contained in the factor $1/E_d$, in the arguments of the Legendre polynomials $(VII.24)$ and in the quantity [cf. *eqs.* $(II.30)$ and $(II.31)$]

$$\eta = \frac{1}{\hbar}\sqrt{m\left[\frac{1}{2}\left(\frac{Q^2}{E_d} + E_d\right) - (\varepsilon_1 + \varepsilon_2)\right]}. \qquad (VII.29)$$

To integrate the differential cross section we shall only retain the Λ-dependence of $d \simeq \frac{n+\Lambda}{k}$ in the exponential of the transfer probability and consider all other slowly varying quantities independent of Λ. We evaluate the latter at the value $\Lambda = \bar{\Lambda}$ such that the integrand in *eq.* $(VII.20)$, $\Lambda\, P^{tr}_{\Lambda-1/2}\, |S_{\Lambda-1/2}|^2$, is maximum. To a good approximation, $\bar{\Lambda} = \Lambda_0$ (grazing angular momentum defined later on). If d_0 is the distance of closest

approach for a Coulomb orbit with angular momentum Λ_0 (d_0 is the strong absorption radius discussed later on) we obtain

$$E_d \simeq E_0 = \frac{A_1 + A_2}{A_1 A_2}[E_{c.m.} - V(d_0)]. \qquad (VII.30)$$

Then *eq.* $(VII.23)$ gives

$$P^{tr}_{\Lambda-1/2}(\ell_2, \ell_1) = \frac{\pi}{4}(2\ell_2 + 1)\frac{(\hbar c\ C_{\ell_1} C_{\ell_2})^2}{mc^2} P_{\ell_1}(\cos\omega_{01}) P_{\ell_2}(\cos\omega_{02}) \frac{e^{-2\eta_0 a_c}}{E_0 \eta_0 d_0}\ e^{-\frac{2\eta_0}{k}\Lambda}, \qquad (VII.31)$$

where $\cos\omega_{0\alpha}$ and η_0 are defined by *eqs.* $(VII.24)$ and $(VII.29)$ by substituting E_0 to E_d and

$$a_c = n/k = \frac{Z_1 Z_2 e^2}{2E_{c.m.}}$$

is half the distance of closest approach in a Coulomb head-on collision.

The transmission coefficient in *eq.* $(VII.20)$ is

$$|S_{\Lambda-1/2}|^2 = \exp[-4\,\mathrm{Im}\,\delta(\Lambda)],$$

where δ is the elastic scattering phase shift. We parametrize the imaginary part of the phase shift by

$$\mathrm{Im}\,\delta_N(\Lambda) = \frac{\ln 2}{4}\ e^{\frac{\Lambda_0 - \Lambda}{\Delta}}. \qquad (VII.32)$$

This form gives $|S|^2 \approx 0$ for small Λ's (strong absorption) and $|S|^2 \simeq 1$ for big Λ's (no absorption). The parameters Δ and Λ_0 can be related approximatevely to the imaginary part of the optical potential, as we show at the end of this section. The factor in front of the exponential in *eq.* $(VII.32)$ ensures that $|S|^2 = \frac{1}{2}$ for $\Lambda = \Lambda_0 = L_{grazing} + 1/2$.

By substituting *eqs.* $(VII.32), (VII.31)$ and $(VII.21)$ into *eq.* $(VII.20)$ we have

$$\sigma(I_{a_1}, I_{c_2} \to I_{c_1}, I_{a_2}) = \frac{(\pi\hbar c\ C_{\ell_1} C_{\ell_2})^2}{4mc^2} \frac{2I_{a_2}+1}{2I_{c_2}+1}$$

$$\cdot (1 - D_{j_1} D_{j_2} R_0)\, P_{\ell_1}(\cos\omega_{01}) P_{\ell_2}(\cos\omega_{02})$$

$$\cdot \frac{\Lambda_0\ e^{-2\eta_0 a_c}}{k^2 E_0 \eta_0 d_0} \int_0^\infty e^{-\frac{2\eta_0}{k}\Lambda}\ e^{-\ln 2 \exp\left(\frac{\Lambda_0-\Lambda}{\Delta}\right)}\ d\Lambda. \qquad (VII.33)$$

The integral in *eq.* $(VII.33)$ can be calculated analytically:

$$\int_0^\infty e^{-\frac{2\eta_0}{k}\Lambda}\ e^{-\ln 2 \exp\left(\frac{\Lambda_0-\Lambda}{\Delta}\right)}\ d\Lambda = \Delta \int_0^1 y^{\alpha\Delta-1} e^{-\beta y}\ dy$$

$$= \Delta\ \beta^{-\alpha\Delta}\ \gamma(\alpha\Delta, \beta), \qquad (VII.34)$$

where we put $y = e^{-\frac{\Lambda}{\Delta}}$, $\alpha = \frac{2\eta_0}{k}$, $\beta = \ln 2\ e^{\frac{\Lambda_0}{\Delta}}$ and the incomplete gamma function(Abramowitz and Stegun 1970, p. 260)

$$\gamma(a, x) = \int_0^x t^{a-1} e^{-t} dt.$$

Since β is very large

$$\gamma(\alpha\Delta, \beta) \simeq \int_0^\infty t^{\alpha\Delta-1} e^{-t} dt = \Gamma(\alpha\Delta). \qquad (VII.35)$$

By substituting *eqs.* $(VII.35)$ and $(VII.34)$ into $(VII.33)$, our final result for the angle-integrated cross section is

$$\sigma(I_{a_1}, I_{c_2} \to I_{c_1}, I_{a_2}) = \frac{(\pi\hbar c\ C_{\ell_1} C_{\ell_2})^2}{4mc^2} \frac{2I_{a_2}+1}{2I_{c_2}+1}$$

$$\cdot (1 - D_{j_1} D_{j_2} R_0)\, P_{\ell_1}(\cos\omega_{01}) P_{\ell_2}(\cos\omega_{02})$$

$$\cdot \frac{\Lambda_0 \Delta}{k^2 E_0 \eta_0 d_0} (\ln 2)^{-2\frac{\Delta}{k}\eta_0}\ e^{-2\frac{n+\Lambda_0}{k}\eta_0} \Gamma(2\frac{\Delta}{k}\eta_0). \qquad (VII.36)$$

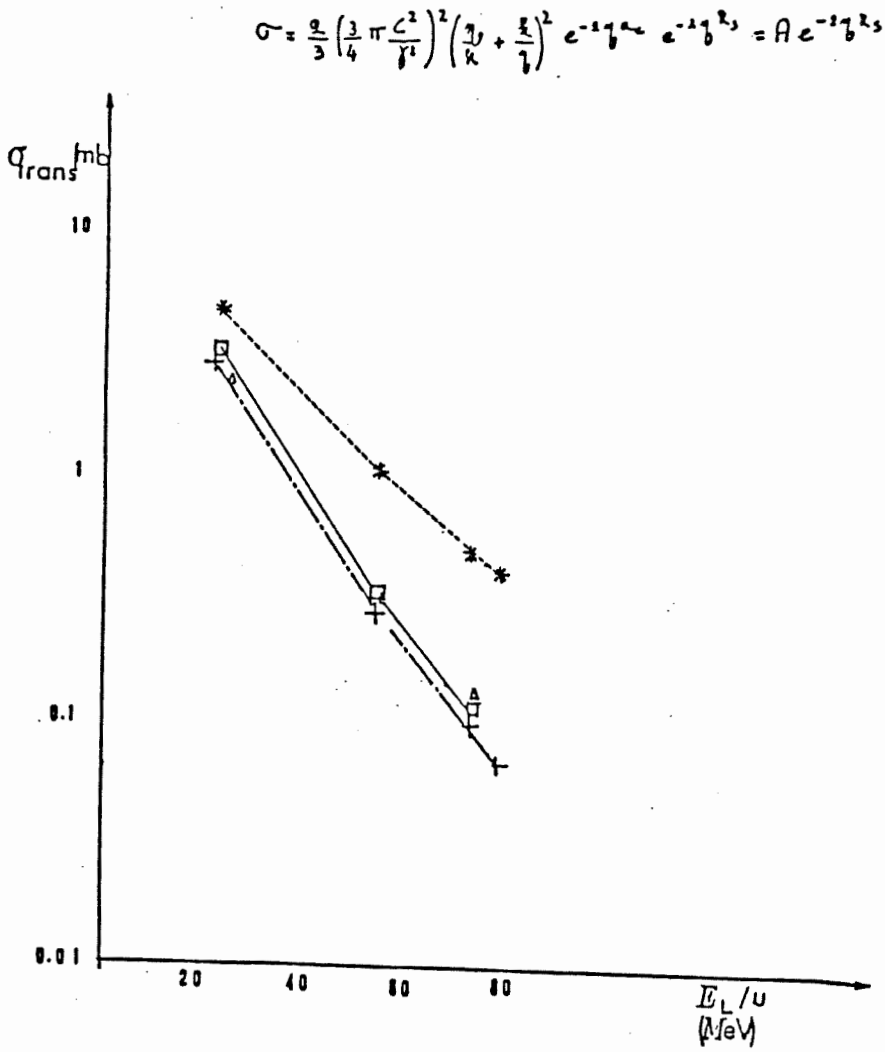

Fig. VII.7. Angle-integrated transfer cross section for the reaction $^{12}C\,(^{13}C, ^{12}C)\,^{13}C_{(1/2^-g.s.)}$ as a function of incident energy per nucleon. The squares are DWBA calculations by Von Oertzen (1985). The crosses and the stars are the results of the calculations of Bonaccorso, Brink and Lo Monaco (1985) for two different choices of the strong absorption radius R_s: + correspond to R_s such that $|S|^2 = 1/2$ and $*$ to R_s such that $P^{tr} \cdot |S|^2$ be maximum. These results are obtained by the analytical formula for the cross section shown on top of the figure, which uses the sharp cut-off approximation for the reflection coefficient $|S|^2$. The symbols have the same meaning as in the present work. Finally, the triangles are obtained by integrating over the angle the differential cross section given by eqs. (III.28)-(III.31). It can be seen that the agreement between this calculation (triangles) and DWBA (squares) is better than for the other two approximation.

All factors in *eq.* $(VII.36)$ depend slowly on energy, except the exponential $e^{-2\frac{n+\Lambda_0}{k}\eta_0} \simeq e^{-2\eta_0 d_0}$ and the Legendre polynomials. The parameters Λ_0 and Δ can be related to the depth W_0 and diffuseness a_w of the imaginary part of the optical potential $W(r)$. By using an exponential form of the nuclear potential (Broglia and Winther 1981, p. 112) and the parametrization (VII.32) of the phase shifts, we find

$$\Delta = k a_w,$$

$$\Lambda_0 = k a_w \ln\left[\frac{2}{\ln 2} W_0 \sqrt{\pi \frac{mc^2}{(\hbar c)^2} \frac{A_1 A_2}{A_1 + A_2} \frac{a_w R_{CB}}{E_{c.m.} - E_{CB}}}\right] + k R_w - n.$$

The expressions given above for Λ_0 and Δ have been tested with the results of reflection coefficients calculated numerically by solving the radial Schrödinger equation.

By extrapolating the parameters of $W(r)$ given in table IV.1 to higher energies, we calculated the angle-integrated cross section, eq. (VII.36), for the reaction $^{208}Pb(^{16}O, ^{15}O)^{209}Pb$ in a wide range of energies above the Coulomb barrier. For incident energy $E_{lab} > 20$ MeV/nucleon the cross section decreases exponentially with increasing energy. At high energy the dependence of the cross section is very similar to that of the transfer probability in fig. VII.1

Chapter VIII. Conclusions

The evaluation of the amplitude presented in this work provides a practical way of calculating angular distributions for single nucleon transfer between heavy ions. At the same time, the semiclassical approach makes it easier to understand the physics of the process.

The perturbative treatment of chapter II is accurate enough for heavy ion reactions above the Coulomb barrier, because of the strong absorption in the interior region. The analytical form shows the explicit dependence of the amplitude on the distance of closest approach (d.c.a.), the relative velocity, the Q-value and the angular momenta of the initial and final states. This gives the condition between Q and the incident energy for maximum transfer and allows the spin selectivity of the reaction to be studied.

The physical interpretation of the process is also quite transparent, as we showed with the approximate factorization of the amplitude in § II.3 or by introducing the double Fourier transform $\tilde{\tilde{\Phi}}$ in § II.5. The transfer amplitude is essentially given by the overlap of two factors: the amplitude that before transfer the nucleon be on the surface Σ between the two nuclei with specified momentum k_{1z} times the amplitude that it is found bound in the final nucleus with momentum k_{2z}. The momenta k_{1z} and k_{2z} are given by the kinematic condition (II.17) that comes out from our calculation, but can also be deduced from the addition of velocities.

One aim of our work was to see how reliable semiclassical calculations are for a quantitative descripton of transfer reactions. The calculations done with the appropriate for-

malism of Hasan and Brink (1978) and the analytical form of the semiclassical amplitude derived in this work show that the shapes of our angular distributions are very similar to those obtained by DWBA. However, the magnitude of our cross section is sensitive to the choice of the distance of closest approach in the initial or final channel. This may be particularly serious at lower energies for a transfer with a large Q-value. The sensitivity to the choice of the orbit makes such a calculation unreliable to extract spectroscopic factors. The evaluation of the absolute cross section could be improved if one finds a consistent way of treating the angular momentum loss from the relative motion to the intrinsic degrees of freedom.

An interesting observation about the partial wave formalism of Hasan and Brink (1978) for calculating angular distributions is that it gives the same angle-integrated cross section as the classical product-of-probabilities formula, as we showed in chapter III. Therefore one can use the simpler classical formula to study spin selectivity and energy dependence of the reaction.

The semiclassical neutron transfer amplitude is easily extended to the case of proton transfer. A new definition of effective Q-value is necessary for a consistent formalism.

A new j-coupling scheme was introduced to study the spin selectivity of the reaction with respect to the incident energy. This gives a formula for the transfer probability and accounts for the observed 'spin-flip' preference at low energies and vice-versa at higher energies. The change occurs at an incident energy such that the relative velocity v at the distance of closest approach satisfies the condition (II.32). This condiion is equivalent to saying that v matches the change in the nucleon velocity caused by the transfer from the

initial level with energy ε_1 to the final level with energy $\varepsilon_2 = \varepsilon_1 - Q$.
Cross sections calculated within this coupling scheme could be used for j identification of single-particle levels.

Also an approximate analytical formula for the angle-integrated cross section has been obtained. This formula can be used in conjunction with transfer probabilities in the new j-coupling scheme to study the spin dependence at high energy.

Another problem is the calculation of the optical potential. It has been stressed several times that transfer plays an important rôle in the depopulation of the elastic channel. As we mentioned in chapter I, transfer form factors have a longer range than those for inelastic excitation. Therefore they affect more the 'tail' of the absorptive potential. The analytical formula (II.28) for the semiclassical transfer amplitude has been used to calculate the imaginary part of the optical potential W (Brink and Stancu 1985). One result of that calculation is that transfer to the continuum states should be included in the calculation of the W, especially at higher incident energy. Therefore an extension of the present formulation to transfer in the continuum would be interesting.

References

Entries with more than two authors appear as "1st Author et al. ", *unless ambiguity arises.*

Abramowitz M. and Stegun I. A., 1970, Handbook of Mathematical Functions, Dover, New York;

Anantaraman N., 1973, Phys. Rev. C8, 2245;

Anyas-Weiss N. et al., 1974, Phys. Rep. **12**, 201;

Ascuitto R. J. and Seglie E. A., 1984, in Treatise on Heavy Ion Science, edited by D. A. Bromley, Vol. 1, Plenum Press, New York and London, p. 463;

Bass R., 1980, Nuclear Reactions with Heavy Ions, Springer-Verlag, Berlin;

Bilwes B. et al., 1983, Nucl. Phys. **A 408**, 173;

Bonaccorso A., Brink D. M. and Lo Monaco L., 1985, contribution to the Conference on Nuclear Structure with Heavy Ions, Legnaro, Italy, to be published;

Bonaccorso A., Piccolo G. and Brink D. M., 1985, Nucl. Phys. **A 441**, 555;

Bond P. D., 1980, Phys. Rev. **C 22**, 1539;

Bond P. D., 1983, Comments Nucl. & Part. Physics (GB) **11**, 231;

Bouldin D. P., anf Goldfarb L. B. J., 1973, Phys. Lett. **47B**, 203;

Brink D. M., 1972, Phys. Lett. **40 B**, 37;

Brink D. M., 1978, in Nuclear Physics with Heavy Ions and Mesons, ed. R. Balian et al., North -Holland, Amsterdam;

Brink D. M., 1985, Semi-Classical Methods for Nucleus-Nucleus Scattering, Cambridge University Press;

Brink D. M. and Satchler G. R., 1971, Angular Momentum, Oxford University Press;

Broglia R. A. and Winther A., 1972 a, Nucl. Phys. **A 182**, 112;

Broglia R. A. and Winther A., 1972 b, Phys. Rep. **4**, 153;

Broglia R. A. et al., 1974, Phys. Rep. **11**, 1;

Broglia R. A. et al., 1981, Nucl. Phys. **A 361**, 307;

Broglia R. A. and Winther A., 1981, Heavy Ion Reactions, vol. I, Benjamin/Cummings, Amsterdam;

Broglia R. A. and Winther A., 1985, Heavy Ion Reactions, vol. II (Transfer Reactions), to be published;

Butler S. T., 1950, Phys. Rev. **80**, 1095;

Butler S. T., 1951, Proc. Roy. Soc. (London) **A208**, 559;

Buttle J. A. and Goldfarb L. B. J., 1971, Nucl. Phys. **A 176**, 299;

de Vries R. H., 1973, Phys. Rev. **C 8**, 951;

Dodd L. R. and Greider K. R., 1969, Phys. Rev. **180**, 1187;

Ericson T. O., 1966, in Preludes in Theoretical Physics, A. de Shalit, H. Feshbach and L. Van Hove eds., p. 321;

Erskine J. R. et al., 1962, Phys. Rev. **128**, 720;

Esbensen H. et al.,1983, Ann. og Phys. **146**, 149;

Frahn W., 1985, Diffractive Processes in Nuclear Physics, Oxford University Press;

Franey M. A. et al., 1979, Nucl. Phys. **A234**, 193;

Glendenning N. K., 1983, Direct Nuclear Reactions, Academic Press, New York;

Goldfarb L. B. J., 1966, in Lectures in theoretical physics, vol. VII-C (eds. P. D. Kunz, D. A. Lind and W. E. Brittin), University of Colorado Press, Boulder, p. 445;

Goldfarb L. B. J. and Von Oertzen W., 1979, in Heavy Ion Collisions, vol. 1, (ed. R. Bock), North-Holland, Amsterdam, p. 215;

Hasan H., 1976, D. Phil. Thesis, University of Oxford (unpublished);

Hasan H. and Brink D. M., 1978, J. Phys. G: Nucl. Phys. **4**, 1573;

Hasan H. and Brink D. M., 1979, J. Phys. G: Nucl. Phys. **5**, 771;

Helmotz et al., 1947, Phys. Rev. **72**, 1003;

Hodgson P. E., 1971, Nuclear Reactions and Nuclear Structure, Clarendon Press, Oxford;

Hodgson P. E., 1978, Nuclear Heavy-Ion Reactions, Clarendon Press, Oxford;

Kahana S. and Baltz A. J., 1977, Adv. Nucl. Phys. **9**, 1;

Källne J. and Fagerström B., 1975, Physica Scripta **11**, 79;

Koeling T. and Malfliet R. A., 1975, Phys. Rev. **22C**, 181;

Landowne S. et al., 1976, Nucl. Phys. **A259**, 99;

Lawrence E. O. et al., 1935, Phys. Rev. **48**, 493;

Lawson R. D., 1980, Theory of the Nuclear Shell Model, Clarendon Press, Oxford;

Lo Monaco L. and Brink D. M., 1985, J. Phys. G: Nucl. Phys. **11**, 935;

Messiah A., 1969, Mécanique Quantique, Dunod, Paris;

Milek B. et al., 1985, Phys. Lett., **B 150**, 512;

Nogami M., 1973, Genshikaku, Shokabo Co. Ltd., pp. 10-13;

Nörenberg W. and Weidenmüller H. A., 1980, Introduction to the Theory of Heavy Ion Collisions (2nd Edition), Springer-Verlag, Berlin;

Olmer C. et al., 1978, Phys. Rev. **C 18**, 205;

Oppenheimer J. R., 1928a, Phys. Rev. **31**, 66;

Oppenheimer J. R., 1928b, Phys. Rev. **31**, 349;

Oppenheimer J. R. and Phillips M., 1935, Phys. Rev. **48**, 500;

Paschopoulos I. et al., Nucl. Phys. **A 252**, 173;

Pieper S. C. et al., 1978, Phys. Rev. **C 18**, 180;

Révai J., 1985, Nucl. Phys., **A 438**, 512;

Satchler G. R. et al., 1969, Phys. Rev. **187**, 1491;

Satchler G. R., 1983, Direct Nuclear Reactions, Oxford University Press;

Serber R., 1947, Phys. Rev. **72**, 1008;

Siemens P. J., 1971, Phys. Lett. **36 B**, 24;

Stancu Fl. and Brink D. M., 1985, Phys. Rev. **C 32**, 1937;

Strutinsky V. M., 1964, Sov. Phys.-JETP **19**, 1401;

Strutinsky V. M., 1973, Phys. Lett. **44 B**, 245;

Traber A., Trautmann D. and Alder K., 1977, Zeit. Phys. **A281**, 391;

Von Oertzen W., 1985, Phys. Lett. **151 B**, 95;

Whittaker E. T. and Watson G. N., 1927, A Course of Modern Analysis, 4th edition, Cambridge University Press;

Wildenthal B. H. et al., 1967, Phys. Rev. Lett. **19**, 965.